PhD degree in Molecular Medicine (curriculum in Molecular Oncology)

European School of Molecular Medicine (SEMM),

University of Milan and University of Naples "Federico II"

Settore disciplinare: bio/10

Characterization of the E3 ligase dHecw, a novel member of the *Drosophila melanogaster* Nedd4 family

Fajner Valentina

Fondazione IFOM, Milan

Matricola n. R10751

Supervisor: Dr. Polo Simona

Fondazione IFOM, Milan

Anno accademico 2017-2018

TABLE OF CONTENTS

LIST OF ABBREVIATIONS

AMPK	AMP-activated protein kinase
APC/C	Anaphase promoting complex
CAT-1	Cationic amino acid transporter
CNS	Central nervous system
Co-IP	Co-immunoprecipitation
DUB	Deubiquitinating enzymes
EC	Endothelial cell
EGFR	Epidermal growth factor receptor
ENaC	Epithelial cell sodium channel
ENS	Enteric nervous system
fALS	Familiar amyotrophic lateral sclerosis
FC	Follicle cell
FE	Follicular epithelium
GC	Germ cell
Grk	Gurken
HECT	homologous to E6-AP carboxyl terminus
HGS	hepatocyte growth factor-regulated tyrosine kinase substrate
IB	Immunoblot
IGF-1R	Insulin-like growth factor-1 receptor
IF	Immunofluorescence
IP	Immunoprecipitation
K	lysine
KO	Knock out
M	Methionine
Nos	Nanos

NEDD4	Neuronal precursor cell-expressed developmentally downregulated gene 4
NF1	Neurofibromastosis Type I
Osk	Oskar
PTEN	Phosphatase and tensin homolog
Pyd	Polychaetoid
RING	Really interesting new gene
RBP	RNA binding protein
RBR	Ring between ring
SOP	Sensory organ precursor
Su(dx)	Suppressor of deltex
Tj	Traffic jam
UAS	Upstream activation sequence
vISH	Virtual *in situ* hybridization
YAP	Yes-associated protein

FIGURE INDEX

TABLE INDEX

ABSTRACT

Ubiquitination is one of the most abundant and versatile post-translation modifications in eukaryotes, and it plays an important role in many biological processes by affecting protein activity, interactions, localization and stability. E3 ligases (E3s) have a key function as molecular ubiquitin-substrate matchmakers, providing specificity to the reaction, yet little is known about the targets and functions of the majority of E3s.

In this thesis, we identified and characterized dHecw, a novel member of the *Drosophila melanogaster* Nedd4 family of ubiquitin E3s. dHecw is the single ortholog of the human HECT ligases HECW1 and HECW2, which are the less characterized members of the family. We proved that dHecw is a catalytically active enzyme, whose expression is tightly regulated in the central nervous system and in the ovary, and is down-modulated during aging. To investigate dHecw function *in vivo*, we generated catalytic inactive dHecw and KO fly mutants by CRISPR/Cas9 technology. Both types of mutants are viable in homozygosis but presented signs of neurodegeneration, such as short lifespan, limited motor function and brain tissue vacuolarization. They also showed premature decline in fertility due to germline specific defects in oogenesis, including aberrant number of nurse cells, compound egg chambers and misspecification of additional oocytes. The interactome of dHecw was identified by mass spectrometry analysis and includes several ribonucleoparticles (RNPs) components, including dFmr1, a translational repressor that controls localized mRNA translation in developing fly egg chambers. Interestingly, *dfmr1* loss of function flies presented ovarian phenotypes that closely resemble the ones of dHecw mutants and KO flies. We demonstrated that dFmrp is a dHecw substrate *in vitro*, and we found a genetic interaction among the two proteins. Our investigation of the functional outcome of dFmrp ubiquitination suggests that it does not cause dFmrp degradation but, instead, it impacts on its function/interaction network. Indeed, we found that the expression of Orb, a known target of dFmrp repression, is upregulated in dHecw fly mutants. On the contrary, Orb levels are down-modulated upon dHecw overexpression in

the germline tissue. Altogether, our data suggest that dHecw is a novel player involved in the dynamic regulation of RNPs required for neuronal health and fertility.

INTRODUCTION

1. The multifunctional role of Ubiquitin

Ubiquitination is a post-translational modification that has a critical impact on proteins and can influence their localization, activity, interaction network, and ultimate fate [Kercher, 2006]. Ubiquitination consists in the covalent attachment of one or more ubiquitin molecules to the ε-amino groups of protein lysines (K) [1]. Ubiquitin is a 76 amino acids peptide and is highly conserved in all eukaryotic cells [2], and is present both in the cytoplasm and in the nucleus of the cell in a free monomeric and target-conjugated form. The ubiquitin protein is extremely stable and adopts a compact β-grasp fold with a very flexible tail of six residues at the C-terminal [3].

Ubiquitination is involved in a multitude of processes, including membrane protein trafficking [4] and sorting, protein quality control, protein localization, protein activity and protein-protein binding ability [5], signal transduction [6], transcriptional regulation [7], DNA repair [8], viral infection, immune response and cell-cycle control [9]. The key to the versatility of ubiquitination relies on its ability to form structurally and functionally different ubiquitin polymers: ubiquitin can be attached to the target protein, as a single moiety (mono and multi-monoubiquitination) or as a polymeric chain (polyubiquitination) [10] .

Ubiquitin has seven internal lysine (K 6, 11, 27, 29, 33, 48 and 63) and one methionine residues at the N-terminus (M1), all of which can be used as an attachment site for chain assembly. Ubiquitin -chains can adopt distinct topologies depending on how the ubiquitin molecules are connected: chains where ubiquitin is always linked through the same residue are classified as homotypic, while they are defined as heterotypic if there are different linkages within the same polymer. Among the heterotypic chains, we can distinguish between mixed chains, with different lysine linkages at successive chain positions, and branched chains, where one

ubiquitin moiety is decorated with at least two ubiquitin molecules, forming a fork-shaped polymer [11] (**Fig. 1**).

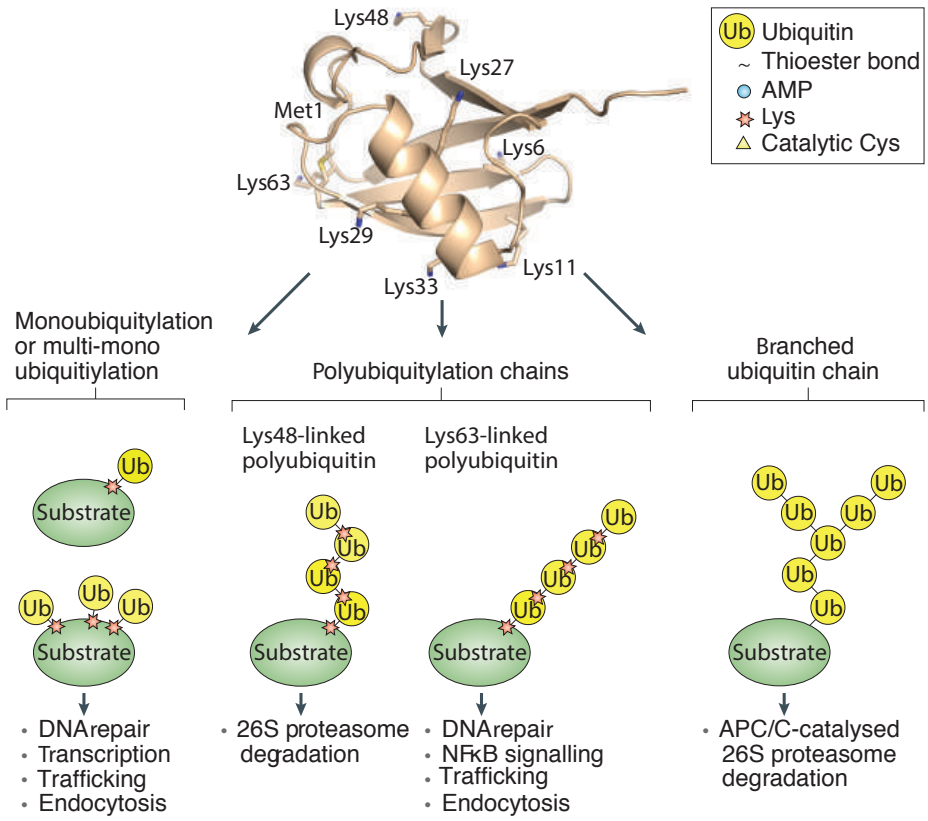

Figure 1. The Ubiquitin code.

The Ubiquitin molecule. The N-terminus methionine and all the lysine residues involved in chains formation are highlighted. Schematic representation of different types of substrate ubiquitination (Ub in yellow) such as mono, multi-monoubiquitination, polyubiquitin chains and branched ubiquitin chains. Potential outcomes of substrate proteins conjugated with the given ubiquitin linkage are indicated. [Adapted from Buetow and Huang, Nature Reviews Molecular Cell Biology, 2016].

As in a code, different ubiquitin modifications are interpreted by the cell as a distinct signal, leading to different outcomes. The first described role of ubiquitination, targeting of proteins to proteasomal degradation, has now been complemented with numerous other functions: mono-ubiquitination changes interaction or localization patterns [12] and acts preferentially as a non-proteolytic signal to control gene expression, viral budding, DNA repair, and endocytosis [13].

Poly-ubiquitin chains are specialized for other cellular functions: K63- and K48-linked chains are the best characterized chain linkages in terms of structure and biological role. It is well established that ubiquitin chains connected through K48 trigger degradation by the 26S proteasome and are structurally characterized by a closed conformation [6]. K48 linkages are the most abundant ubiquitin chain types in the cell and their levels increase rapidly when the proteasome is inhibited [14]. On the contrary, K63-linked chains fold in an extended, open conformation and are non-proteolytic signals involved in the regulation of many cellular processes, such as DNA repair [15], [16] , membrane protein trafficking, and endocytosis [17]. K63-linked chains also regulate the assembly of protein complexes [18], such as the mRNA splicing machinery - one of the most dynamic complexes in human cells - and part of its rearrangements during distinct steps of the splicing reaction was suggested to be regulated by K63-linked chains [19].

The functional role of the other ubiquitin chains is less characterized [10]. The function of K6, in particular, is currently unclear: recent works linked K6 chains with mitochondria quality control, but the exact role in this context needs still to be clearly defined [20]. K11 was shown to be involved in proteasomal degradation of cell cycle proteins [21]. The anaphase-promoting complex (APC/C) is the crucial E3 ligase for mitotic degradation of cell cycle regulators, as cyclin B and securin; it has been shown to generate K11 ubiquitin chains on its substrates, promoting their degradation via the proteasome [21]. K27 linkages are involved in DNA damage response [22] and innate immunity, while K29 chains were suggested to contribute to the negative regulation of Wnt signaling [20]. K33- ubiquitin chains appear to have non-degradative functions, working as negative regulators of T-cell antigen receptors and of AMPK (AMP-activated protein kinase)-related protein kinase [20]. Recently, they were implicated in post-Golgi protein trafficking [23]. Linear ubiquitin chains, like M1-linked chains, play a key role in inflammatory and immune responses by regulating the activation of the transcription factor NF-κB [24].

Ubiquitin chain formation is a dynamic and reversible process and deubiquitinating (DUB) enzymes may team up with E3 ligases to edit or remove ubiquitin chains [25]. During the editing process, one chain type is replaced by a chain of different topology, which changes the fate of the modified substrate. Interestingly, ubiquitin molecules can be further modified by other post-translational modifications, like acetylation and phosphorylation, increasing the signal repertoire of this multifunctional protein [26].

1.1 E3 ligases: catalysts and matchmakers of the Ubiquitin cascade

Ubiquitination is a highly controlled process and it is catalyzed by the sequential action of three classes of enzymes: ubiquitin-activating enzymes (E1s), ubiquitin -conjugating enzymes (E2s) and ubiquitin-ligases (E3s) [27]. For covalent conjugation to occur, the ubiquitin C-terminus has to be activated. The E1 enzyme is responsible for the activation of the C-terminal glycine (G76) of ubiquitin in an ATP-dependent manner, resulting in a high energy thioester linkage between ubiquitin and the catalytic cysteine of the enzyme. Then, the activated ubiquitin is transferred to the catalytic cysteine of the E2 enzyme in a transthiolation process. This second enzyme carries the ubiquitin moiety to the E3 ligase, which catalyzes the transfer of ubiquitin to the ε-amino group of a substrate lysine residue, or to the growing end of a poly-ubiquitin chain [2]. It is interesting to notice the number of enzymes that are present per class: only two E1 enzymes are involved in the activation and the transfer of ubiquitin to a limited number of E2s (around 40), which interact with more than 600 E3s, determining the increase in specificity along the cascade. In this way, each E3 is able to recognize and to ubiquitinate a panel of substrates with high specificity [28]. The recognition of the right target is a key step in the ubiquitination process. The E3 ligases act as a catalyst for the reaction, greatly increasing the rate of ubiquitin transfer. They also play an essential role as molecular matchmakers, capable of conferring a high degree of specificity towards substrates and the ubiquitin chain linkage built on them [27], [28]. According to their structure and mechanism of action, E3

ligases are divided into three major classes (**Fig. 2**): really interesting new gene (RING), homologous to E6-AP carboxyl terminus (HECT) and ring between ring (RBR).

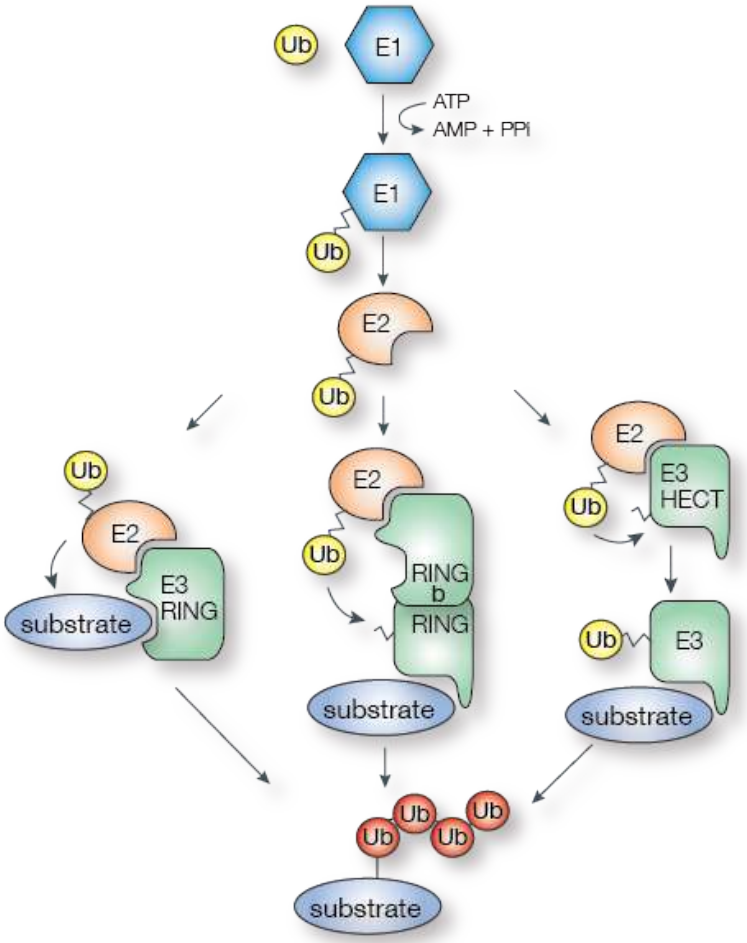

Figure 2. The Ubiquitin cascade.

Schematic representation of ubiquitination reaction mediated by an E1 ubiquitin-activating enzyme (E1, blue), an E2 ubiquitin-conjugating enzyme (E2, orange) and an E3 ubiquitin ligase (green). Three classes of E3 ubiquitin ligases have been identified: RING ligases (left), RBR (RING-between-RING) ligases (middle), and HECT ligases (right). [adapted from Woelk et al. Cell Div. 2007].

1.1.1 RING ligases

The vast majority of E3 ligases belong to the group of Really Interesting New Gene (RING) that regulate crucial cellular functions, such as cell cycle, DNA repair, cell signaling and responses to hypoxia [29]. The RING is their catalytically critical domain, and is characterized by a cross-brace structure with two zinc ions coordinated by cysteine and histidine residues [30]. The E3s

of the RING family have a dual role in substrate ubiquitination: first, they act as a molecular scaffold, and simultaneously bind the E2~Ub and the substrate to bring them in close proximity. Second, they induce conformational changes in the complex to correctly orient the thioester bond and prime to donor ubiquitin carried by the E2 for the nucleophilic attach of the substrate lysine [31], [32]. Members of the RING ligases can work as monomers, as dimers (either homodimer or heterodimer) or as multi-subunit complexes. Cbl is a well characterized RING E3 that acts as a monomer [33] and has a key role in the regulation of protein tyrosine kinases [34] One example of homodimers is represented by the Rnf8 E3 ubiquitin-protein ligase complex that regulates DNA damage signaling [35]. In the case of heterodimers, like BRCA1–BARD1 (BRCA1-associated RING domain 1), generally one RING E3 does not have intrinsic catalytic activity and helps the stabilization and activation of the other active RING ligase [29]. A well-studied example is given by the E3 ligase Mdm2, that can function as a homodimer or a heterodimer with MDMX in the regulation of the tumor suppressor p53 [36]. The two multi-subunit RING ligases are APC/C (anaphase-promoting complex/cyclosomes) and SCF (Skp1-Cul1-F-box); both of which have a critical role in the regulation of cell cycle progression [37].

1.1.2 HECT E3 ligases

The HECT E3 ligases are implicated in protein trafficking, signaling pathways that regulate cell growth, proliferation, and immune response [38]. HECT E3 ligases are defined by a 350 residues module, first characterized in the human E3 ligase E6-associated protein, E6AP [39], invariably positioned at the C-terminal. Differently from the RING, the enzymatic activity of HECT occurs in two distinct reactions: first, with a transthiolation reaction between the E2 and the E3, the ubiquitin is transferred to the cysteine on the active site of the HECT domain. In the second step, the ubiquitin moiety is transferred from the HECT intermediate to a lysine on the target substrate [38]. The HECT domain is necessary and sufficient for both reactions: it was proved that isolated HECT domains are able to bind E2~ubiquitin, form an E3~ubiquitin

intermediate, ligate the E3-linked ubiquitin to one of the HECT lysine and build a polyubiquitin chain, reviewed in [40]. In mammals, the HECT enzymes are further divided into three subgroups according to their domain architecture: Nedd4/ Nedd4-like are the HECT E3s with C2 and several WW domains, HECTs with RLDs (regulator of chromosome condensation 1-like _ RCC1-like domains) are called HERC, and the last group contains the HECTs that neither have C2, RLDs nor WW domains (like HUWE1, HACE1, UBE3B) [41].

1.1.3 RBR ligases

The last class of E3 ligases is represented by the RBR ligases and was recently defined as a mechanistically distinct class; to date, these E3 enzymes are not well understood, and their substrates and E2 partners are poorly defined [42]. RBR ligases are defined as RING-HECT hybrids, as they show characteristics of both classes; they possess two RING domains, one that acts as a scaffold and an atypical RING domain (RING2) containing a catalytic cysteine involved in the formation of the catalytic intermediate [43], [42]. Members of this E3 family mediate diverse processes, such as regulation of post-translation modifications and protein stability, cellular and stress signaling, cell-cycle control, transcription, RNA metabolism and translation [44]. One of the most studied RBR enzyme is Parkin, whose mutations in the RBR domain are associated with Parkinson's disease [45].

2. NEDD4 family

2.1 Domain description

The NEDD4 (neuronal precursor cell-expressed developmentally downregulated gene 4) family of HECT E3 ligases is the most intensively studied family and is well conserved from yeast to mammals (**Fig. 3**). In the human genome, the NEDD4 family has diverged with nine homologs: NEDD4 (also known as NEDD4-1), NEDD4L (also known as NEDD4-2), AIP4/ITCH, SMURF1, SMURF2, WWP1, WWP2, HECW1 and HECW2 (also known as NEDL1 and NEDL2). All these proteins share common domain architecture with unique functional proprieties [46], [38]. Starting from the N-terminus, they display a C2 domain responsible for the regulation of

cellular localization, and two-to-four WW domains, in charge of substrate selection. Both regions are also involved in a regulatory intramolecular interaction with the C-terminal catalytic HECT domain [41], [47].

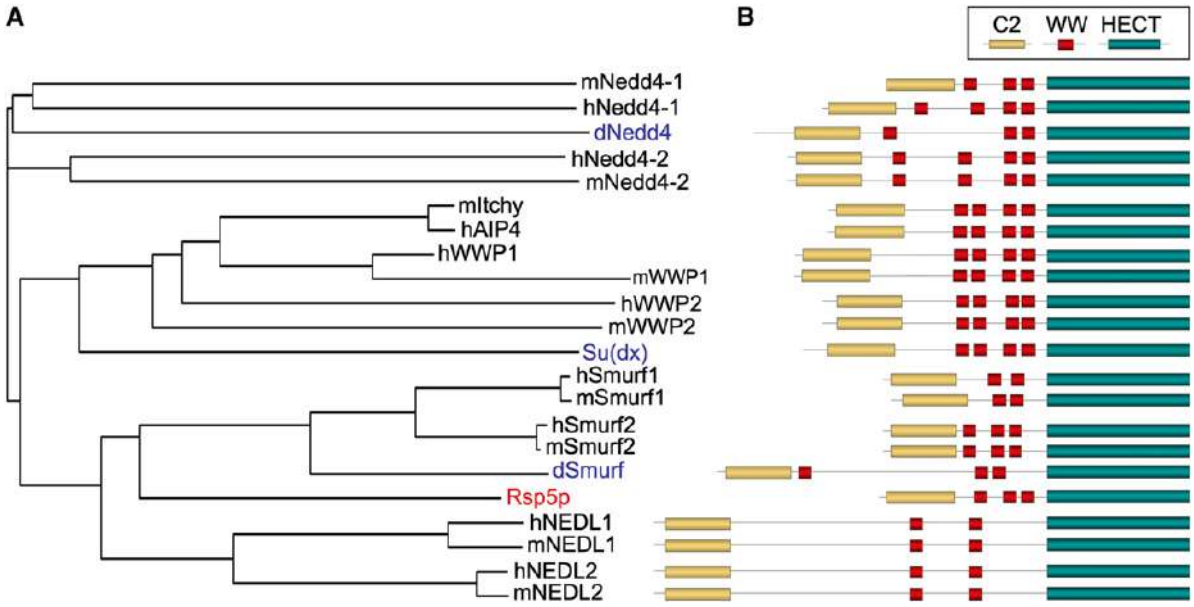

Figure 3. Phylogenetic relationship tree of different members of C2-WW-HECT family of E3s.

*(**A**) Orthologs of Nedd4 have been identified in yeast (red), fly (blue), and mouse and human (black). Itch clusters with WWP1 and WWP2, while Nedd4-1 and 2, the Smurfs and HECW1 and 2 forms separate clusters. (**B**) The C2-WW-HECT E3 modular structure consist of an N-terminal Ca2+/ lipid-binding (C2) domain (yellow rectangles), a central region containing WW domains (red squares), and a ubiquitin-protein ligase HECT domain (teal rectangles). [Adapted from Bernassola et al., Cancer Cell, 2008].*

The C2 domain is a ~130 residues module, folded in an eight-stranded beta-sandwich structure and was originally described as a calcium-dependent phospholipid binding domain of the protein kinase C [48]. Since the discovery of the C2 domain, a wide array of C2-bearing proteins has been identified, pointing to a great functional diversity of this domain. Indeed, the C2 domain can bind calcium, phospholipids, inositol phosphate but also proteins, and has different binding affinities according to each domain [49].

The WW domain contains two conserved tryptophan residues that are spaced 20–22 amino acids apart, hence the name 'WW domain'. This domain is a compact module folded in three stranded antiparallel beta-sheets, forming a hydrophobic core where ligand binding occurs [50]. The WW domain is often present in multiples copies within the same protein and

is found in a variety of unrelated proteins (e.g., dystrophin, Pin1, YAP65). WW domains have a key role in mediating protein–protein interactions via recognition of proline-rich motifs and phosphorylated serine/threonine-proline sites. WW domains are classified into four classes according to the sequence motifs they recognize [51], [52]. NEDD4 E3s bear class I type domains, able to bind PY motifs (L/PPxY). Notably, WW domains from the same E3 may function independently and can have distinct binding preferences [53]. Thus, the WW-rich region in NEDD4 family members serves as a scaffold to recruit proteins and regulators, and provides these enzymes with a versatile platform that remains to be fully characterized.

The HECT domain is the defining structural element of this class of ligases. The HECT domain is composed of a bi-lobed structure with a bigger N-terminal lobe (N-lobe) that contains the E2 binding site and a non-covalent ubiquitin-binding site, and a smaller C-terminal lobe (C-lobe) carrying the catalytic cysteine involved in the ubiquitin transfer [54]. The two lobes are connected by a flexible hinge region that permits the C-lobe to span virtually 360° around the hinge, as underlined by the different conformations adopted in the solved structures of the HECT domains. The flexibility of the hinge loop has a critical role in ligase activity, and it is required to bring the cysteine residues of the E2 and the E3 in close proximity during ubiquitin transfer and for the nucleophilic attack of the target lysine to the HECT~ubiquitin [55], [56], [57]. In addition to the key catalytic cysteine, some strictly conserved acidic residues present in the C-terminal part of the HECT domain were demonstrated to be fundamental for a proper catalysis [58], potentially contributing to the formation of the active catalytic site, and helping to position the acceptor ubiquitin.

The ability to build linkage-specific ubiquitin chains is an intrinsic feature of the HECT domains, independently from the E2 that they are coupled with [59]. In detail, the C-terminus of HECT E3 ligases has a key role in determining chain specificity; it was shown that the substitution of the last three NEDD4 amino acids with the E6AP sequence (not a NEDD4 family member) changes the specificity of the ubiquitin-chain product from pure K63-linked chains,

typically created by this family through a sequential addition mechanism, to a mixture of K48- and K63-linked chains [58], [60]. Although the NEDD4 family is known to generate mainly K63 ubiquitin chains, several studies reported that NEDD4 substrates undergo proteasome-mediated degradation [61]. An explanation provided recently by French and colleagues is that chain synthesis might works in two different phases: a more stringent initial phase that results in K63-specific ubiquitin tetramers, and one less defined phase, in which chains are elongated via different lysines [62]. These final longer and branched structures are well recognized by the proteasome [62]. In addition, NEDD4 can also generate K11 linkages, even if at lower efficiency, and substrates modified in this way are targeted for degradation [63].

2.2 Regulation of HECT activity

Accurate control of E3 ligase activity is fundamental to ensure functional restriction until they are activated. This is crucial to prevent excessive ubiquitination of substrates or misdirected auto-ubiquitination that may cause E3 instability. The ligase activity of NEDD4 family proteins is finely regulated at several levels, spanning from intra-molecular interactions to adaptor protein interactions, and post-translational modifications [38], [64] (**Fig. 4**). Interestingly, despite the conserved domain architecture, NEDD4-family E3s seem to have evolved distinct mechanism of auto-regulation, maybe as a consequence of a different spacing between the domains. A pioneering work of Wiesner and co-workers demonstrated that in the absence of bona fide substrates, a subset of NEDD4-family E3 ligases (SMURF2, NEDD4, NEDD4L and WWP2) are kept in a catalytically inactive state by intramolecular interaction between the N-terminal C2 domain and the C-terminal HECT domain [65]. A following structural study showed that in this close conformation, the C2 binds the HECT near to Ub-binding exosite of the N-lobe and locks the C-lobe in a catalytically incompetent conformation, preventing conjugation of ubiquitin to the substrate [66] (**Fig. 4 A**).

Recent studies of the other NEDD4 members ITCH, NEDD4L and WWP2 extend the self-regulatory role also to the central region of the enzyme, which contains the WW domains

[67], [68], [69]. A crystal structure of WWP2 finally provided the key element for this auto-inhibition in the linker between the WW2 and the WW3 domains, called the 2,3-linker [70]. This 26-residues alpha-helix is able to interact extensively with the N-lobe and the C-lobe of WWP2 HECT, maintaining the enzyme in a close conformation [70] (**Fig. 4 B**). Interestingly, secondary structure prediction indicates that NEDD4 holds a similar alpha-helix C-terminal in the WW1, that may well be part of the inhibitory mechanism, but this hypothesis awaits structural validation. All the inhibitory conformations identified so far may easily coexist and synergize in the same HECT E3 to achieve full enzyme inhibition [47].

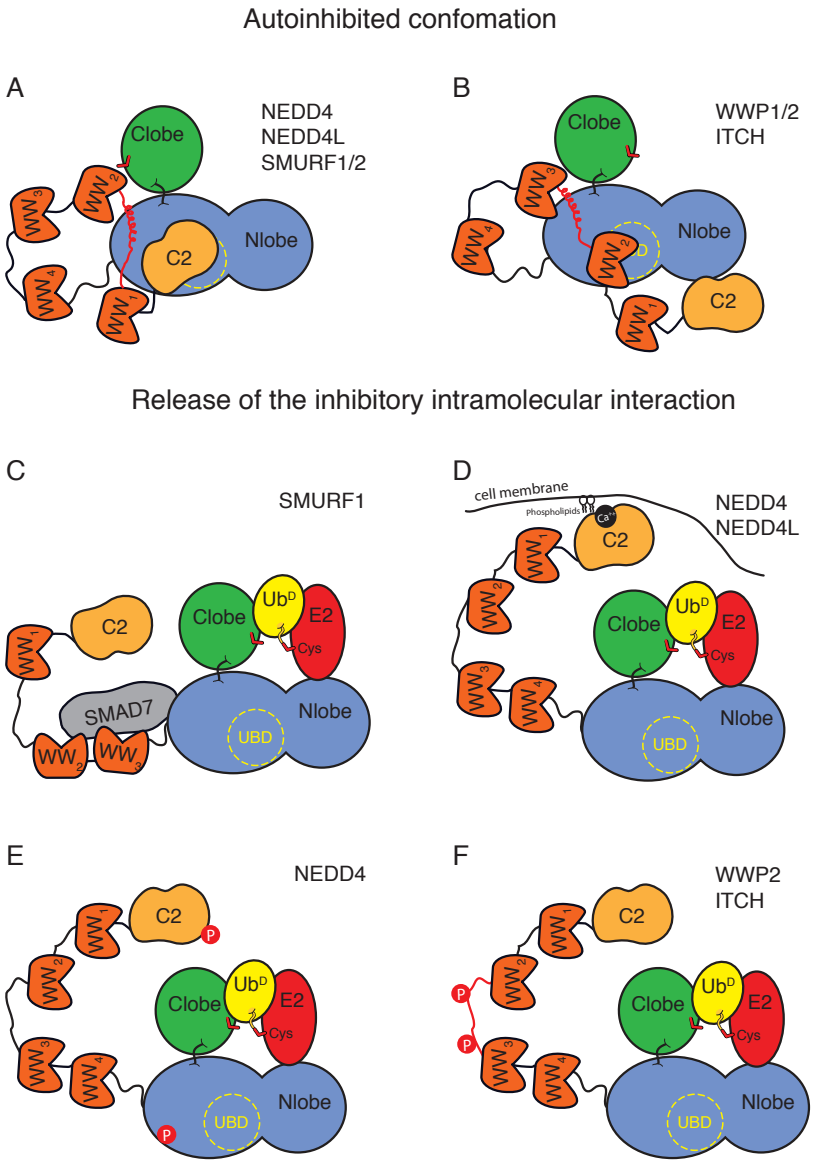

Figure 4. Mechanisms of NEDD4 HECTs regulation.

*Schematic representation of the intramolecular interactions occurring in NEDD4 family members: N-lobe is in blue, C-lobe is in green, WW domains in orange and C2 in dark yellow. (**A**) In NEDD4, NEDD4L and*

*SMURF1-2 the C2 domain mediates the autoinhibited conformation. The C2-binding surface overlaps with the ubiquitin-binding exosite of the N-lobe and locks the C-lobe in a catalytically incompetent conformation. (**B**) In WWP1-2 and ITCH, the linker between WW2 and WW3 domain locks the HECT domain in an inactive conformation, blocking the ubiquitin -binding exosite (depicted as yellow dashed circle on the N-lobe). (**C**) Inactive conformations can be released by adaptor binding, (**D**) Ca2+ flux, (**E,F**) phosphorylation events [adapted from Fajner et al, FEBS letters, 2017].*

A critical issue is how upstream signaling events may trigger the complete release of the auto-inhibitory interactions, leading to full ligase activation [71]. In a few cases, adaptor proteins may work as activators, like the case of SMURF2 that is activated by its adaptor protein SMAD7. By releasing the C2-mediated auto-inhibition, stimulating the binding of E2, and recruiting SMURF targets, SMAD7 functions at multiple levels to control E3 activity and to ensure specificity in SMURF-catalyzed ubiquitination [72] (**Fig. 4 C**). In other cases, as for NEDD4 and NEDD4L, signaling is the driving force: it is well-established that calcium-mediated membrane translocation of the C2 re-localizes NEDD4L, releasing the HECT activity [73], [74] (**Fig. 4 D**). Persaud and colleagues demonstrated that NEDD4 activity is also modulated by tyrosine phosphorylation induced by receptor tyrosine kinases (RTKs) [53]: upon EGFR and FGFR activation, a set of phosphorylation events occur at the C2 and HECT domains, mediated by the tyrosine kinase Src [53]. A similar phosphorylation-based mechanism of activation was demonstrated also for Itch [67], and, recently, Chen et al. suggested that also for the 2,3-linker of WWP2 [70] (**Fig. 4 E,F**). Additional studies are needed to establish if this model where post-trnslational modifications caused by upstream signaling events result in the dissociation of the auto-inhibitory HECT interaction is a common way to activate also other HECT members.

2.3 Function in physiology and disease

Each member of the NEDD4 family is diversely implicated in a wide range of biological processes, such as endocytosis, protein trafficking, viral budding, signaling, cellular growth, and proliferation [38]. It is, thus, not surprising that their alteration is implicated in several diseases, from cancer to neurological disorders [41].

NEDD4L is closely related to the prototype of the family, NEDD4: they share ~60% similarity, but show different expression profiles. While NEDD4 is ubiquitously expressed, NEDD4L is selectively expressed in liver, kidney, brain, lung, and heart [75]. Both NEDD4 and NEDD4L were originally implicated in the regulation of fluid and electrolyte homeostasis, controlling the surface abundance of epithelial cell sodium channel (ENaC) subunits [76], [77]. ENaC is a channel expressed in the apical part of epithelial cells, highly expressed in kidney, lung, heart, brain and colon, where it regulates sodium homeostasis in response to hormones [78]. NEDD4 and, especially, NEDD4L are able to bind the PPxY motifs in the C-terminal tail of ENaC, and to ubiquitinate the channel [79], causing its internalization and lysosomal degradation [80], [81]. Mutations or deletions of the PPxY motif result in the disruption of the interaction between NEDD4/L and ENaC, causing the Liddle's syndrome, a severe disorder that consists in sodium retention and hypertension [82]. NEDD4L activity has been associated with the ubiquitination of other transporters, as in the case of the dopamine transporter (DAT). Both NEDD4 and NEDD4L were shown to be responsible for the ubiquitination of the cationic amino acid transporter (CAT-1) in a cell-type dependent manner [83].

The NEDD4 family has a major role in the regulation of endocytosis and sorting of numerous signaling receptors and transmembrane protein [71], including the epidermal growth factor receptor (EGFR) [84], the insulin-like growth factor-1 receptor (IGF-1 R) [85], the hepatocyte growth factor-regulated tyrosine kinase substrate (HGS) [84], the guanine nucleotide exchange factor CNrasGEF [86], the lysosomal protein LAPTM5 [87], and the β2-adrenergic receptor through the adaptor function of β-arrestin proteins [88]. The role of the family was extensively characterized, leading to the conclusion that the NEDD4 family functions either as a positive or a negative regulator of transmembrane receptors.

NEDD4 is a positive regulator of IGF-1/Akt kinase signaling in mouse embryonic fibroblasts (MEFs). NEDD4−/− MEFs show a decreased abundance of cell surface IGF1 receptor (IGF1R), reduced mitogenetic activity, and cell growth [85]. Differently from IGF1R,

NEDD4 has been implicated in the down-regulation of the EGFR [84]. EGF stimulation promotes ubiquitination of the EGFR, which recruits the ubiquitin interacting motif (UIM)-containing endocytic adaptors EPS15 and EPSIN-1 to the plasma membrane, and, subsequently, HRS to the endosomal membrane. These adaptors are ubiquitinated by NEDD4 through a process known as coupled monoubiquitination, which directs the progression of the ubiquitinated receptors towards lysosomal degradation [89], [71]. Furthermore, NEDD4 plays a role in viral budding where it ubiquitinates HTLV-1 Gag protein, favoring the release of HTLV-1 viral particles from the cell [90].

From the pathological point of view, NEDD4 is frequently overexpressed in different types of cancers, including non-small cell lung cancers, gastric carcinomas, bladder carcinoma, prostate carcinoma and colorectal carcinomas, and is thought to be a promising anti-cancer drug-target [91]. The possible oncogenic role of NEDD4 in the context the tumor suppressor PTEN (Phosphatase and tensin homolog) is, however, still controversial; NEDD4 was initially identified to be responsible for the poly-ubiquitination and proteosomal degradation of PTEN [92]. However, the role of NEDD4 on PTEN fate has not been validated in NEDD4 knockout studies [93], leaving the issue open for further studies.

Another member of the NEDD4 family is AIP4 (atrophin-1 interacting protein 4), also called ITCH. This HECT has been involved in the ubiquitination and endocytosis of the Notch receptor and of the G-coupled receptor CXCR4 [94], [95]. AIP4 plays a role in the immune response, and regulates T lymphocyte differentiation, by promoting ubiquitination of Jun proteins [96]. Furthermore, an emerging number of ITCH protein targets have been implicated in tumorigenesis and chemosensitivity, such as the p53 family members p63 and p73 [97].

An oncogenic role has been proposed for the WW containing protein 1 (WWP1) based on its gene amplification in 40% of breast and prostate cancers [98]. Further studies revealed that p53 is a WWP1 substrate, and that 53 ubiquitination by WWP1 causes its stabilization and accumulation in the cytoplasm, while inactivating its transcriptional activities [99].

Additional WWP1 substrates include Kruppel like factors KLF2 and KLF5, two tumor suppressor proteins [100]. Interestingly, WWP1 was shown to negatively regulates TGF-beta signaling [101], as demonstrated for the other NEDD4 proteins SMAD ubiquitination regulatory factor 1and 2 (SMURF1 and SMURF2). SMURF1\2 antagonize the transforming growth factor-β (TGFβ) signaling by targeting receptors themselves or receptor-associated signaling molecules (SMADs) adaptor proteins [102]. SMURF1 targets specifically Smad1 and Smad5, while SMURF2 has a broader specificity [103]. The role of these E3 ligases is probably not redundant, since WWP1 and SMURFs are expressed in distinct patterns in human tissues and carcinoma cell lines, suggesting unique pathophysiological roles of WWP1 and SMURFs. SMURF2 overexpression was reported in several types of cancer, in particular in pancreatic and in esophageal squamous cells carcinoma where its aberrant expression was correlated with higher invasiveness [104].

2.3.1 HECW1 and HECW2

HECT, C2 and WW domain-containing E3 ubiquitin ligase 1 (HECW1) and HECW2 represent the largest but the less studied members of the Nedd4 HECT family. Their genes are located on chromosome 7 and 2, respectively. These proteins share 69% sequence identity: the C-terminal part is the most conserved one, with 93% identical catalytic HECT, and the substrates binding domains WWI and WWII show 97% and 82% identity, respectively. The major differences lie in the N-terminal unstructured region of the proteins.

According to the Human Protein Atlas, HECW1 is more selectively expressed, being predominantly expressed in the central nervous system, and weakly expressed in the kidney. Similarly, HECW2 is expressed in the central nervous system, but also in lung, spleen, testis and placenta. The overlapped expression in the brain might suggest a redundant role for the two paralogs, while they probably have a unique function in the other tissues.

2.3.2 HECW1

Nakagawara and coworkers first identified HECW1 in 2004 as a component of Lewy body-like hyaline inclusions, along with the translocon-associated protein-*∂* (TRAP-*∂*), Dishevelled-1 (Dvl-1), and mutant forms of superoxide dismutase-1 (SOD1). Interestingly, HECW1 was shown to ubiquitinate wild type Dvl-1 and mutant SOD1, but not wild-type SOD1 [105]. The authors suggested that mutant SOD1, HECW1, Dvl-1 and TRAP-*∂* form a complex of ubiquitinated protein aggregates that may play a critical role in neuronal cytotoxicity in amyotrophic lateral sclerosis (ALS). Since the sequestration of Dvl-1 by mutant SOD1 is enhanced by the overexpression of HECW1, pharmacological inhibitors of HECW1 could prove an effective ALS therapy. In following studies, the Nakagawara group generated HECW1 transgenic mice expressing human HECW1 [106]. These mice showed motor dysfunctions, degeneration of neuron in the lumbar spinal cord and muscle atrophy, recapitulating ALS-like symptoms. These data, together with the preferential expression of HECW1 in neuronal tissue, suggest the involvement of HECW1 in the pathophysiology of neurodegenerative diseases. In addition, HECW1 is expressed significantly at higher levels in favorable neuroblastomas relative to unfavorable ones [105].

In SH-SY5Y neuroblastoma cells, p53 is induced in association with an increased level of HECW1 upon cisplatin (CDDP)-mediated apoptosis [107]. A luciferase reporter assay showed that HECW1 enhances the transcriptional pro-apoptotic activity of p53 in a catalytically independent manner. Furthermore, the C-terminus of p53 was identified as the binding region for HECW1. The mechanism, by which HECW1-mediated enhancement of p53 remains unclear, although these findings suggest that HECW1 may regulate cell proliferation and differentiation, stress response, and DNA-damage response, and has a pro-apoptotic function in the cells [107]. Moreover, the RING ubiquitin ligase (RNF43), highly expressed in colorectal cancers, interacts with HECW1 and p53, and suppresses the transcriptional activity of the latter in colorectal carcinoma cells [108]. In this case, the association of HECW1 with

RFN43 and p53 attenuates p53-mediated apoptosis [108]. It is, however, unclear whether the interaction between RNF43, HECW1 and p53 contributes to posttranslational modifications of p53 [108].

ErbB4 is the latest identified target of HECW1. ErbB4 is a member of the EGFR family and is important for mammary epithelial cell proliferation and survival [109]. Other two HECT members, WWP1 and AIP4, negatively regulate the ErbB4 protein expression in T47D breast cancer cell line. Knockdown of WWP1, AIP4 and HECW1 additively increase the endogenous ErbB4 protein levels in T47D cells, suggesting a beneficial role of these three E3 ligase in suppressing the ErbB4 expression and function in breast cancer [109].

Finally, HECW1 may have a role in Neurofibromastosis Type I (NF1); a common autosomal dominant inherited disease characterized by the development of both benign and malignant tumors. Interestingly, profiles of malignant samples revealed that recurrent amplification was observed for a 43 kb region in chromosome band 7p14 (4309182 bp to 43132835 bp), which partially contained the HECW1 gene. This region was shown to be amplified in 16 of 24 (67%) patients [110], corroborating its involvement in cancer.

2.3.4 HECW2

Nakagawara and co-workers also identified the HECW2 E3 ligase (also known as NEDL2) in 2003 while they screened for p73 interactors, and found that HECW2 is able to bind the C-terminal PY motifs of p73 and to catalyze its ubiquitination *in vitro*. Interestingly, the ubiquitination of p73 by HECW2 leads to its stabilization, resulting in enhanced p73-dependent transcriptional activation [111]. Thus, it seems that both HECW1 and HECW2 are involved in the stabilization and the enhancement of the transcriptional modulatory functions of p53 family members [111], [105].

HECW2 has been shown to be regulated during cell cycle and is degraded by Anaphase promoting complex (APC)/Cdh1 at mitotic exit [112]. HECW2 depletion prolongs metaphase and its overexpression induces earlier activation of APC/C, leading to chromosome lagging,

which may cause tumorigenesis [112], but its exact role during mitosis is not clear. HECW2 knock out mice helped unveil one of its physiological function *in vivo*: these mice show a low body weight, bowel motility defects and died two weeks after birth [113]. Further experiments revealed that HECW2 plays an essential role in regulating enteric nervous system (ENS) development, and positively regulates enteric neural precursor proliferation through the Glial cell line-derived neurotrophic factor (GDNF)/Akt signaling pathway [113]. Intriguingly, this pathway is essential also for kidney development, and it was shown that HECW2 is essential for proper kidney development as 1/3 of HECW2 knock out mice present unilateral or bilateral kidney hydronephrosis [114].

O'Donnel and colleagues demonstrated that HECW2 is expressed also in the human colon, and investigated its potential involvement in Hirschsprung's disease (HSCR); a heterogeneous genetic disorder characterized by the absence of ganglion cells in the distal intestine due to a failure of neural crest cells migration [115]. Decreased expression of HECW2 in the aganglionic colon suggests that this E3 ligase may play a role in the pathophysiology of HSCR and further studies are needed to clarify the exact function of HECW2 during enteric neurogenesis [115].

Recently, a novel substrate of HECW2 was identified, AMOTL1, and a novel role for this E3 ligases as potential angiogenesis regulator [116]. AMOTL1 is a member of the angiomotin family, fundamental regulators in the control of endothelial cell (EC) junction stability and permeability. HECW2 binds AMOTL1 and enhances its stability via lysine 63-linked ubiquitination. Indeed, HECW2 depletion in human ECs decreases AMOTL1 stability, loosening cell-to-cell junctions and altering subcellular localization of yes-associated protein (YAP) from the cytoplasm into the nucleus [116].

2.4 Model organism to study the NEDD4 family

Drosophila melanogaster model organism

Drosophila melanogaster is a versatile model organism that has been productively used to shed light on a broad range of biological processes, including genetic inheritance, embryonic development, learning, behavior, and aging [117]. Despite notable differences between human and fruit flies, it is now well established that most of the fundamental biological mechanisms and signaling pathways are conserved between the two. Striking features that make *Drosophila* an attractive model system are that it requires an easy handling and maintenance; it has a rapid life cycle (10-12 days); it produces a large number of offsprings (up to 100 eggs per day). Furthermore, each developmental stage (embryo, larva, pupa, and adult) offers advantages in studying different developmental aspect and pathways: the embryo is generally used to study fundamental processes of development, like pattern formation, cell fate determination, organogenesis, and neuronal development. The larva is used as well in developmental studies and to investigate some simple behaviors, such as foraging. The adult fly is a good system to study a wide range of pathways, having structures that perform the equivalent functions of the mammalian heart, lung, kidney, gut, and reproductive systems [118](**Fig. 5**). *Drosophila* possesses a compact genome (122 million bases versus 3.3 billion bases in humans) organized in 4 diploid chromosomes (versus 23 in humans), and it was the first major metazoan to have its genome sequenced [119]. In over a century of research, scientists have created a huge repertoire of genetic tools that is still in expansion.

Drosophila provides an ideal model system for studies aimed at the characterization of genes implicated in human disease; it was estimated that about 75% of the genes implicated in human diseases have functional orthologs in flies [120]. Often, similar genes of the same family in humans have a single ortholog in *Drosophila,* avoiding redundancy and allowing to reduce the complexity of the studies.

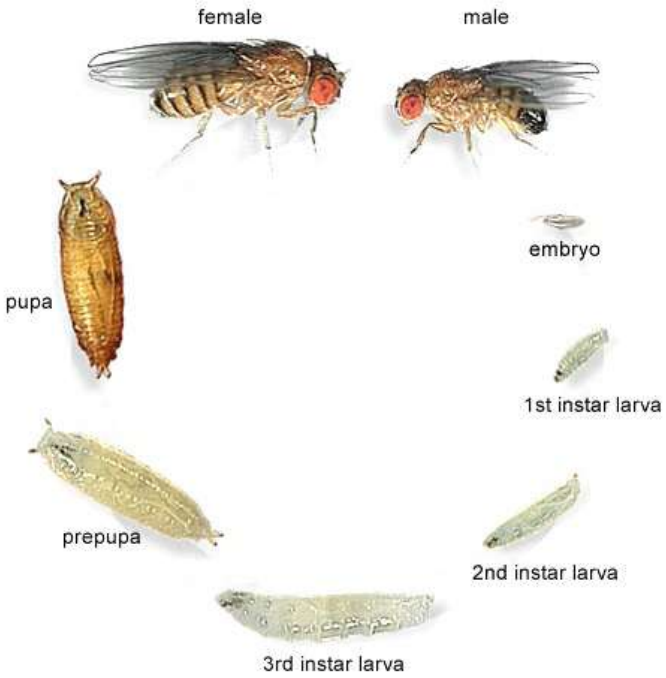

Figure 5. Drosophila melanogaster life cycle.

Drosophila life cycle include four stages: embryo, larva (whose development is further divided in 1st, 2nd, and 3rd instar larva), pupa, and adult flies. [Adapted from FlyMove].

For example, the human disease genes FMR1, FXR1 and FXR2, have a single orthologous in flies, called dFmr1. Several fly disease models proved relevant to human disease, especially in the field of neurodegeneration [121]. Overexpression of human pathological proteins in flies has allowed the establishment of numerous disease models like Alzheimer and related tauopathy [122], Parkinson disease [123] and polyglutamine disease [124]. Furthermore, *Drosophila* has been helpful in studying neuropathology caused by non-coding trinucleotide repeats expansions, like Fragile X syndrome [125], in which the pathology is caused by silencing of the FMR genes. In the last decade, the diversity of *Drosophila* models has greatly increased to include models for diabetes [126], obesity [127], cardiomyopathy [128], neurodevelopmental disorder like autism [129], and cancer [130]. Overall, these model systems have been helpful in the discovery of new genes involved in pathogenesis, as well as for the testing of potential therapeutic compounds [118].

Drosophila melanogaster Nedd4 family

Drosophila has been instrumental also for unravelling the function of the NEDD4 family of E3 ligases. In flies, three members of the dNedd4 family have been characterized so far: dNedd4, Suppressor of deltex (Su(dx)) and dSmurf, which regulate trafficking of transmembrane receptors. In particular, both dNedd4 and Su(dx) act as negative modulator of Notch signaling, regulating the routing of the Notch receptor towards endosomal degradation [131], [132] . In particular, Su(dx) was shown to bind the Notch intracellular domain (NICD) and to promote its transport to endosomes by a clathrin-independent endocytic route [133]. Baron and co-workers also demonstrated that Su(dx) binds polychaetoid (Pyd), the unique *Drosophila* ZO homologue, in part through a non-canonical WW-binding motif [134]. Pyd has different effects on Notch signaling in different model systems: it positively regulates Notch signaling during sensory organ precursor (SOP) development, but it also acts negatively on Notch to restrict the ovary germline stem cell niche. Genetic assays show that Pyd and Su(dx) act antagonistically in these organs, impacting Notch activity [134]. It was suggested that Su(dx) participates to the temperature compensation mechanism in the Notch signaling pathway, to ensure the maintenance of stable developmental Notch signaling in different environmental conditions [133]. Su(dx) prevents excessive Notch signaling at high temperatures, diverting the receptor into the Glycophosphatidylinositol-positive endocytic route and promoting its entry into the multivescicular body. At lower temperatures, instead, Su(dx) increases the basal activity of Notch signaling and Notch is then retained on the endosomal limiting membrane where it is available for activation [133].

In addition to the regulation of Notch [135], [132], dNedd4 is also involved in axon guidance and neuromuscular synaptogenesis by promoting the endocytosis of Commissureless from the muscle surface, a pre-requisite step for muscle innervation [136], [137]. Interestingly, only the short isoform of dNedd4 (dNedd4S) has a positive role in neuromuscular synaptogenesis, while the long form (dNedd4Lo) has an opposite effect [138].

Even if the precise mechanism has not been elucidated, proper synaptogenesis is granted by a different temporal regulation of the two splicing isoforms [138].

dSmurf has a key role in the regulation of decapentaplegic (Dpp, the fly TGF-beta ortholog) signaling during development; it restricts Dpp activity by targeting phosphorylated MAD (Smad1/5 ortholog) to degradation [139]. Spatial and temporal restriction of Dpp signaling is crucial during *Drosophila* embryogenesis for the formation of dorsoventral patterning in the developing embryo [139] and in wing imaginal disc for proper wing development [140]. Recently, dSmurf has been implicated also in the control of the Hippo pathway by modulating the turnover of Warts (Wts) kinase [141].

Overall, *Drosophila* Nedd4 family members have a role in the regulation of multiple cargoes in the cells, and target them mainly to degradative endocytic pathways.

3. mRNA localization and local translation

Over the past 30 years, it has been recognized that not all mRNAs are programmed for immediate translation, but some mRNAs undergo delayed translation, allowing transcripts to be transported or stored until developmental or environmental cues call for their translation. Coupling gene expression with its site of function within the cell is a conserved process through evolution [142]. Local mRNA translation was initially believed to occur only in eukaryotes, but recent studies proved that also in prokaryotes gene transcription and translation can be compartmentalized, emphasizing its relevance in all the domains of life. Super resolution microscopy showed that in *Escherichia Coli* (*E.coli),* mRNA encoding inner-membrane proteins are enriched at the membrane [143], [144]. This process is fundamental both in germ cells and in somatic cells, in particular in polarized cells, to establish functionally distinct compartments and structures. During development, localized maternal mRNA guides the formation of body axes, as shown both in *Drosophila* and *Xenopus* oocytes [145], [146]. In neurons, axonal growth cones require local synthesis of cytoskeleton regulators [147]. In mature neurons, translational control of localized mRNAs allows protein expression in specific

subdomains and confers the ability to rapidly trigger protein synthesis at distant synaptic surfaces; this process is fundamental for plasticity and may participate in long-lasting changes in synaptic strength [148]. Cytoskeleton remodeling is also necessary for directional movement, and is the results of local translation of beta-actin mRNA at the leading edge of fibroblast [149] (**Fig. 6**).

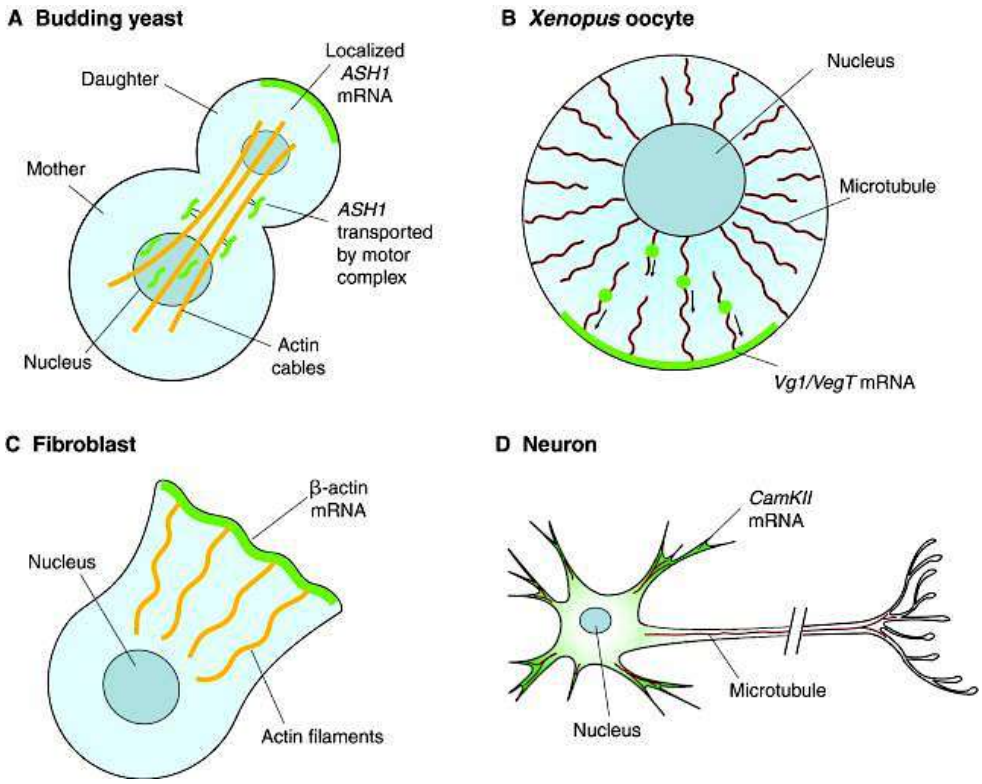

Figure 6. The fundamental role of localized mRNA translation.

*Key examples of localized mRNAs (green). (**A**) In budding yeast, ASH1 mRNA is localized and translated in the daughter cell, repressing mating type switching. (**B**) In Xenopus embyo, germ layer specification relies on the asymmetrically distributed Vg1 and VegT mRNA at the vegetal pole of the oocyte. (**C**) Beta-actin mRNA is specifically localized at the leading edge of migrating fibroblast, providing local concentration of actin monomers for the assembly of actin filaments necessary for migration. (**D**) In mature neurons, dendritic localization of calcium/calmodulin-dependent protein kinase IIα (CaMKIIα) mRNA facilitate a rapid response to synaptic activity, contributing to learning and memory-related synaptic plasticity [Becalska A. N, and Gavis E.R., Development, 2009].*

Restricting protein synthesis in space and time has several functional benefits for the cells. First of all, the transport of a single or a few mRNA molecules is energetically advantageous in comparison to trafficking of bulk proteins. Then, the mRNA that can undergo multiple rounds of translation generates a large amount of proteins where it is required. Having a pool of mRNA ready to be translated in a functionally relevant location confers also an advantage in time, allowing a faster response to external stimuli, which is particularly important in the context of cell migration and neuronal plasticity [148]. Local mRNA and protein concentration not only help to gather them where they are needed the most, but also prevent proteins from being wasted or localized in areas where their function could be deleterious [150]. For example, the mRNA of myelin basic protein is restricted to the distal processes of oligodendrocytes where membrane compaction and myelin formation occurs. The distribution of this gluey protein would be deleterious elsewhere in the cells, causing aberrant membranes aggregation and impairing cellular functions [151], [152].

3.1 RNA granules

Locally transcribed mRNAs are assembled and transported in large ribonucleoprotein particles (RNPs), which have been referred to as RNA granules [152]. They generally contain several ribosomal subunits, translation factors, decay enzymes, helicases, scaffold and RNA binding proteins. In the last decade, different sub-cellular structures correlated with post-transcriptional regulation have been described, in particular processing bodies (P-bodies) [153] and Stress Granules (SG) [154]. These structures differ in terms of composition and function: PB contains components of both non-sense mediated decay pathway and RNA-induced silencing complex, being a main site of irreversible mRNA silencing, and do not contain any ribosome. SGs, instead, contain temporally stalled mRNA of housekeeping genes, whose translation is stopped in response to environmental stress, such as heat, oxidative stress, UV irradiation, and hypoxia [155]. Being the consequence of abortive translation, SG contain specifically stalled 48S pre-initiation complex, translation initiation factors, together

with several other mRNA binding and scaffold protein. Despite the differences, several evidences suggest that these granules can interact physically and functional. Anderson and Kedersha proposed a model where SGs act as site of mRNA triage, where messengers can be sorted either for temporal storage, re-initiation, or degradation [155]. Certain transcripts targeted for decay will be delivered to associated PBs for degradation [156]. These structures are related to other kinds of cytoplasmic granules, like neuronal RNA granules [157] and germ granules [158], which play important roles in the localization and the control of mRNAs specifically in neurons, oocyte and embryos, harbouring highly specific mRNA cargos, whereas SGs and P-bodies seems to be less discriminating [155]. Neuronal granules carry, together with mRNA, translation initiation factors, RBPs and both small and large ribosomal subunits [159]. Despite the presence of intact ribosomes, mRNA is transcriptionally silent until its final destination at the dendritic synapses is reached [160].

Germ granules will be described in details in the following paragraphs, taking *Drosophila* as reference model system.

3.1.1 mRNA regulation in ribonucleoparticles

To achieve a temporal and spatial control of mRNA translation, the messenger RNA must be sequestered from the translational machinery until it reaches the proper subcellular localization. To this end, mRNAs are packed in ribonucleoprotein (RNP) complexes that regulate their stability, trafficking and translation.

A growing body of evidence shows that RNP assembly begins co-transcriptionally in the nucleus, followed by substantial remodeling in the cytoplasm [161]. A key feature for the proper RNP assembly are cis-regulatory elements or the zip-code, generally localized in the 3' untranslated region (UTR) of the mRNA where obstacles to the translation are unlikely to be found and secondary structures like loops and hairpins are generally formed [162]. They are specifically recognized by trans-actin RNA-binding proteins (RBPs), building up the ribonucleoparticle. Furthermore, nuclear maturation events have a key role in the regulation of

transcript cytoplasmic fate, as is the case for the *Drosophila oskar* mRNA, for which pre-mRNA splicing of the first exon and EJC deposition are required for the formation of the Spliced Oskar Localization Element (SOLE), necessary for proper cytoplasmic localization in the oocyte [163]. [164].

Messenger RNA are generally translationally silenced during transport and their repressed state is controlled by RBPs, together with other factors present in in the RNP, such as small non-coding RNA [165].

Protein synthesis is a multistep process and its main phases are initiation, elongation and termination. In order to prevent messenger RNA translation during transport, different repressors can act at different levels of the process, and most of the repressors inhibit the initiation phase [142]. During initiation, the eukaryotic translation initiation factor complex eIF4F (composed of the cap-binding factor eIF4E, the RNA helicase eIF4A and the scaffold protein eIF4G) binds the methylated guanosine cap at the mRNA 5' end. Thereafter, the messenger RNA is circularized through the interaction between eIF4G and the 3'polyadeninde tail binding protein (PAPB), facilitating the recruitment of 40S ribosomal subunit and the pre-initiation complex. Translation repressors commonly bind the cap-binding protein eIF4E, inhibiting the interaction between eIF4E and eIF4G. This type of repressors, called eIF4E-BP (binding protein), block the formation of the initiation complex [142]. An example of eIF4E-BP is the protein CYFIP1/Sra1, which contributes to the translational repressor activity of the Fragile X Mental Retardation Protein (FMRP) in neurons [166]. The other initiation factors can also be targeted by repressors: in yeast, Khd1 blocks initiation by interacting with eIF4G to represses translation of the ASH1 mRNA [167]. Lin et al. identified the helicase eIF4A as a target of the mammalian non-coding RNA BC1 in dendrites [168]. An additional mechanism to inhibit translation initiation involves the block of 60S subunit recruitment, as is the case of the repressor ZBP1, which prevent assembly of a competent ribosome on beta-actin mRNAs [169].

A second, efficient mechanism to control translation relies on the modulation of the mRNA poly-A tail. Indeed, long poly-A tails promote recruitment of PABP and initiation of translation, some RNPs take advantage of this mechanism and act as repressors by recruiting the deadenylation complex that reduces poly-A length. In *Drosophila* embryos, Smaug binds the 3'-UTR of *nanos* mRNA and recruits the CCR4-NOT deadenylation complex, leading to rapid poly-A shortening and subsequent decay of the un-localized messenger RNA[170]. Interestingly, it was shown that the messenger RNA can be silenced also by oligomerization into dense particles, which is inaccessible to ribosomes, as demonstrated for *oskar* mRNA [171].

Strikingly, the mechanisms just described are not mutually exclusive. In fact, to ensure a precise control of translation, localization of mRNA is controlled by several repressors that act redundantly at multiple levels of translation.

3.1.2 RNP cytoplasmic transport and de-repression following localization

Up to now, three main modes of transcript localization have been described: direct mRNA transport along the cytoskeleton, random diffusion followed by local entrapment, and general transcript degradation coupled with local protection at the target site [172], [173]. Among these modes, the most prominent localization mechanism is the transport on a cytoskeletal 'highway' [174], [175], [150]. RBPs, together with adaptors, aid the recruitment of motor proteins, acting as a bridge between mRNAs and the cytoskeleton. The type of recruited motor protein and the transport kinetic are both dictated by cis-regulatory regions within the mRNA itself [176, 177]. Once the mRNA reaches its final destination, it has to be stably anchored. This step is controlled in several systems by the actin cytoskeleton, but also motor proteins seem to be involved [178]. Translational de-repression can then be achieved by different mechanisms, either immediately after localization at the final destination, or later, in response to specific stimuli [142].

Translational de-repression in response to spatial cues is mainly caused by decreasing repressor affinity for target mRNAs. Changes in affinity can be induced by competitive binding with locally expressed proteins, as in the case of the *Drosophila* Oskar. *Oskar* mRNA is translated into protein at the posterior pole of the oocyte where it binds the *nanos* repressor Smaug, reducing its translational inhibition and allowing translation in a spatially restricted fashion [170]. Another mechanism to reduce repressor affinity is achieved by local phosphorylation, as demonstrated both *in vitro* and *in vivo* for the beta-actin mRNA binding protein ZBP1, whose repression is inactivated by Src kinase [169].

In specific cell types, like neurons and germ cells, localized mRNAs are kept in a quiescent state until specific cues induce their translation. In dendrites, the stimulus is synaptic signaling, while in developing axonal growth cone is guidance signals [159]. Upon stimulus, both the general components of the translational machinery and the RBP are regulated to activate translation, in some case by phosphorylation as for CPEB (cytoplasmic polyadenylation element binding protein), that upon phosphorylation promotes poly-A tail elongation. In vertebrates, the kinases responsible for CPEB phosphorylation belong to the Aurora-kinase family (es., Eg2) [179]. The stimuli that induce its activation could be different, like metabotropic glutamate receptor (mGluR) stimulation in neurons [180] or exposition to progesterone, as occurs in *Xenopus* oocyte [181].

Another well characterized example of regulation by phosphorylation is the repressor Fmrp: differently from CPEB, in its phosphorylated state Fmrp is found associated with stalled ribosomes [182], causing repression of mRNA translation. In contrast, upon neuronal stimulation by mGluR, Fmrp is dephosphorylated by the protein phosphatase 2A (PP2A), ultimately leading to de-repression [183].

3.2 Studying RNA localization in *Drosophila* ovaries

Drosophila melanogaster has been a fundamental system in the characterization of mRNA localization and local translation [184]. In the developing embryo, axial polarity is determined by asymmetric distribution of four key maternal mRNAs: *gurken* (grk), *bicoid* (bcd), *oskar* (osk) and *nanos* (nos).

3.2.1 Drosophila ovaries

Axial polarity is set up during oogenesis [145]. The *Drosophila* ovary is constituted by 14 to 20 ovarioles, each of which is composed by a succession of developing egg chambers where oocyte maturation takes place. Each egg chamber is made up of 16 interconnected germline cells, constituting the cyst, surrounded by a somatic follicular epithelium. Every cyst arises from asymmetric division of a germline stem cell (GSC), 2-3 of which are localized at the anterior tip of the ovariole in an organ called germarium [185] (**Fig. 7**).

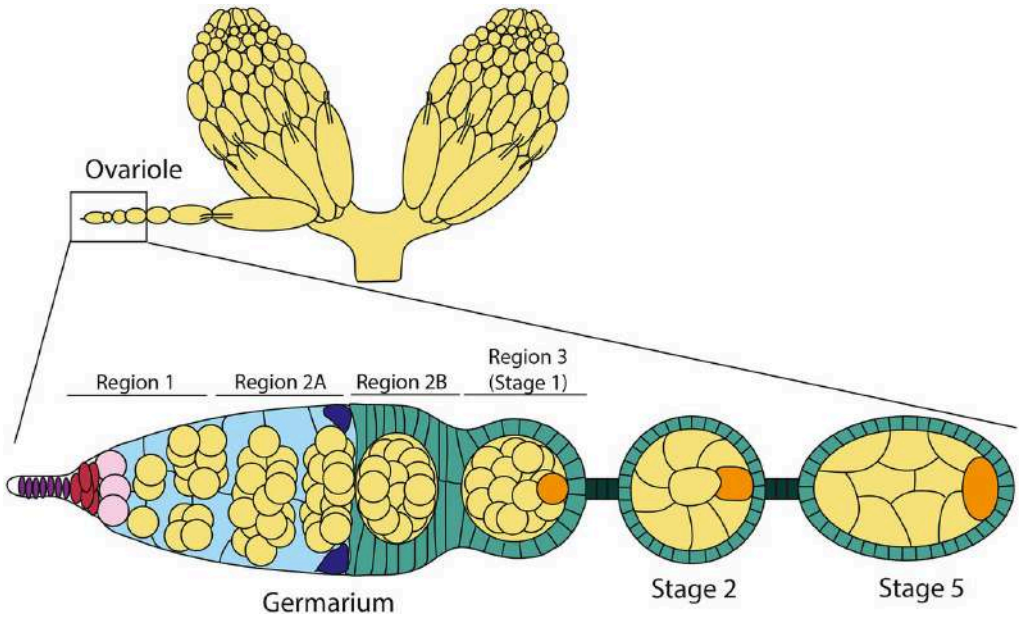

Figure 7. The Drosophila ovary and oogenesis.

The ovary is composed of 14–20 ovarioles. At the anterior end of each ovariole there is a structure known as 'germarium', which provides the germline cells and somatic follicle cells that compose the subsequent egg chambers. Germline stem cells (light pink), and germline cysts (yellow), follicle stem cells (dark blue), follicle cells (green), and oocyte (orange) [adapted from Silva, Genetics, 2015].

The GSC self-renovate and produces a cystoblast that undergoes 4 rounds of synchronous division with incomplete cytokinesis. The cells in the resulting syncytium are interconnected by actin-rich cytoplasmic bridges called ring canals [185]. One of the two oldest germ cells, possessing 4 ring canals, will differentiate into an oocyte. The oocyte's nucleus becomes transcriptionally quiescent committed to meiosis, forming stable synaptonemal complexes and arresting at meiotic prophase I in region 2b of the germarium [185]. The nucleus remains in prophase I for most of the oogenesis; during the late stage of oogenesis the oocyte progresses to metaphase I and is further arrested until ovulation [186].

Cyst divisions are supported by the formation of the fusome, a vesicle-rich and highly branched structure connecting all 16 germ cells. The fusome originates as a spectrosome in the GSC and imposes synchronicity and correct geometry to cyst division [187] (**Fig. 8**).

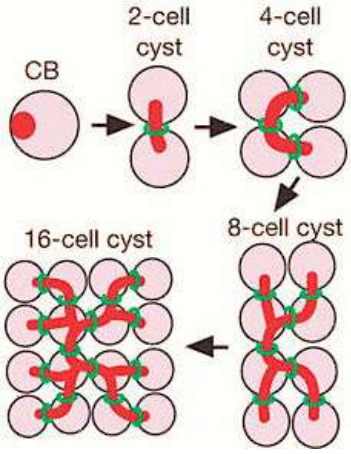

Figure 8. Fusome and cyst division.

Representation of cyst mitotic division, starting from the cystoblast (CB). Fusome is indicated in red, ring canals in green [adapted from Kei and Spradling, Nature, 2004].

The fusome might be a critical element for oocyte specification: in fact, it was suggested that, among the two oldest cystocytes, the one that retains more fusome material will differentiate into an oocyte [188]. Furthermore, the fusome acts as a platform for recruitment of factors that are important for cell division. Among these factors there are dynein, which aids spindle formation and orientation during mitosis, bam (bag of marbles), which promotes oocyte differentiation [188], and CycA, which is crucial to count and synchronize rounds of

division. Indeed, overexpression of CycA leads to 5 rounds of mitosis but only in the presence of an intact fusome [189].

Concomitant with oocyte specification, the remaining 15 germline cells specialize as nurse cell undergo several rounds of endoreplication to become polyploid. As suggested by their name, nurse cells provide a supporting role for the oocyte that is largely transcriptionally quiescent by producing maternal mRNAs and cytoplasmic components that are delivered to the oocytes via the ring canals [184], [145]. At the later stages of oogenesis, the nurse cells extrude their content into the oocyte and their cytoplasm is mixed through a vigorous ooplasmic streaming. The nurse cells are then eliminated by apoptosis, while the follicle cells migrate to surround the oocyte and secrete both the vitelline membrane and the chorion to protect the mature egg [145].

3.2.1 RNA localization in *Drosophila* oocyte

The oocyte matures within the egg chamber thought 14 morphologically distinct stages. During early (stage 2-6) and mid-oogenesis (stage 7-10), transport of cargoes from nurse cells to the oocyte is continuous and mainly selective on the 'microtubule (MT) highway'. This structure is highly dynamic and undergoes major rearrangements during oogenesis [190]: MTs nucleate from a microtubule organizing center (MTOC) at the posterior pole of the oocyte (minus end) and extend anteriorly into the nurse cells (plus end). In early and mid-oogenesis, mRNA localization has two key roles: first, the establishment of the anterior-posterior (A/P) and dorso-ventral (D/V) axes, both initiated by two temporally and spatially different round of *gurken* (*grk*) mRNA translation [191]. Second, local translation of the *oskar* (*osk*) mRNA specifies the posterior of the future embryo and is responsible for the establishment of the future germline [192].

In early oogenesis, *grk* mRNA is transported to the MT minus end by Dynein, and it is locally translated at the posterior pole of the egg chamber. The protein product of *grk* mRNA is a TGF-alpha ligand homolog with epidermal grow factor (EGF) repeats, and is recognized by

Torpedo, a *Drosophila* homolog of EGF receptors on the apical surface of the follicle cells, inducing them to adopt a posterior fate [193]. The follicle cells signal back to the oocyte, causing a first rearrangement of the MT cytoskeleton, which reverts its polarity and re-localizes the minus ends and of the nucleus to the anterior margin of the oocyte [194]. During mid-oogenesis, *grk* mRNA is bound by Egl and the dynein adaptor BicD is transported to the anterior-dorsal corner of the oocyte. Here, a second round of translation and signaling to the adjacent follicle cells determines their dorsal fate, thus defining the dorso-ventral axis [195].

During mid-oogenesis, *osk* mRNA is localized and anchored to the posterior pole where it sets up the future pole plasm, a specialized cytoplasm that contains factors, such as Nanos, required for germ cell and abdomen formation [192]. *osk* localization has been extensively characterized: several mRNA binding proteins, like Staufen, are essential for its correct localization, while actin and the actin-binding proteins Cappucino, Myosin V, Spire and Lasp are required for proper anchoring of *osk* mRNA [196].

During late oogenesis (stage 10-14), the MT cytoskeleton undergoes a second major re-arrangement and MTs are reorganized in bundles at the cortex following nurse cell cytoplasm dumping and ooplasmic streaming [197], which helps to mix the ooplasm and prevents further mRNAs transport to the posterior pole. At this stage (**Fig. 9**), the *nos* mRNA is localized and translated at the posterior pole, while *bcd* mRNA is transported inside the translationally repressed RNP and is positioned at the anterior margin of the oocyte, where it remains silent until after fertilization. Following fertilization and egg deposition, opposite protein gradient of Bicoid and Nanos define and set up the embryonic A/P axis [184].

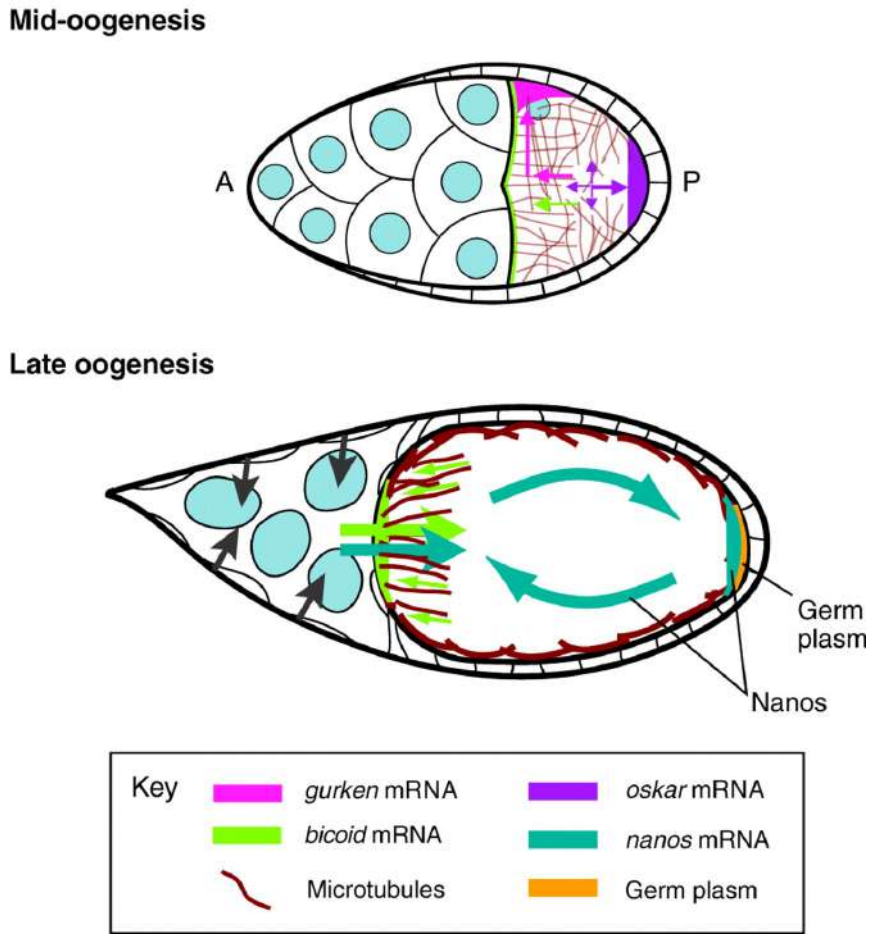

Figure 9. Locally translated mRNAs in oogenesis.

Representation of mRNA and protein distribution in mid- and late stage egg chambers. Gurken (pink), oskar (violet) and bicoid (green) mRNA are transported along microtubules (brown) in mid-oogenesis and localized as indicated in the upper panel. Colored arrows indicate the direction of the movement. In the lower panel (late stage egg chambers), nurse cells contraction is indicated by the gray arrows. Large green and dark green arrows indicate entry of bicoid and nanos mRNA in the oocyte. Curved dark green arrows represent diffusion of nanos facilitated by ooplasmic streaming. Small green arrows indicate bicoid transport on anterior microtubules [Adapted from Becalska and Gavis, Development, 2009].

3.2.2 mRNA regulation in the germline

During the RNPs transport through the nurse cells and oocyte, maternal mRNAs are maintained in a translationally silent state. In particular, *osk* translational control has been extensively characterized. *osk* translational inhibition occurs at multiple levels, thanks to several repressors, among which the RBP Bruno binds the Bruno response element (BRE) in *osk* 3'UTR, inducing its oligomerization [198], [199] and inhibiting recruitment of the small

ribosomal subunits to the 5' cap [171]. Furthermore, the Bruno-*osk* interaction recruits the 4E-BP protein Cup that blocks the association of eIF4E with eIF4G and eIF4A, and the formation of the translation initiation complex. Cup also works through the repression of the oo18 RNA binding protein (Orb), the *Drosophila* homolog of CPEB [200]; [201]. Orb, in its phosphorylated active state, function as a translational activator by promoting cytoplasmic polyadenylation of mRNA containing cytoplasmic polyadenylation element (CPE) in their 3'UTR [179]. *In primis*, Orb is required for the translation of several essential mRNAs, *osk* and *grk* [202], [203]. Davison and colleagues recently proposed a model for spatial regulation of *grk* mRNA local translation, that differs from that of *osk* mRNA local translation, which is mainly regulated by the binding of the translational repressors previously cited. Immunofluorescence analysis and electron microscopy show that RNPs contain significantly less Orb in nurse cells than in the oocyte: therefore, *grk* transcript is probably kept silent in nurse cells by the limiting amounts of Orb [203]. In the oocyte, the *grk* mRNA is anchored at the edge of the RNP, a ribosome enriched area [204], and associates with Orb to be locally transcribed [203]. Orb is highly expressed in the oocyte thanks to a feedback loop mechanism by which Orb protein promotes translation of its own mRNA [205]. This loop is controlled by the negative action of the mRNA binding proteins Cup, Ypsilon Schachtel (YPS) and the fragile X mental retardation protein (dFMRP) [201], [206], [207].

3.2.3 dFmrp contributes to mRNA regulation in the ovaries

Costa and colleagues demonstrated that dFmrp associates with Orb in a RNAse resistant complex, and show that dFmrp acts as a negative regulator of Orb autoregulatory circuit [206]: *dfmr1* loss of function flies present, indeed, an accumulation of Orb. The authors also show that dFmrp is required for proper cyst formation and oocyte specification, although the underlying molecular mechanism needs to be further investigated. It would be interesting to verify whether the connection between Orb and dFmr1 in fly ovaries is relevant for the neurological phenotypes of the Fragile X syndrome in humans and in mice.

3.2.4 Ubiquitination in RNPs regulation.

Dynamic changes in the composition of protein-mRNA complex are critical for mRNA regulation. Despite significant progress made in identifying RNP components and dynamics, the precise regulation of RNP assembly, disassembly and transport is not completely understood. A growing body of evidence indicates that post-translational modifications (PTM) might have a crucial role in this process. As previously mentioned, phosphorylation is a key factor in the regulation of translational repressor/activator activity [179], [182], [183].

Similarly, ubiquitination is assuming a crucial role in mRNA regulation. In yeast, it was found to be important for the export of translation-competent RNPs: the HECT E3 ligase Tom1 ubiquitinates the adaptor factor Yra1 (Aly/REF in mammalian), causing its dissociation from nuclear mRNPs and allowing efficient mRNA export [208]. In mice, ubiquitination can impact directly on translational repressor/activator regulation [209], [210]. Indeed, mGluR stimulation at the synapses triggers FMRP ubiquitination by APC/Chd1 and its subsequent degradation [211].

Interestingly, NEDD4 was recently found to control the turnover of mRNP components in mice testis, by ubiquitinating and destabilizing NANOS2, thereby allowing differentiation of spermatogonial progenitor cells (SPC) [212]. This regulatory mechanism in important in physiological conditions, in which it controls the size of the SPC pool, as well as in stress condition, in which it is required for clearance of stress granules [212].

4. Autophagy

Autophagy is a lysosome-mediated catabolic process that plays key roles in ensuring cellular homeostasis under physiological conditions, for instance by turning over aggregated macromolecules and damaged organelles [213]. During autophagy, cargoes are sequestered from the cytosol by formation the autophagosome, which delivers them to the lysosome for degradation and recycling. The autophagy pathway is dramatically activated in response to many types of stress: a) metabolic stress, such as nutrient deprivation, to generate basic

elements to sustain new synthesis and energy production; b) damaging stress, to remove injured organelles and macromolecules; c) therapeutic stress (drug treatment), d) morphogenetic changes occurring during development and differentiation, to remove disused cellular structures; e) pathogenic infection, to eliminate invasive microbes and to generate degradation products required for the activation of innate immune system and antigen presentation.

4.1 The autophagic pathway

The pathways that regulate autophagy are evolutionarily conserved among eukaryotes [214]. Under normal nutritional conditions, the protein kinase Target of Rapamycin (TOR) phosphorylates ULK1, which blocks the ULK1-ATG13-FIP200 pre-initiation complex and prevents its interaction with AMPK. During starvation, AMPK phosphorylates ULK1, favouring its release from TORC1 and its association to the site of isolation membrane formation. This induce the recruitment of the components of the ubiquitin-like conjugation systems responsible for the generation of LC3-II, an essential proteolipid molecules required for autophagosome biogenesis [215], [216]. The parent molecule, LC3-I, is generated by the proteolytic cleavage of ATG4, which cleaves LC3 to produce LC3-I, which is bound by the E1 activating enzyme, ATG7, and transferred to the E2 conjugating enzyme, ATG3. The E3 ligase is a complex composed of ATG12-5-16; the latter is produced by another reaction that requires the E1- Atg7 and the E2-like conjugating enzyme Atg10. Cytosolic LC3-I is then modified by the attachment of phosphatidyl-ethanolamine (PE), and anchored to the isolation membrane, forming LC3-II and contributing to the elongation of the autophagic membrane. LC3-II is widely used as a marker of autophagosomes, since it is the only autophagic protein that stably associates with the mature autophagosome, and remains associated with them until it is trafficked to the lysosome [217]. When the outer membrane of the autophagosome fuses with the lysosome, Atg4 releases LC3-II from PE and the autolysosome is formed. In this

compartment, the inner membrane of the autophagosome and its contents are degraded by lysosomal hydrolases, and nutrients are released into the cytosol for recycling (**Fig. 10**).

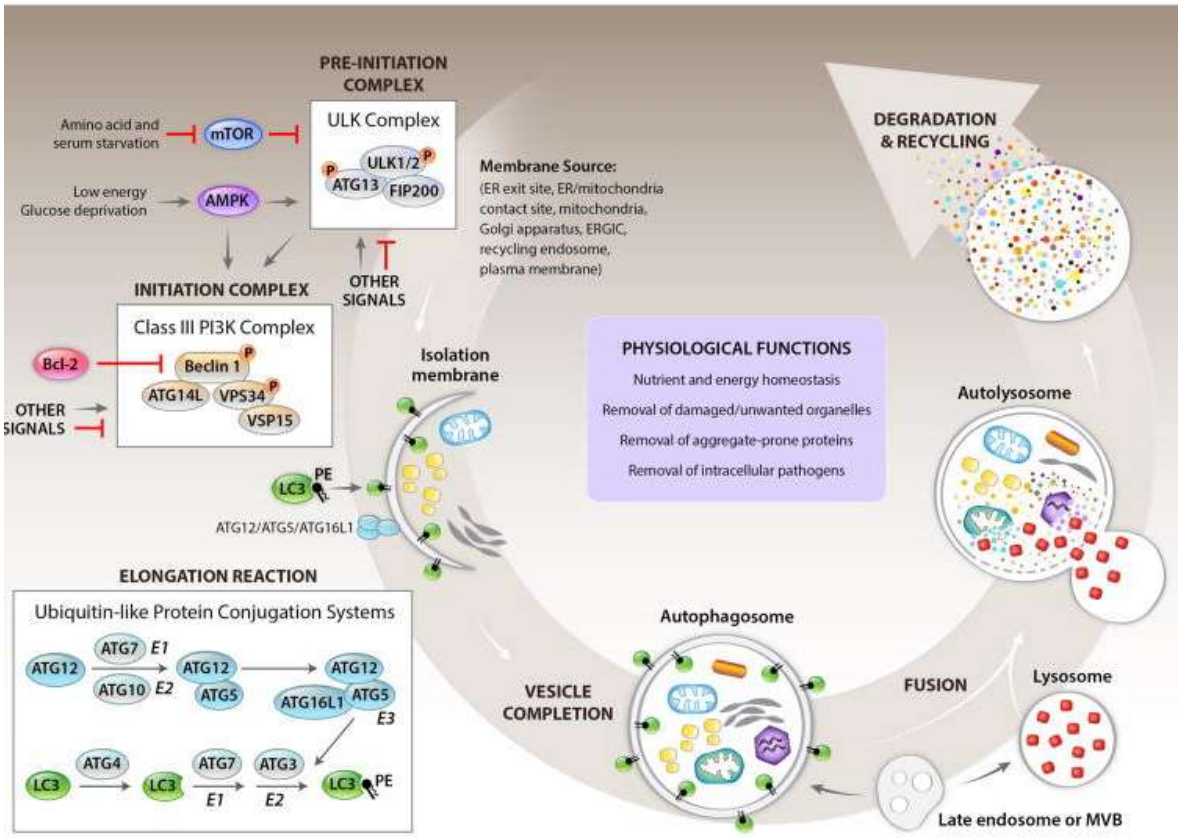

Figure 10. Autophagic pathway.

Autophagic pathway description from Green D.R., et al., Cell, 2014.

4.2 Ubiquitin in Autophagy

Ubiquitin is critical in the regulation of the autophagy pathway [218], [219]. Ubiquitination regulates the autophagy response at least at three different levels: i) ubiquitin selectively labels autophagy targets, such as damaged mitochondria or protein aggregates, which are then bound by a family of sequestome-like protein receptors, like p62. These proteins act as a bridge between ubiquitin and the autophagosome protein LC3, allowing cargo engulfment by the forming the autophagosome [218], [219]; ii) upon nutrient starvation or Toll-like receptors activation, the main upstream autophagy regulators ULK1 and Beclin1 are labeled with non-degradative ubiquitin chains that favor protein complex assembly and activation; iii) the

stability of pro-autophagy factors, such as Ambra1, Pink1 and Deptor is negatively regulated by ubiquitin and proteasomal degradation [220], [221].

Some ubiquitin E3s have been shown to be clearly involved in autophagy [220]; the best-studied example is represented by Parkin, which orchestrates a cycle of ubiquitination events occurring at the membrane of the damaged mitochondria that ultimately results in the degradation of the organelles [218]. Most of the ubiquitin ligases identified act on upstream regulators rather than on the autophagy machinery components. However, it remains to be determined whether specific ubiquitin ligases dedicated to control of the core autophagy pathway may exist.

4.2.1 The NEDD4 family and Autophagy

Recently, some evidence suggested the involvement of a few members of the NEDD4 family in autophagy, however, a systematic analysis has not been pursued. A regulatory connection between NEDD4 and BECLIN 1 was demonstrated; NEDD4 is able to bind and ubiquitinate BECLIN-1 with K11 and K63 Ub-chains to regulate its turnover [63]. NEDD4 involvement in autophagy and its association with the mTOR signaling pathway was also suggested by Li and colleagues [222]. Recent work confirmed the positive regulation of NEDD4 in autophagy, as NEDD4 knock down impaired starvation or rapamycin-induced activation of autophagy and autophagosomal biogenesis [223]. In this work, Nedd4 was found to interact with the autophagy components LC3 and p62: NEDD4 binds LC3, through a conserved WXXL LC3-binding motif in a region between the C2 and the WW2 domains, and ubiquitinates p62 [223]. Interestingly, a genome-wide siRNA screen identified an ubiquitin ligase-independent function for Smurf1 in viral autophagy and mitophagy, which seems to be tissue specific and dependent on the C2 domain, but the molecular mechanism has not been elucidated yet [224].

4.3 RNA and Autophagy

An increasing body of evidence indicates that RNA and ribonucleoprotein complexes can be object of autophagic degradation, providing an additional mechanism for cytoplasmic RNA

catabolism [225]. Pioneering observations in the 1980s established that RNA turnover is significantly increased in starved human fibroblast via the lysosome-dependent pathway [226]. Follow-up experiments showed that lysosome and autophagosome inhibition effectively bocks starvation-induced RNA degradation, reinforcing the evidences of a role for autophagy in RNA degradation [227], [228]. Moreover, recent genome wide screens and large scale proteomic-based approaches identified a considerable number of autophagy regulators with RNA-related functions [229], [230].

4.3.1 Autophagic clearance of RNPs

Multiple evidence attributes a role to autophagy also in the regulation of clearance of ribonucleoprotein complexes, in a process named 'granulophagy' [231], [225]. Autophagy was shown to clearly affect SG clearance both in yeast and mammalian cells, since mutations inhibiting autophagy upstream of autophagosome or vacuolar formation cause SG accumulation. Indeed, *Atg7*$^{-/-}$ MEF cells exhibit a basal level of constitutive SG in standard conditions, and the impairment is even more evident after heat stress in SG resolution [231]. SGs, rather than PB, seem to be preferential targets of autophagy, possibly due to the dynamic nature of the latter [231]. Studies in *Caenorhabditis elegans* (*C. elegans*) suggested that also maternal germ granules are degraded through selective autophagy during embryogenesis, and their interaction with LGG-1 (the worm Atg8 homolog) is mediated through the adaptor protein SEPA-1 (suppressor of ectopic P granule in autophagy) [232], [233]. Whether this mechanism of germ granule clearance described in *C. elegans* is utilized by other organisms still needs to be defined [233].

4.3.2 Pathological implications of altered RNP homeostasis

RNPs are critical for proper regulation of RNA metabolism in a wide range of biological pathways. Thus, altered homeostasis of RNPs of different nature can be detrimental for the cell and has been proposed to occur in several diseases from cancer to neurodegeneration as review in [234].

Persistence of large RNPs like P-bodies, in particular SGs, was shown to be involved in several degenerative diseases, such as amyotrophic lateral sclerosis (ALS), frontotemporal lobar degeneration (FTLD), fragile X-syndrome (FXS) and spinocerebellar ataxia-1, spinal muscular atrophy (SMA) [235], [236], [237], [231]. A common hallmark of ALS, FTLD and other neurodegenerative diseases is the accumulation of cytoplasmic aggregates that contain also SG-related proteins, RBP and RNA [238], [235]. TDP43 is a well characterized example of disease-related RNA binding protein; TDP43 mutations are not only associated with ALS and FTLD, but the protein is also a major constituent of pathological intracellular inclusions observed in diseased neurons [238]. It was proposed that, being an aggregation-prone protein, TDP43 is sequestered from its physiological function and, at the same time, gains a toxic function [238]. mRNA binding proteins possess a natural tendency to aggregate due to the peculiar structure imposed by the necessity of binding RNAs. Unfolding and aggregation of such 'prion-like domains' or 'low complexity domain', has important implications in the pathogenesis of RNP-centered diseases [239]. Indeed, mutations in the prion-like domains have also been associated with the formation of toxic hyperaggregates, as seen in ALS, frontotemporal dementia (FTD), Alzheimer disease (AD), FXS, and Huntington's disease (HD) [240], [241].

At the molecular level, multiple RNA-processing steps were found to be defective in pathological conditions: malfunction in RNA splicing, like in the case of hnRNP proteins, whose altered splicing ability has been correlated not only with ALS and AD [242], but also with cancer [243]. Alterations in RNA stabilization is a key point for the RNA binding protein FUS in FTD [244], while RNP translocation along axons is defective in SMA [245], causing aberration in mRNA local translation. These defects are particularly critical for certain type of cells, like neurons and muscle cells, possibly due to their longevity that allows age-related damage to accumulate and reach pathological levels [246]. Local translation is crucial also during the development of neurons, for the assembly of a functional neural circuits and during oogenesis:

aberration at any point of this pathway can compromise the proper development of the future organism. During development, alteration of proper mRNA local translation in neurons can result in neurodevelopmental disorders, as in the Fragile X syndrome, the most common form if inherited mental retardation and is caused by CGG expansion of over 200 triplets in the 5' UTR *FMR* genes, causing its hypermethylation and silencing. As reviewed by Till [247], the RNA binding protein FMRP has a key role during neural development: by controlling local translation in axon and dendrites, it guides growth cone mobility for the assembly of functional neural circuits [147]. It is not surprising that Fragile X patients present an abnormal connectivity of several cortical regions increased density of dendritic spines and an abundance of spines exhibiting immature morphologies, causing many cognitive and behavioral impairments [247]. *FMR* alleles with an intermediate number (55–200) of CGG repeats are referred to as premutation alleles, and are linked to two other distinct disorders: fragile X–related primary ovarian insufficiency (FXPOI) and fragile X–associated tremor/ataxia syndrome (FXTAS). FXPOI patients present hypergonadotropic hypogonadism and cease menstruating before age 40, and its etiology is still poorly understood [248]. FXTAS is a late-onset neurodegenerative disease, characterized by accumulation of CGG-*dFMR* mRNA in nuclear Ub-positive foci, with low level of protein expressed [249].

So far, therapeutic developments have been limited due to incomplete knowledge of the specific role of RNPs in disease pathogenesis. Although great improvements have been made in the past decade and potential therapeutic targets have been found in order to control defective RNA processing in disease [234], it is fundamental to gain detailed insight into the molecular mechanism and regulation of such complex processes, which are governed by an interconnected network of functionally related proteins.

AIM OF THE THESIS

The aim of this study was to characterize the physiological and potential pathological functions of the NEDD4-E3 ligases HECW1 and HECW2, taking advantage of the genetically tractable *Drosophila* model. To this end, we generated catalytic inactive and knock out mutants of the single fly ortholog dHecw, together with all the tools necessary for the analysis of dHecw expression, localization and function.

MATERIAL AND METHODS

1. Cell culture

Cell culture experiments were performed using the *Drosophila* Schneider-2 (S2, macrophage-like cells derived from late embryos) cell line provided by IFOM Cell Culture Facility. S2 cells were cultured in Schneider's medium (GibCO) supplemented with 1% Glutammine (Euroclone) and 10% of Fetal Bovine Serum (FBS) (Euroclone) at 28°C. Cells were plated to a density of 1.000.000 cells/ml every three days.

1. Gene knock down by RNA interference in S2 cells

2.1 Synthesis of double stranded RNA

To silence the expression of dHecw gene in S2 cell line, were generated dsRNA specifically targeting dHecw transcript, according to the following steps:

1) synthesis of DNA fragments carrying the consensus sequence for T3 and T7 RNA polymerase;
2) in vitro transcription of single stranded RNA molecules;
3) assembling of dsRNA.

1) DNA fragments carrying consensus sequences for T3 and T7 RNA polymerase for dHecw were generated and amplified through PCR (Polymerase Chain Reaction).
The following primers containing consensus sequences for T7 (lower case) and T3 polymerase (lower case) were used:
dHecwKD T7For: 5'-taa tac gac tca cta tag g gagaGGATAATTGCCACGATTGGT-3'
dHecwKD T3Rev: 5'-aat taa ccc tca cta aag g gagaGGCGCCAATCGTTTGTG-3'

S2 cells cDNA was used as DNA template for the PCR reactions.

Reaction mixture:

REAGENTS	FINAL CONCENTRATION	FINAL VOLUME
5X Phusion Buffer	1X	10 µl
dNTP mix, 10 mM	0.2 mM	1 µl
Forward primer 10 µM	0.5 µM	2.5 µl
Reverse primer 10 µM	0.5 µM	2.5 µl
Phusion DNA Polymerase (5U/µl)	1.25 U	0.5 µl
Template DNA	< 250 ng	100 ng
Water		up to 50 µl

The PCR reaction (denaturation, annealing and extension) was repeated for various number of cycles (see table below). PCR reactions were performed with a termocycler (GeneAmp® PCR sytem 9700) using the following program for amplification.

Step	**Temperature**	**Time**	**Cycles**
1	98°C	30 seconds	1
2	98°C 50°C 72°C	10 seconds 30 seconds 30 seconds	3
3	98°C 65°C 72°C	10 seconds 30 seconds 30 seconds	25
4	72°C	5 minutes	1
5	4°C	∞	1

PCR products were analyzed by electrophoresis in a 1,5% agarose gel in Tris-Acetate pH7.8 4 mM, EDTA 1mM (TAE) buffer. The DNA marker Gel Red Dye (1:10.000) (Biotium) was added to the gel. Samples were prepared mixing the entire volume of PCR products with the loading buffer 6X (NEB) and then loaded for 30' minutes at 100 mV. DNA fragments were visualized by an UV transilluminator at 260 nm.

After the electrophoresis DNA fragments were isolated and purified using QIAquick Gel Extraction Kit protocol (QIAGEN). DNA samples were eluted in RNAse free water and their concentrations were measured at the spectrophotometer (NanoDrop ThermoScientific) using a wavelength of 260 nm.

2) In vitro transcriptions were performed in RNAse free conditions.

For each DNA sample two reactions, containing respectively T3 and T7 RNA polimerases, were set up. T3 and T7 polymerases bind to the specific consensus sequences, placed respectively at the 5'-end and 3'-end of the generated amplicons, and synthesize the antisense and sense RNA strands. The reaction mix for each in vitro transcription was performed as follows:

REAGENTS	**T3 (final vol.)**	**T7 (final vol.)**	**Final concentration**
5X Buffer	8 μL	8 μL	1X
rATP, 2,5 mM	4 μL	4 μL	1 mM
rCTP, 2,5 mM	4 μL	4 μL	1 mM
rUTP, 2,5 mM	4 μL	4 μL	1 mM
rGTP, 2,5 mM	4 μL	4 μL	1 mM
DTT, 100 mM	4 μL	4 μL	10 mM
RNAsin Ribonuclease inhibitor, 40U/μL	1 μL	1 μL	20 u
DNA template	400 ng	400 ng	400 ng
Polymerase	2,4 μL	2,4 μL	40 u
RNAse free water	Up to 40 μL	Up to 40 μL	

DNA samples were added to the reaction mix and incubate at 37°C O.N. according to the manufacturer protocol (Promega). RNA concentration was measured at the spectrophotometer using a wavelength of 260 nm. In order to avoid DNA contamination, 1 μg of RNA samples were treated with RNase-free DNase (Promega kit). Samples were incubated at 37°C for 30 minutes. To block the reaction, for each μg of RNA we used for DNAse digestion, 1μL of Stop Solution (Promega) was added and the enzyme was inactivated at 65°C for 10 minutes. Then, RNA samples were subjected to precipitation in 2,5 volumes of cold ethanol 100% and 0,1 volumes of sodium acetate (3 M, pH 5,2) and then were incubated O.N. at -80°C.

Samples were centrifuged for 30' at 13.200 rpm at 4°C, washed in cold ethanol 70% and centrifuged 10' at 13.200 rpm 4°C. In order to avoid any ethanol residues, samples were placed under chemical hood 10' and then eluted in RNase free water. RNA concentration was then measured.

3) To assemble dsRNA, 15 µg of antisense (T3) and sense (T7) synthesized RNA strands were incubated 15 minutes at 68°C and then 30 minutes at 37°C. dsRNA were stored at -80°C or directly used for knockdown experiments.

2.2 dsRNA mediated knocked down in S2 cells

10^6 S2 cells were seeded in a 6 well plate and left adhere for 24 hours. Cells were starved for 30 minutes in Schneider's medium without serum and then dsRNAs were added directly to the medium. After 5 minutes incubation Schneider's medium with 20% FBS was added to cells and they were incubated at 28°C for 48 hours.

2. *Drosophila* S2 Cells immunostaining

For immunostaining S2 cells were plated on coverslips coated with poly ornithine. S2 cells were rinsed two times with PBS 1X and fixed in 3,7% paraformaldehyde (PFA) for 15'. Then, cells were rinsed three times in PBS 1X and permeabilized with PBS 1X - 0,1% Triton (PBS-T) for 20'. In order to minimize aspecific antibodies interactions PBS-T 1% BSA (Blocking solution) was added for 30 minutes and incubated with primary antibody diluted in PBS-T 0,1% BSA (anti-dHecw purified antibody, 1:50) for two hours at room temperature (RT). After three washes in PBS 1X, cells were incubated with secondary antibodies conjugated with fluorophores (anti-rabbit Cy3, 1:400) diluted in PBS 1X for 2 hours at RT. Cells were washed three times in PBS 1X. To label nuclei, DAPI (Sigma-Aldrich) diluted 1:5000 in PBS 1 X was added to the cells for 10' at RT and then washed once in PBS 1X. Coverslips were mounted on slides using Mowiol Mounting Medium (Calbiochem) or glycerol 70%.

3. Fly strains

Flies were maintained on standard yeast/cornmeal/agar media. All experiments were performed at 25°C, unless differently specified.

Overexpression and knock down was obtained using the UAS-Gal4 system

Overexpression was obtained using the following Gal4-driver lines: MS1096-Gal4; UAS-CD8:GFP (larval wing disc pouch, Bloomington), nanosGal4-VP16 (germline, kindly provided by A. Ephrussi), traffic jam-Gal4 (follicle cells, Bloomington). Atg7 mutant ($Atg7^{D77/D14}$) were nicely provided by G. Juhasz. $Atg7^{D77/D14}$ are two null alleles, generated for P-element excision: deletion D77 lacks exon 4, 5, 6 that encode for E1-like domain, while allele D14 present a large deletion that include the transcription and translation start sites and the majority of the Atg7 coding region [Juhasz 2007]. The Fmr1 mutant used was the $fmr1^{\Delta 113M}$/TM6B, that present deletion of the first two coding exons (Bloomington). For knock down experiments, we used the UAS-CG42797 RNAi #104394 (Vienna Drosophila Stock Centre).

4. UAS-RFP dHecw line generation

For overexpression experiments, transgenic fly lines carrying tagged-dHecw wild type were generated by standard techniques using the attP/attB recombination system. The vector contains the attB donor sequence for site-specific integration by the PhiC31 system, the white gene as an eye pigmentation marker, and an ampicillin resistance cassette. *dHecw* gene was amplified from LD10978 vector (DGRC), sequenced and cloned in a pUASattb vector, where was previously cloned an RFP tag, using the Infusion HD cloning system (Contech). This system relies on a proprietary In-Fusion Enzyme, which fuses DNA fragments (e.g., PCR-generated inserts and linearized vectors) by recognizing 15-bp overlaps at their ends. The oligonucleotides used to generate the *dHecw* PCR insert are as follows (vector complementary sequence is indicated in upper case, BglII and XhoI restriction site are lower case, dHecw sequences are highlighted):

Forward: 5'- GTCCGGACTCagatctATGGAGCCACCAGCTGCA-3'

Reverse: 5'- TAGAGGTACCctcgagCTACTCAATGCCGAACGTGTTG-3'

Amplifications were performed with the GeneAmp® PCR system 9700 termocycler using the following cycling conditions:

Step	Temperature	Time	Cycles
1	98°C	30 seconds	1
2	98°C 40-45°C (calculated for each primer pair) 72°C	10 seconds 30 seconds 30 sec/Kb of target lenght	5
3	98°C 50-55°C (calculated for each primer pair) 72°C	10 seconds 30 seconds 30 sec/Kb of target lenght	25
4	72°C	7 minutes	1
5	4°C	∞	1

1 mg of pUASattb-RFP vector was digested for 2 hours at 37°C with 20 units of restriction enzyme (New England Biolabs). Digested vector and PCR products were isolated and purified using QIAquick Gel Extraction Kit protocol (QIAGEN). DNA samples were eluted in RNAse free water and their concentrations were measured at the spectrophotometer (NanoDrop ThermoScientific) using a wavelength of 260 nm.

50 ng of digested vector and 50 ng of PCR insert were ligated with 5 ml of In-Fusion HD Enzyme Premix and incubate the reaction for 15 min at 50°C. 50 µl of competent cells Stellar (InFusion) were transformed with 2,5 ml of ligation reaction. The correct sequence of the generated vector was verified by sequencing with the primers used for PCR amplification, that cover the beginning and the end of the gene.

The transgenic vector was sent to BestGene.inc to perform site-direct injection in ZH86fb embryo. The φC31 integrase mediates recombination between attB and attP sites, resulting in the integration of UAS RFP dHEcw into the attP2 landing site on the third chromosome. Transgenic offspring was screened by eye-color (white marker) and sequencing with the following primers:

1140_for: 5'-GGTGCCGGTCCACCAGAGCT-3'

1200_re: 5'-TATTCGGCGACGAAGATGAC-3'

2440_for: 5'-CAGTTCTTTATTGATCACCA-3'

2500_for: 5'-CGTACCACACGAGGACACTC-3'

3040-for: 5'-GGGCTTTGTTCCTATTGAAG-3'

5. Targeted overexpression and knock down in *Drosophila*

Targeted gene overexpression and knock down was obtained using the Gal4-UAS system [250]. As schematized in the following figure, this system is composed by two main parts: the *Gal4* gene, encoding the *Saccharomyces cerevisiae* transcription activator protein Gal4, and the UAS (Upstream Activation Sequence), an enhancer to which GAL4 specifically binds to activate gene transcription. Flies carrying a UAS-transgene (e.g. wild type gene/tag-gene/mutated gene/RNAi) are mated to flies carrying a Gal4 driver, thus the progeny contains both elements of the system. *Gal4* expression is under the control of a tissue specific promoter (commonly referred as 'driver'), ensuring the UAS-transgene expression in a controlled spatial and temporal fashion. Gal4 activity is temperature dependent: minimal Gal4 activity is present at 16°C, while 29°C provides a balance between maximal activity and minimal effects on fertility and viability due to growth at high temperature. Simply by altering the temperature, a wide range of expression levels of any responder can be achieved, thereby increasing the flexibility of the system.

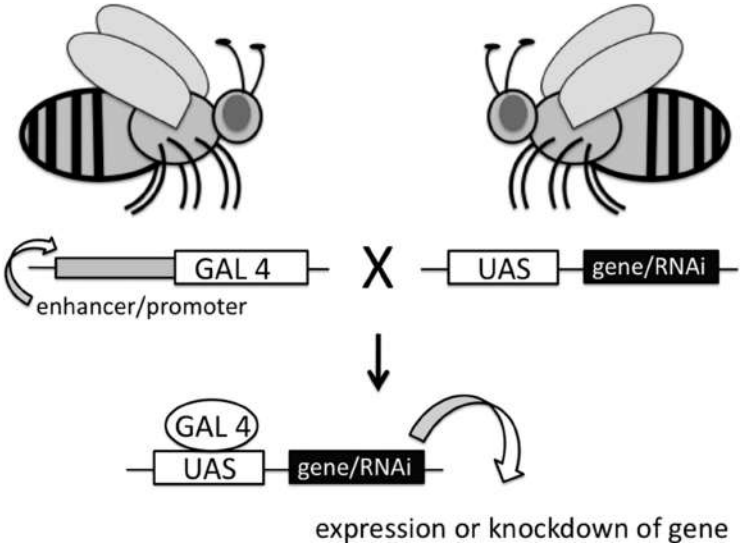

The Gal4-UAS system *[Adapted from Neckameyer,et al. American Journal of Physiology 2012]*

6. CRISPR Cas9 mutant generation

To express Cas9 endonuclease in *Drosophila* germ cells, we took advantage of a nos-Cas9 line (y2 cho2 v1; P[nos-Cas9, y+, v+]3A/TM6C, Sb Tb) available from NIG-fly stock center. In these flies, the *Cas9* gene expression is controlled by the nanos-Gal4 promoter (nos), which has been shown to drive highly specific germline expression.

For the design of guide RNAs we used the MIT CRISPR design tool (http://crispr.mit.edu/, Zhang Lab, MIT). Target sequence requires a 'G' nucleotide (nt) as starting base and 20 nt length, preceding a NGG Protospacer Adjacent Motif (PAM), that serves as a binding signal for Cas9 [251]. We discarded all the sgRNA that had predicted off-target on the X chromosome, where the *dHecw* gene is located. We selected those sgRNA sequences that had fewer predicted off-targets that fell on non-target chromosomes. To create the catalytic inactive mutants, we choose a sgRNA that include the catalytic cysteine C1394W, and for the knock out a sgRNA on the first exon of the gene. The selected sequences were cloned in the pBFvU6.2 vector (obtained from NIG-fly stock center) between two BbsI restriction sites at the beginning of the sgRNA scaffold, and overhangs were added to the oligonucleotide to allow ligation (sequence highlighted). The oligonucleotides used to construct the sgRNA vectors are as follows:

dHecw inactive mutant F:	F:	5'-CTTCGTGCCCACACATGCTTCAAT-3'
	R:	5'-AAACAATGAAGCATGTGTGGGCAC-3'
dHecw knock out	F:	5'-CTTCGCCTTCTACGAGGCGCGCAA-3'
	R:	5'-AAACTTGCGCGCCTCGTAGAAGGC-3'

This expression vector contains 399 base pairs of the Drosophila snRNA:U6:96Ab gene promoter sequence and 81 base pairs of the sgRNA scaffold. The attB donor sequence, for site-specific integration by the PhiC31 system, the vermilion gene as an eye pigmentation marker, and an ampicillin resistance cassette are also incorporated into the transformation vector. The sgRNA-carrying vectors were sent to BestGene.inc to perform site-direct injection into 'y,w P(nos-phiC31); attP2' embryos (landing site on the third chromosome).

To obtain founder animals that expressed an active Cas9-sgRNA complex specifically in the germ cells, the U6-sgRNA strain was crossed to the nos-Cas9 strain. As indicated in the scheme below, founder males were crossed with compound-X chromosome and 50 flies with potentially mutated chromosomes were recovered from founder animals over the balancer FM7. Balancers are chromosomes with inversions that suppress recombination with their normal homologues, allowing the maintenance of lethal and sterile mutations as a balanced heterozygote. The presence of a balancer is recognizable by visible dominant marker mutations. Cas9 and sgRNA element were removed from the background thanks to selection for the v^+ eye color.

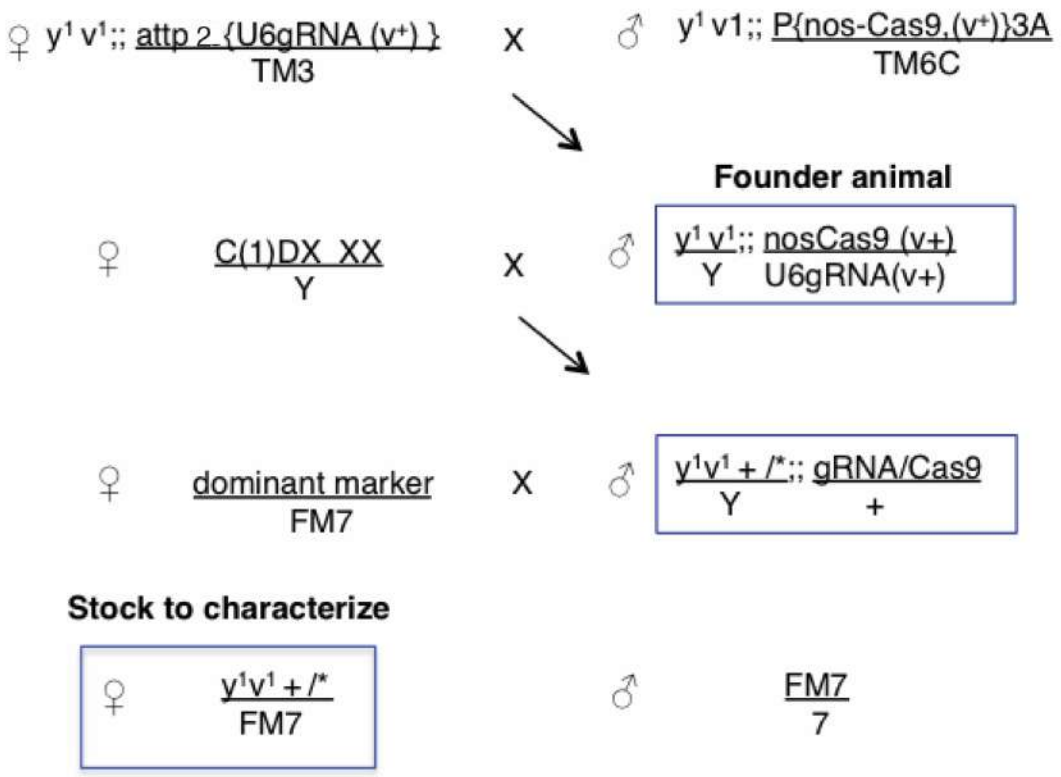

Crosses performed to generate dHecw mutants.

To recover mutated alleles (indicated by a star), male founders were crossed to females carrying the attached-X chromosome (C(1)DX XX) so that the mutated paternal X chromosome could be paternally inherited. Mutated chromosomes were subsequently balanced over the first chromosome balancer FM7.

7.1 CRISPR Cas9 mutant screening

To identify mutated chromosomes, genomic DNA from individual flies was extracted and target regions were amplified by Polymerase Chain Reaction (PCR). Oligonucleotide used for PCR were designed to anneal approximately 250 base pairs upstream and downstream from the expected cut site, as follows:

dHecw inactive mutant F: 5' CCGAGAGTTGGAGCTGGTTA 3'

R: 5' AAACTAGTGGGATGCCATGC 3'

dHecw knock out F: 5' ATGGAGCCACCAGCT 3'

R: 5' AGCTGGTGGCTCCAT 3'

PCR reactions were performed using the following reagents:

REAGENTS	FINAL CONCENTRATION	FINAL VOLUME
5X Phusion GC Buffer	1X	10 µl
dNTP mix, 10 mM	0.2 mM	1 µl
Forward primer 10 µM	0.5 µM	2.5 µl
Reverse primer 10 µM	0.5 µM	2.5 µl
Phusion DNA Polymerase (5U/µl)	1.25 U	0.25 µl
Template DNA	< 250 ng	variable
DMSO	3%	1.5 µl
Water		up to 50 µl

Amplifications were performed with the GeneAmp® PCR system 9700 termocycler using the following cycling conditions:

Step	**Temperature**	**Time**	**Cycles**
1	95°C	2 minutes	1
3	95°C primer Tm °C 72°C	45 seconds 45 seconds 1 minute	30
4	72°C	5 minutes	1
5	4°C	∞	1

PCR product size was controlled on Agarose Gel (0,8%) and analyzed by sequencing, in collaboration with the campus sequencing facility with the primers used for PCR amplification.

7. *Drosophila* behavior assay

8.1 Lifespan Analysis

For the lifespan experiment, cohorts of 200 (100 females and 100 males, unless otherwise stated) 1-3 days old flies of the same genotype were collected and kept at 25°C or 29°C on standard cornmeal food (for 2 liters of medium: 2180 ml water, 18 gr agar, 51 gr dry yeast, 187 gr corn flour, 230 molasses, 10% tegosept, 13 ml propionic acid). Flies were housed in group of 25 flies/vial, in mixed-sex groups. Flies were transferred onto fresh food every two/three days and the number of dead animal was recorded. Percentage of survival was calculated over 200 animals per genotype. Survival analysis was repeated twice and data were analyzed with PRISM GraphPad software: survival fraction were calculated using the product limit Kaplan-Meier method and log rank test was used to evaluated significance of differences between survivorship curves.

8.2 Climbing Assay

For the climbing assay 10 flies/genotype were placed in a 9 cm plastic cylinder. After a 30-s rest period, flies were tapped to the bottom of the cylinder. Negative geotaxis was quantitated by counting the number of flies that able to cross a 7 cm threshold during a 15-s test period. The test was repeated 10 times for each genotype (total of 200 flies/genotype). Flies were not exposed to CO^2 at least 24 hours before the assay, as carbon dioxide quickly anesthetizes the insects. The climbing ability was measured in 1 days-old flies (T0) and monitored every 5 days after the 25th day of the lifespan, when started emerging significant differences between dHecw mutants and control. The climbing index was calculating as the number of succeeding flies over the total. Data were analyzed both with multiple comparison test (one-way ANOVA, Kruskal–Wallis) and Mann Whitney test for single comparison. Data were presented as mean of 10 repetitions +/- SEM.

8. Nucleic acid assays

9.1 Genomic DNA extraction

Each fly was homogenized with a pestle in 10 µl of lysis buffer (100 mM Tris-HCl pH 7.5, 100 mM EDTA, 100 mM NaCl, 0.5% SDS) and then 1 µl of Proteinase K (10 mg/ml) was added to allow proteins digestion. After an incubation at 70°C for 30 minutes, 100 µl of LiCL/KAc solution were added to the mix and the mixture was left in ice for at least 20 minutes. Samples were centrifuged at 13200 rpm for 15 minutes at RT and the supernatant, which contains nucleic acids, was transferred into a new tube. 100 µl of isopropanol were added and a centrifugation at 13200 rpm for 10 minutes at RT allowed DNA precipitation. The aqueous upper phase was discarded and the pellet was washed by adding 150 µl of 70% ethanol before being centrifuged at 13200 rpm for 10 minutes at RT. The pellet was dried for few minutes under a chemical hood and resuspended in 20 µl of DNAse free water.

9.2 RNA extraction and reverse transcription

Drosophila tissues were collected and RNA was extracted using TRIZOL Reagent (Invitrogen) and RNAse Mini kit (QIAGEN). Concentration and purity was determined by measuring optical density at 260 and 280 nm using a Nanodrop spectrophotometer. cDNA was generated from 1µg of RNA using the QuantiTect Reverse Transcription kit (QIAGEN), according to manufacturer's protocol. Samples were analyzed by the Real Time PCR facility with Dm01837439_g1 Dm01837441_g1 assays (Applied Bioscience). They recognized region respectively at the 5' and 3' of dHecw. Amplicon expression in each sample was normalized to its RpL32-RA mRNA content.

9. Protein assays

10.1 dHecw antibody production

For the production of the anti–dHecw antibody, the first 1-390 nt of dHecw were cloned in a pGEX6P1 vector and the GST-dHecw fusion protein was produced in Rosetta competent cells.

Bacteria were lysed in GST lysis buffer [50 mM Hepes, 200 mM NaCl, a mM EDTA, 0,1% NP40, 5% glycerol PMSF 0,1 M and protease inhibitors (Calbiochem)] and lysate was incubated with GST beads. Fusion protein (2 mg) was then eluted with 50mM glutathione dialyzed in PBS o.n. and sent to Eurogentech S.A. for animal immunization. Rabbit polyclonal antibody was affinity purified by Cogentech and validated by immunoblotting using S2 cells RNAi or mock depleted.

10.2 Protein extraction and quantification

Cells and *Drosophila* tissues were collected washed twice in PBS 1X. Then, cells were homogenized in RIPA buffer (50 mM Tris-HCl, 150 mM NaCl, 1 mM EDTA, 1% Triton X-100, 1% sodium deoxycholate, and 0.1% SDS) supplemented with a protease inhibitor cocktail (CALBIOCHEM) and incubated for 20 min on ice. Lysates were cleared by centrifugation at maximun speed for 10 minutes. Supernatants were recovered and quantified by BiCinchonic acid Assay (BCA Assay, Thermoscientific) according to the manufacturer procedure. The BCA Protein Assay combines the reduction of Cu^{2+} to Cu^{1+} by protein in an alkaline medium with the highly sensitive and selective colorimetric detection of the cuprous cation (Cu^{1+}) by bicinchoninic acid. In the first step copper binds with proteins in an alkaline environment resulting in the formation of a light blue complex. In the second step of the color development reaction, bicinchoninic acid (BCA) reacts with the reduced cation (Cu^{1+}) that was formed in step one. When two molecules of BCA are chelated by one cuprous ion a purple-coloured reaction is produced. The BCA/copper complex exhibits a strong linear absorbance at 562 nm with increasing protein concentrations. The absorbance of the BCA/copper complex formed in each sample was analyzed at the Victor Wallac (PerkinElmer) spectrophotometer. Then, proteins concentrations were determined according to Lambert-Beer law.

10.3 Immunoblot analysis

Proteins were denatured by adding Laemli Buffer 2X (Tris-HCl 6.25 mM pH 6.8, glycerol 1%, SDS 2%, β-mercaptoethanol 2%, bromophenol blue 0.0012%) and by boiling them for 5 min. Proteins were then separated on precast gradient gel (4–20% TGX precast gel, Bio-Rad) by

SDS/PAGE and transferred to nitrocellulose by Transblot Turbo (BIO-RAD). The membrane was blocked in PBST 5% milk, before incubation with primary antibodies. Primary antibody used were rabbit polyclonal anti-dHecw (this study) 1:250, mouse anti-Orb 4H8-s and 6h4-s mix together 1:250 (Developmental Studies Hybridoma Bank, DSHB), mouse anti-tubulin 1:5000, mouse anti-dFmrp 1:300 (DSHB), mouse anti-ubiquitin 1:1000 (FK2, Enzo Life Science), rabbit anti-Ref2p 1:1000 (kindly provided by Rusten T.E.). Secondary antibodies used were anti-mouse and anti-rabbit linked to HRP (GE Healthcare), and detected with ECL (GE Healthcare). Immunoblots were visualized using Chemidoc (Bio-Rad).

10.4 Immunoprecipitation analysis

S2 cells were cultured under standard conditions and lysed in JS buffer [Tris–HCl pH 7.6, NaCl 150 mM, glycerol 10%, $MgCl_2$ 1.5 mM, Na pyrophosphate 0.1 M pH 7.5, PMSF 0.1 M, Na vanadate 0.5 M pH 7.5 in Hepes, NaF 0.5 M, with addition of protease inhibitors 1:500 (Calbiochem)] for 20 min on ice. Lysate were clarified by centrifugation and 1 mg were immunoprecipitated with 4 μg of anti-dHecw antibody or anti-GST rabbit antibody as a negative control, in combination with protein G-sepharose. Precipitated immunocomplex were washed, loaded on a precast gradient gel (4–20% TGX precast gel, Bio-Rad) and analyzed by immunoblot.

10.5 Protein production

For the production of the tag- WW domains (dHecw substrate binding domains) pull down assay, the fragment containing the two domains (637-831 aa) was cloned in pGEX6P1 vector. For *in vitro* ubiquitination, the full length *dHecw* gene was cloned in a pGEX6P1 vector and *dFmr1* was clones by PCR into a pET43 using as a template the cDNA obtained from wild type ovaries where the gene is highly expressed. Fusion protein were produced in Rosetta competent cells. Rosetta cells were transformed with the indicated constructs, were used to inoculate 50 ml LB (containing 25 μg/ml ampicillin) and were grown overnight at 37°C. The 50 ml overnight culture was diluted in 1 litre of LB and was grown at 37°C until it reached

approximately OD=0.6. Then, 0.5-1mM IPTG was added and the culture was grown at 18°C overnight. The cells were then pelleted at 4000 rpm for 10 minutes at 4°C and pellets were resuspended in GST-lysis solution or Buffer A for the His-construct (50 mM NaH2PO4 pH 7.8 , 300mM NaCl, 10 % glycerol, 10 mM imidazole, Protease inhibitors (Calbiochem)). Samples were sonicated 5 times for 20 seconds/each on ice and were pelleted at 14000 rpm for 30 minutes at 4°C. 1 ml of glutathione-sepharose beads (Amersham) (1:1 slurry) previously washed 3 times with GST-lysis buffer, were added to the GST-dHecw supernatants. For His-MBP dFmrp Ni-NTA beads (QIAGEN), previously washed 3 times with buffer A, were added to the supernatants. Samples were incubated 3-4 hours at 4°C on a rocking wheel. The beads were then washed 3 times in PBS containing 1% triton, and additional 2 times in PBS alone. The beads were finally resuspended in 1:1 volume of GST-maintenance solution and stored at –80°C.

10.6 Pull-down experiments

For pull-down experiments, 2μM of GST proteins were incubated with 1 mg of S2 lysate for 2 hours at 4°C in YY buffer (50 mM Na-HEPES pH 7.5, 150 mM NaCl, 1mM EDTA, 1mM EGTA, 10% glycerol, 1% triton-100). After four washes of the GST proteins with YY buffer, specifically bound proteins were resolved on precast gradient gel (4–20% TGX precast gel, Bio-Rad) and detection was obtained by immunoblotting using specific antibodies.

10. Immunohistochemical analysis

Adult heads of 1 day, 35 days and 60 days-old flies were dissected in PBS 1X and fixed in 4% paraformaldehyde overnight, at 4°C. After embedding in 1,2 % low melting agar, heads were dehydrated in serial dilutions of ethanol (from 70% to 100%) prior to paraffin embedding, performed in collaboration with the Tissue Processing Unit of the Campus. The paraffin blocks were cut with the microtome into 5 μm frontal sections, stained with haematoxylin–eosin (H&E) and examined by bright-field microscopy. For each time point, at least 5 brains/genotype were analyzed, and vacuoles with diameter >2 μm were counted over 12/15

brain slices.

11. Immunofluorescent analysis in fly tissues

Ovaries and third instar larval brains were fixed in 4% paraformaldehyde, washed in PBST 0,1 % (PBS 1X, 0,1 % Triton-100 X), permeabilized in PBST 1% for 15 to 30 minutes (PBS 1X, 1 % Triton-100 X) and blocked with 5% BSA in PBST for 30 minutes/1 h. Primary antibodies were incubated overnight at 4 ºC and secondary antibody for 2 h at RT. DAPI was incubated for 15 minutes at RT. 3 washes with PBT 0,1% were performed in between each step. Tissues were mounted in 70 % glycerol/PBS. Primary antibodies against the following antigens were used: rabbit polyclonal anti-dHecw (this study) 1:250, mouse anti-Orb 4H8-s and 6h4-s mix together 1:250 (DSHB), mouse anti-ubiquitin FK2 (ENZO Life Science) 1:100, anti-phalloidin TRITC 1:50 Ab, mouse dFmrp 1:300 (DSHB), rabbit anti-Oskar 1:2000 (kindly provided by Ephrussi A.), mouse anti-Gurken 1:400 (DSHB), rabbit Ref2p 1:1000 (kindly provided by Rusten T.E.), human anti-ubiquitin K63 1:200 (Genentec), rabbit anti-Shrub 1;100, guinea pig anti-Hrs 1:200 (kindly provided by Bellen lab), mouse anti-hts 1:200 (DSHB).

12. LC-MS/MS analysis

For Mass Spectrometry analysis, proteins were resolved by SDS-PAGE on a gradient gel and stained with colloidal blue (Colloidal Blue Staining Kit, Invitrogen). Briefly, samples were subjected to reduction in 10 mM DTT for 1 hour at 56ºC. Digestion was carried out saturating the gel with 12.5 ng/µL sequencing grade modified trypsin (Promega) in 50 mM ammonium bicarbonate overnight. Peptide mixtures were acidified with tri-fluoro acetic acid (TFA, final concentration 3%), extracted from gel slices with 30% acetonitrile (ACN)/ 3% TFA, dried in a Speed-Vac and resuspended in 20 µL of 0.1% FA. Three technical replicates of 5 µL injected for each sample were analyzed on a Fourier transformed-LTQ mass spectrometer (Thermo Electron, San Jose, CA). Peptides separation was achieved by a linear LC gradient from 100% solvent A (5 % ACN, 0.1% formic acid) to 20% solvent B (ACN, 0.1% formic acid) over 33

minutes and from 20% to 80% solvent B in 4 minutes at a constant flow rate of 0.3µL/minutes on Agilent chromatographic separation system 1100 (Agilent Technologies, Waldbronn, Germany) Survey MS scans were acquired in the FT from m/z 350-1650 with 100,000 resolution. The five most intense doubly and triply charged ions were automatically selected for fragmentation. Target ions already selected for the MS/MS were dynamically excluded for 60s. Peptides were analyzed by liquid chromatography on an Agilent 1100 LC system (Agilent Technologies, Santa Clara CA, USA). Interactomics results were generated with Scaffold_4.3.4 (Proteome Software Inc., Portland, OR) and protein quantitation was displayed as Total Spectral Count (candidates are reported in **Table 3**). Peptide identifications were accepted if they could be established at greater than 95.0% probability by the Peptide Prophet algorithm with Scaffold delta-mass correction. Protein identifications were accepted if they could be established at greater than 99.0% probability and contained at least 2 identified peptides.

13. Site directed mutagenesis

For the generation of catalytic inactive dHecw (C1394W) to be tested in in vitro ubiquitination it was performed site directed mutagenesis using the Quick Change Mutagenesis Kit (StrataGene), following the manufacturer's instructions. Briefly, a sense and an antisense oligo, carrying the desired mutation in the middle of the sequence, were generated (5'-CCCGTGCCCACACATGGTTCAATCGGCTGGATTTG-3') and used in a PCR reaction using the wild type construct previously cloned in pGEX6P1 vector (50 ng). The PCR was performed using the Pfu TURBO polymerase for 12-18 cycles. After amplification, 1 µl of DpnI restriction enzyme, which selectively cuts methylated DNA at the GATC sequence, was added to digest the wild-type parental DNA. After 1 hour of incubation at 37°C, the PCR product was used to transform competent Escherichia coli cells. Single colonies were picked, plasmid DNA extracted (Miniprep, Promega kit) and sequenced for the presence of the desired mutation and the absence of other, unwanted, base changes. For the amplification step, 12-18 PCR cycles

were performed with a denaturation step of 30 seconds at 95°C followed by an annealing step of 1 minute at 55°C and an extension step at 68°C of 2 minutes/ kb of plasmid length.

14. *In vitro* Ubiquitination assay

15.1 Self-*in vitro* ubiquitination

dHecw full-length and the isolated dHecw HECT domain (1043-1426 aa) were produced as GST-tagged proteins in Rosetta cells. Reaction mixtures containing purified enzymes (20 nM E1, 250 nM His_6-tagged E2-Ube2D3, 250 nM GST-tagged E3 immobilized on glutathione beads), and 1µM Ub were incubated in ubiquitination buffer (25 mM Tris-HCl, pH 7.6, 5 mM $MgCl_2$, 100 mM NaCl, 2 mM ATP) at 37°C. At the indicated time point samples were centrifuged to separate the GST-beads ("pellet"), containing the ubiquitinated E3s. The pellet was washed four times in Ripa buffer before loading on SDS–polyacrylamide gel electrophoresis (SDS-PAGE) gel. Self-ubiquitination detection was performed by immunoblotting using α-Ub antibody. Membranes were stained with Coomassie after immunoblotting to show equal loading of GST proteins.

15.2 Substrate-*in vitro* ubiquitination

For substrate ubiquitination assay 20 nM E1, 250 nM His6-tagged E2-Ube2D3, 250 nM GST-tagged E3, 1µM Ub and 250 nM of HisMBP-dFmrp were added to the reaction mixture. GST-dHecw used was eluted from the beads with glutathione and dialyzed before addiotion to the reaction mixture. At the indicated time points samples were centrifuged to separate the pellet, containing the ubiquitinated substrate, from the supernatant, containing unbound enzymes and the soluble ubiquitin chains. The pellet was washed four times in RIPA buffer (50 mM Tris HCl pH 7.6, 150 mM NaCl, 1% NP-40, 0.1% SDS, 0.5% Deoxycholic acid) before loading on a 3-8% tris-acetate precast gel (Lifetechnologies). Supernatant was loaded on a gradient 4-20% precast gel (Biorad). Detection was performed by immunoblotting, using specific antibody. A

coomassie-stained membrane was used to show the loading of GST/HisMBP-fusion protein after immunoblotting.

RESULTS

1. Characterization of dHecw

While searching for the *Drosophila* ortholog of HECW1 and HECW2, we identified CG42797, a single, uncharacterized gene located on the X chromosome. The protein product of this gene shares co-linearity and an extensive amino acid sequence identity with the human proteins, especially in the functional domains substrate binding-WW and catalytic HECT, as depicted in **Fig. 11**. Compared to human HECW1 and HECW2, the *Drosophila* 1426 aa protein shows no identifiable C2 lipid binding domain, suggesting that the CG42797 may lack the ability of binding to membranes [46], similar to other Nedd4-like proteins, such as the *C.* elegans Ce01588 [46]. Based on the functional and structural similarities with its human orthologs, described in the following paragraphs, we named the CG42797 gene '*dHecw*'.

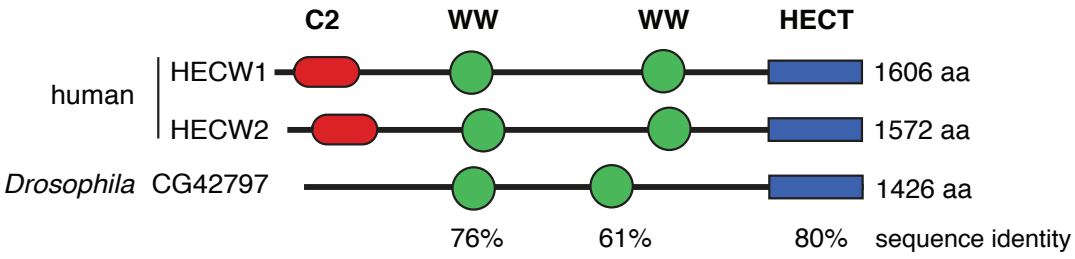

Figure 11. CG42797/dHecw Drosophila E3 ligase.

Schematic representation of human HECW1 and HECW2, and Drosophila CG42797/dHecw proteins. Domain architecture is composed of a C2 (Ca2+ dependent lipid binding) domain (red), 2 WW substrate interacting domains (green), and a catalytic HECT domain (blue). Percentage of identity is reported above the single domains. The fly ortholog shows no C2 lipid binding domain.

1.1 dHecw has a catalytic activity

To verify the enzymatic activity of dHecw as an E3 ligase we tested the functionality of the full-length protein and its HECT domain, which was previously shown to be the minimal region able to sustain the catalysis in the NEDD4 family of ligases [58]. We produced and purified bacterial GST-tagged full-length dHecw and the dHecw HECT domain alone (see methods) and

performed an *in vitro* self-ubiquitination assay with the purified components, using the human HECW1 HECT as a positive control for the reaction and Ube2D3 (also called UbcH5c) as E2, which resulted the best functional match for human HECW1 (not shown). GST-proteins were separated on SDS-PAGE gel and immunoblotted (IB) against ubiquitin. The ubiquitin signal was visible starting from the molecular weight of the GST-proteins, indicating that both the full length and the dHecw HECT domain alone are able to self-ubiquitinate (**Fig. 12**). Therefore, we concluded that dHecw is a catalytically active HECT ligase.

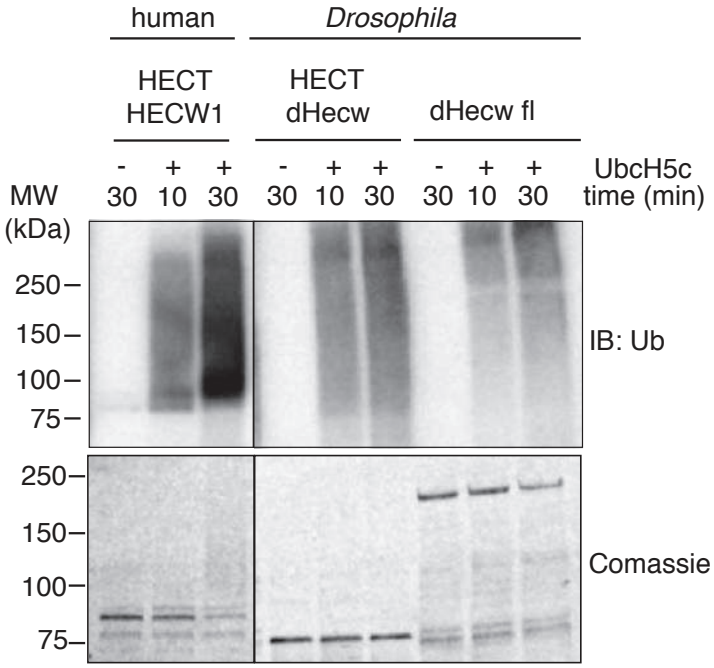

Figure 12. dHecw is an activeE3 ligase.

Ub chain formation assay with the indicated GST constructs analyzed by IB analysis (upper panel). The coomassie staining shows a comparable level of loaded proteins (lower panel).

1.2 dHecw expression and subcellular localization in *Drosophila* tissues

Previous studies indicate that human HECW1 and HECW2 are preferentially expressed in neuronal tissues [111] e [105]. In order to study the physiological function of dHecw, we investigated its expression pattern in different *Drosophila* organs, using different methods. Analysis of messenger RNA expression levels was performed by real time polymerase chain reaction (RT-PCR) on several larval and adult tissues (**Fig. 13A**). To define dHecw expression

and subcellular localization, we produced a rabbit polyclonal antibody against amino acids 1-130, a unique region of the protein (see methods). The specificity of the antibody was tested by immunofluorescence (IF) and IB in *Drosophila* S2 wild type and dHecw knock down (KD) cells (**Fig. 13B**). Both at the mRNA and protein level we observed an enrichment of dHecw in the central nervous system (CNS) and the ovaries in normal physiological conditions (**Fig. 13C**), as also indicated by the annotated RNA-seq data of modENCODE database (not shown).

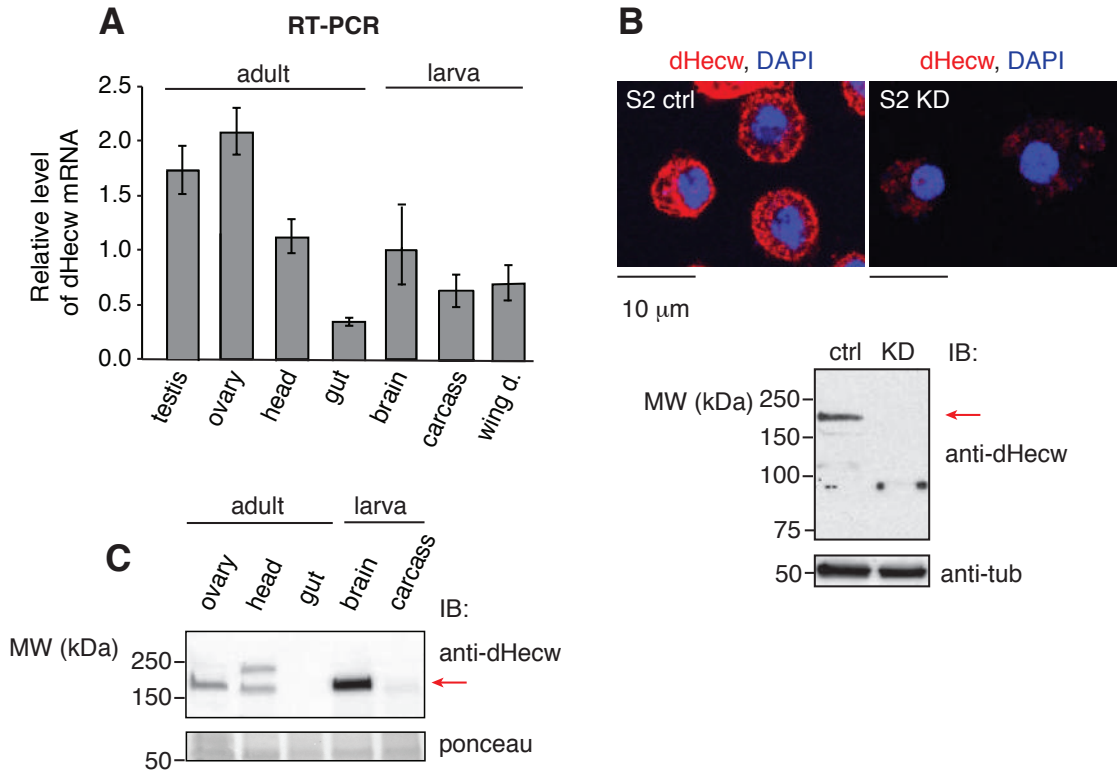

Figure 13. dHecw is expressed in the ovary and the central nervous system.

*(**A**) dHecw mRNA expression was measured by RT-PCR in the indicated wild type Drosophila tissues. For the RT-PCR, the reported expression levels are relative to larval brain and SD is calculated over two experiments (three technical replicates for each). (**B**) Upper panel: IF analysis of S2 cells (ctrl) and S2 cells interfered for dHecw (KD) at 48 hours. dHecw is stained in red, nuclei are stained in blue (DAPI). Scale bar: 10 μm Lower panel: protein levels were measured by IB analysis with the indicated antibodies, in S2 cells (ctrl) and dHecw-interfered S2 cells at 48 hours (KD). dHecw is indicated by the red arrow. (**C**) dHecw protein levels were measured by IB analysis in the indicated wild type Drosophila tissues. dHecw is indicated by the red arrow.*

In immunofluorescence analysis, our antibody localized dHecw mainly to the cytoplasm. In fly ovaries, dHecw appeared to have a broad distribution in both somatic tissue and germline. Interestingly, dHecw co-localized with the oocyte marker Orb, showing a preferential enrichment in this compartment. The thickness of later stage egg chambers (9-10) caused some issues with the penetration of the antibody, but despite that, dHecw and Orb co-localized at the posterior margin of the fly oocyte (**Fig. 14**).

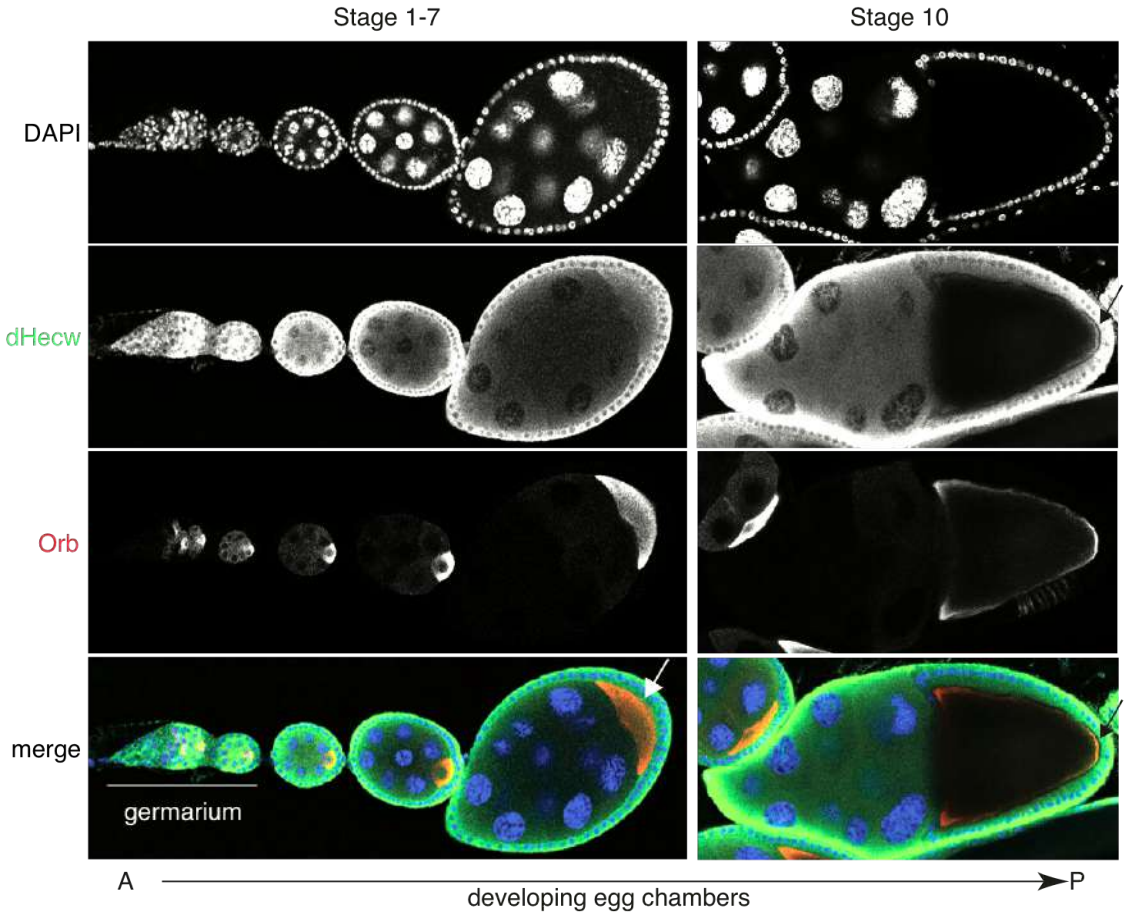

Figure 14. dHecw is cytoplasmic and co-localizes with Orb.

IF analysis of Drosophila ovarioles with the indicated antibodies. Left panel: the chain of egg chambers develops from the germarium (previtellogenic stages 1-7). dHecw localizes both in the follicular epithelium and in the germline. At later stages (egg chamber on the right), dHecw co-localization with the germline marker Orb (white arrow) in the oocyte is more evident. Right panel: stage 10 egg chamber, dHecw localization at the posterior margin of the oocyte (black arrow).

Taking advantage of the online resource tool Drosophila Virtual Expression eXplorer (DVEX), we explored dHecw expression in the *Drosophila* embryo (stage 6) at the single cell level [252]. The analysis with virtual *in situ* hybridization (vISH) confirmed that dHecw expression is generally weak, and is predicted to be mainly expressed in cells on the dorsal/anterior side and posterior of the developing embryo (**Fig. 15**).

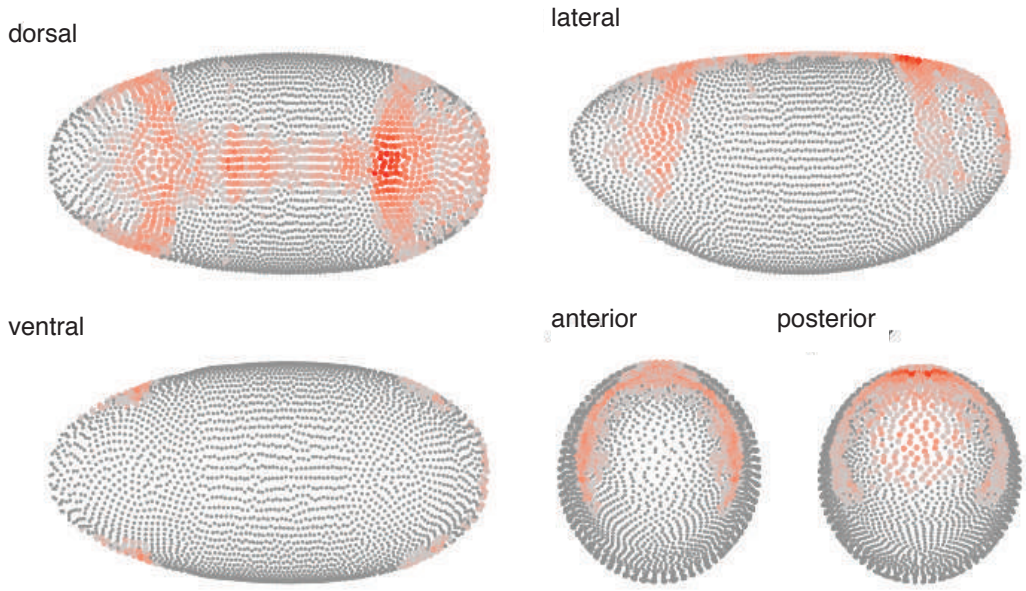

Figure 15. dHecw virtual expression in the fly embryo.

Prediction of spatial expression patterns of the dHecw gene with the virtual in situ hybridization tool DVEX, in stage 6 embryo. Five different embryo orientations are shown. dHecw expressing cells are shown in pink.

---

2. CRISPR/Cas9 mutagenesis of the *dHecw* gene

2.1 Generation and characterization of mutant dHecw flies

In order to identify physiological processes regulated by dHecw, we generated mutant flies using the CRISPR/Cas9 system [251]. To directly target the activity of the protein, we designed a guide RNA complementary to the region that encodes the catalytic cysteine (C1394, see methods for details). Transgenic flies carrying nanos-Cas9 and U6-sgRNA were crossed to obtain founder flies that express an active Cas9-sgRNA complex specifically in the germline. Founder males were mated to recover progeny with putatively mutated chromosomes. 50

independent lines were established and screened by PCR for the presence of mutations in *dHecw* sequence. We identified 3 lines with insertions/deletions that lead to coding alterations as described in **Fig. 16**. Among the mutated protein products, two lack the catalytic cysteine (C1394Afs1461, named m1, and Δ1394-1396, named m2), while one has a 10 bp deletion right after the cysteine 1394 codon, which determines a frameshift with the generation of an aberrant C-terminus (F1395Wfs1457, named m3).

Figure 16. Nucleotide and amino acid sequences of mutations induced by CRISPR/Cas9 system in the dHecw gene.

The wild type (wt) sequence of nucleotides (nt) and amino acids (aa) are shown in the top panel, the catalytic cysteine is marked in green and the stop codon is indicated with an asterisk. In mutant sequences, deletions are indicated with dashes and amino acids that differ from the wild type are marked in red.

Previous studies showed that, in addition to the catalytic cysteine, the conserved C-terminal region of the HECT contains several residues essential for the catalysis [60], [58]. Therefore, the generated mutants were predicted to be catalytically inactive, and to verify whether this is the case, we mutagenized full-length GST-dHecw, replacing the catalytic cysteine with a tryptophan (C1394W) and we purified the corresponding protein to perform an *in vitro* ubiquitination reaction. Consistent with our prediction, while wild type dHecw is able to self-

ubiquitination and generate free polyubiquitin chains, while the C/W mutant is impaired and shows the same ubiquitin signal as that in in the E2-only reaction (**Fig. 17**).

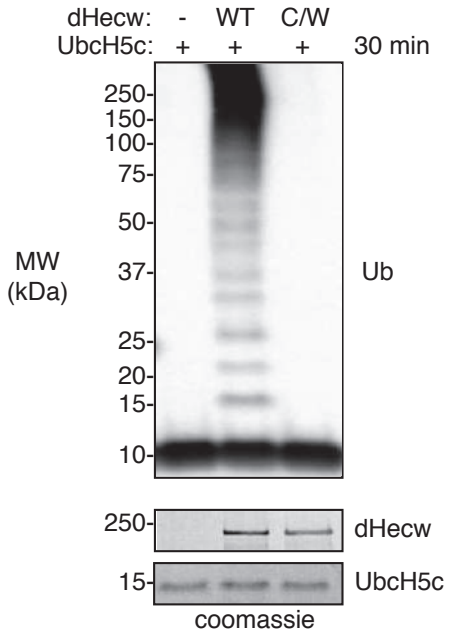

Figure 17. The dHecw mutant is catalytically inactive.

Ubiquitin chain formation assay with the indicated recombinant proteins was analyzed by IB analysis using anti-ubiquitin antibodies (upper panel). The E3 used for the reaction are dHecw wild type (WT) and dHecw catalytic inactive (C/W). The coomassie staining shows comparable levels of loaded protein (lower panels).

Homozygous mutant m1, m2 and m3 flies are viable and do not show macroscopic morphological defects (**Fig. 18A**). Being mutated at the very end of the gene, dHecw mutant flies were expected to be normally transcribed, and not to be targeted by non-sense mediated decay (NMD) [253]. Indeed, we observed no difference in dHecw mRNA expression in mutant third instar larval brain, compared to the control by RT-PCR (**Fig. 18B**). In contrast, the mutant proteins seemed to be unstable since immunoblot (IB) analysis showed a clear decrease in protein level when compared with wild type dHecw, which was visible already at early stages (third instar larval brain, **Fig. 18C**) and was even more evident in the adult fly head (**Fig. 18D**). Remarkably, we observed that also the expression level of dHecw in wild type flies decreases over time in parallel with the behavior of its mRNA, as measured by RT-PCR in the adult fly head (**Fig. 18E**).

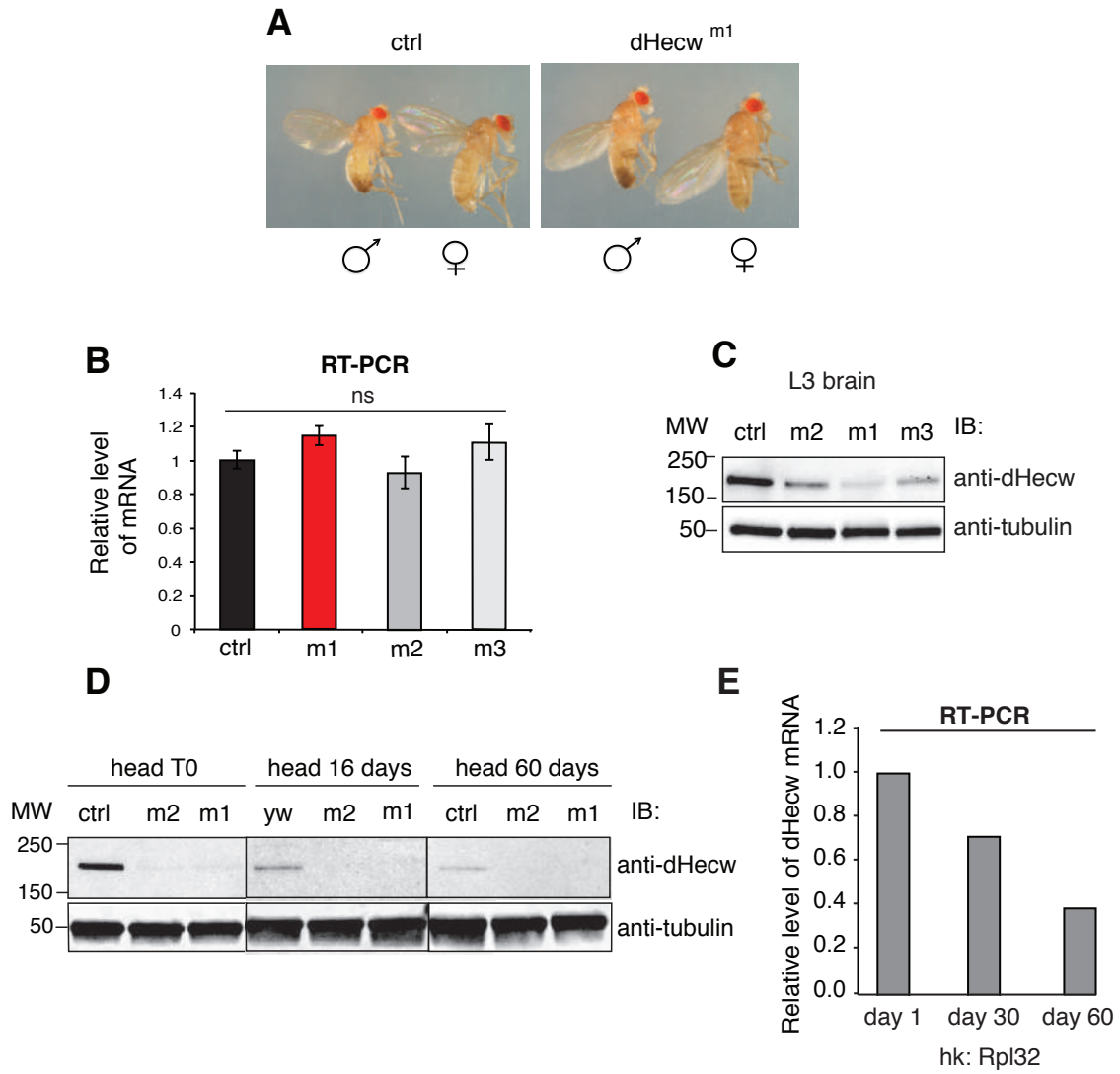

Figure 18. dHecw mutants.

*(**A**) Examples of male and female adult mutant flies (right panel) that are viable in homozygosis and that do not show macroscopic morphological defects in comparison with wild type OR flies (ctrl, left panel). (**B**) The expression levels of all mutated genes m1 (red), m2 (grey), m3(light grey) were measured by RT-PCR. No significant differences were scored. The reported expression levels are relative to wild type larval brain and SD is calculated over three technical replicates. (**C, D**) IB analysis with the indicated antibodies in larval brains (**C**) and adult fly heads (**D**). The expression levels of mutant proteins are reduced in comparison with wild type control (yw). Endogenous levels of wild type protein decrease with aging: compare the levels of new born flies (T0) at 16 and 60 days. (**E**) dHecw expression was measured by RT-PCR in adult heads at different time points: 1 day, 30 days and 60 days. The reported expression levels are relative to day 1 using Rpl32 as housekeeping (hk) gene.*

2.2 dHecw mutant flies exhibit a neurodegenerative phenotype

The progressive decrease of dHecw expression levels with age prompted us to search for possible phenotypes during aging. *Drosophila* adult flies live 60-80 days, a feature influenced by multiple factors, including the genetic background, environment, nutrition and mating [254], [255] . To minimize the influence of these factors, we performed a lifespan assay with mixed-sex groups in standard cornmeal food using a controlled number of animals. Interestingly, dHecw mutant flies displayed a reduced lifespan compared with the isogenic control lines (**Fig. 19A,** left panel). The median survival was reduced by 22%. At 29°C, we found that the defect is exacerbated with a 27% reduction in lifespan compared with the control flies (**Fig. 19A,** right panel).

To test whether the shorter lifespan in dHecw mutant is associated with neuromotor defects, we performed a climbing test, using a standard negative geotaxis assay. Mutant flies displayed a significant premature decline in climbing ability, which was evident at day 25. At 29°C, the climbing defect was significant at earlier time points (**Fig. 19B**, right panel).

A hallmark of neurodegeneration in *Drosophila* is progressive "vacuolization" of the brain due to loss of CNS neurons. To assess the integrity of dHecw mutant fly brains, we performed microscopy analysis using frontal-head paraffin sections stained with hematoxylin and eosin (H&E). We observed that adult (35days old) mutant fly brains present extended vacuolization, compared to age-matched control fly brains (**Fig. 20A**). Vacuoles' quantification revealed that these are larger and significantly more numerous in dHecw mutant fly brains. In addition, the vacuole size rises with age (**Fig. 20B)** and all three fly mutants exhibit the same neurodegenerative defects (not shown). These phenotypes suggest a putative involvement of dHecw in protecting neurons from premature neurodegeneration

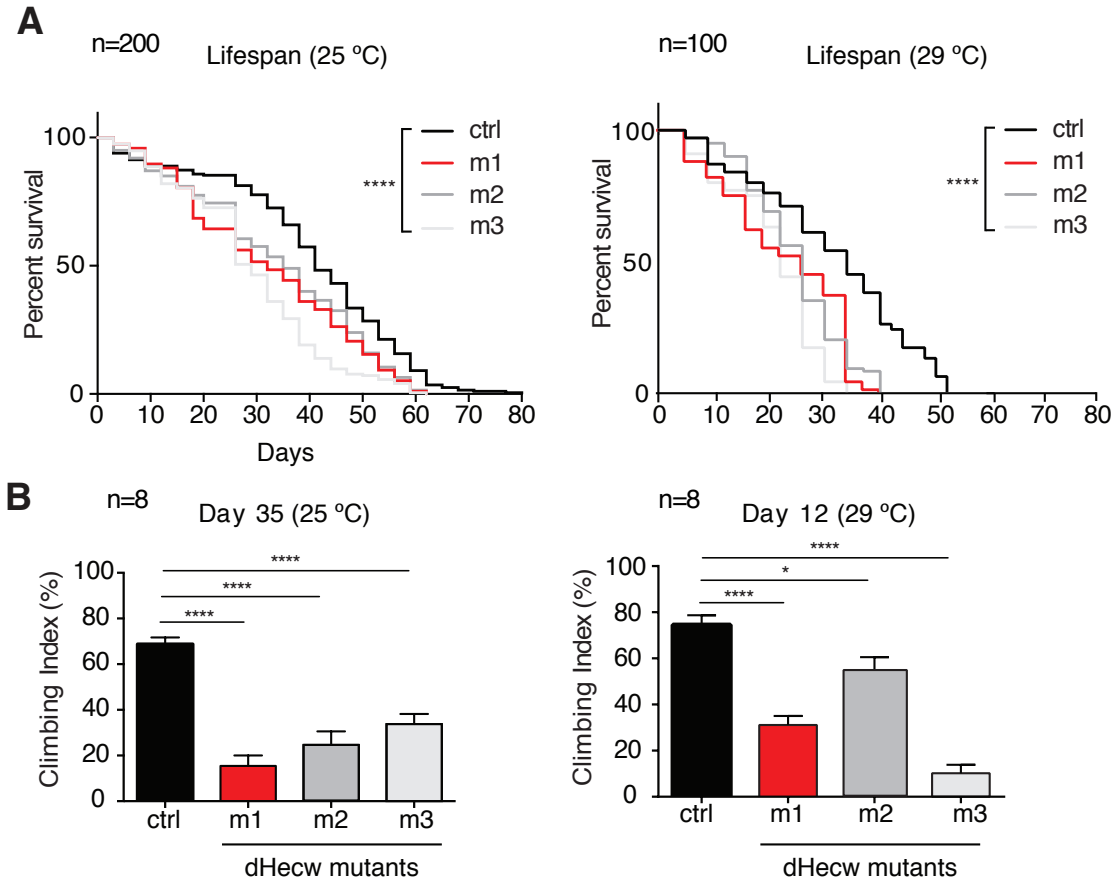

Figure 19. dHecw mutants show a reduced lifespan and premature decline of motor function.

*(**A**) Survival curve of lifespan analysis for each indicated genotype. Flies were kept at a density of 25 flies/vial and maintained in standard cornmeal agar medium. Flies were scored every two/three days for survivorship and percentage of survival was calculated over 200 animals per genotype at 25ºC (left panel), and 100 animals at 29ºC (right panel). dHecw mutants (m1, m2, m3) show a significant decrease in their lifespan compared with the control line (log-rank test, p-value <0,001). (**B**) Motor function was measured during aging, using the negative geotaxis assay. Flies were gently tapped to the bottom of a plastic vial and flies that could climb over the threshold (7 cm) in 15 seconds were scored. Mutant flies show a climbing deficit that becomes more evident with aging, 25ºC (left panel) and 29ºC (right panel). Results are presented as a mean of 8 repetitions ± SEM, and differences were measured with multiple comparison test (one-way ANOVA) and Mann Whitney test for single comparison.*

.

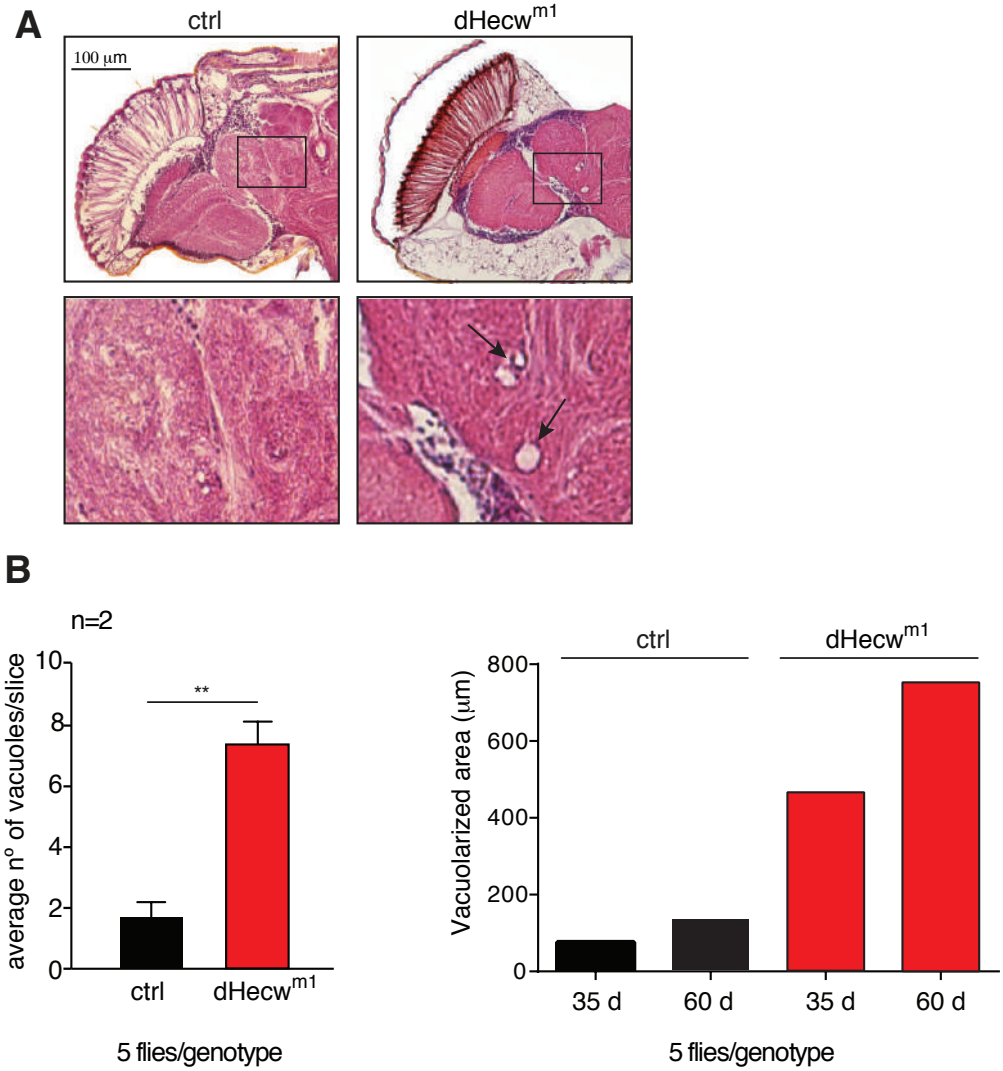

Figure 20. dHecw mutant fly brains show a high tissue vacuolarization.

*(**A**) Frontal sections of 35 days old fly brains were stained with H&E and examined by bright-field microscopy. Scale bar: 100 µm. Magnified views of central brain regions corresponding to the respective boxed areas. (**B**) Left panel: quantification of the vacuoles (>2 µm) in various fly brain slices (5 flies/genotype) in 35 days old flies. Results are presented as mean of two independent experiments ± SEM. Right panel: total vacuolarized area (5 flies/genotype). Wild type control (black), dHecw mutant m1 (red).*

2.3 dHecw mutant flies show reduced fertility and oogenesis defects

As previously shown, dHecw expression is enriched not only in the central nervous system but also in adult fly ovaries (**Fig. 13A**). IB analysis of fly ovary extracts revealed a reduced level of mutant proteins in comparison with wild type dHecw (**Fig. 21A**). These observations

prompted us to ask whether dHecw is required to support fertility, an easily measurable trait in healthy flies. In females, egg-laying varies with age: after a peak at day 4 from eclosion, there is a physiological decline of egg production, which is reduced by 50% at day 40 [256]. By counting the number of laid eggs by equal numbers of age-matched females, we found that 20 days old mutant flies lay significantly less eggs compared to control flies (**Fig. 21B**).

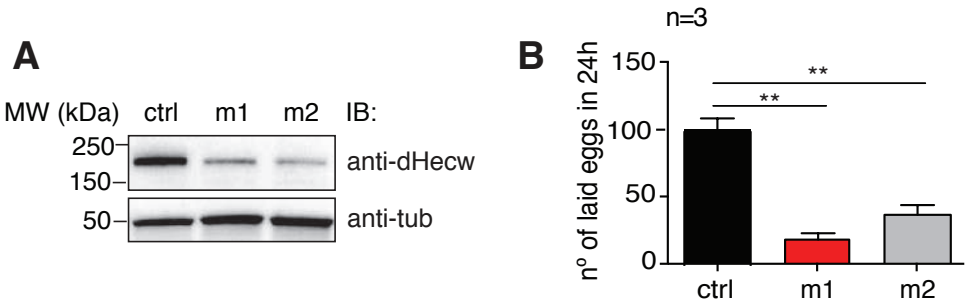

Figure 21. dHecw mutants display premature fertility reduction.

(*A) Protein levels were measured by IB analysis with the indicated antibodies in adult fly ovaries (3 days old). The expression levels of mutant proteins (dHecw m1, dHecw m2) are reduced in compared with wild type control (yw). (****B****) Fertility assay was assessed via the number of egg laid in 24 hours by the indicated 20 days old genotypes. Results are presented as mean ± SEM number of laid eggs. SEM was calculated over three experiments.*

To investigate the cause of the reduced egg laying, we dissected ovaries from adult female flies and performed immunofluorescence analysis of well-fed mated fly ovaries, which revealed the presence of aberrant egg chambers (**Fig. 22-23)**. All three mutants manifested the same defects, and one (m1) of them was used for further analysis of the phenotype. In young flies (3 days old), 21 % of dHecw mutant fly ovaries present egg chambers with an altered number of germ cells. Among these defective egg chambers, the majority (75%) has a reduced number of nurse cells and ring canals, indicating a premature arrest of cystoblast mitotic division. In most of the cases, the number of germ cells was not an exponential of two, indicating a loss of synchrony during cystoblast division. The remaining defective egg chambers possessed more than 16 germ cells and multiple oocytes. In the majority of these cases (70%), we observed a

double or triple number of nurse cells, ring canals and oocytes, suggesting that the alteration is possibly generated by fusion of two or more egg chambers, yielding compound egg chambers. These observations suggest the presence of defects during cyst encapsulation, which occurs in region 2b of the germarium. The remaining 30% defective egg chambers with increased GCs numbers presented one oocyte and a number of nurse cells between 15 and 30; in this case, the defect is likely to be caused by an extra-round of not synchronized mitosis.

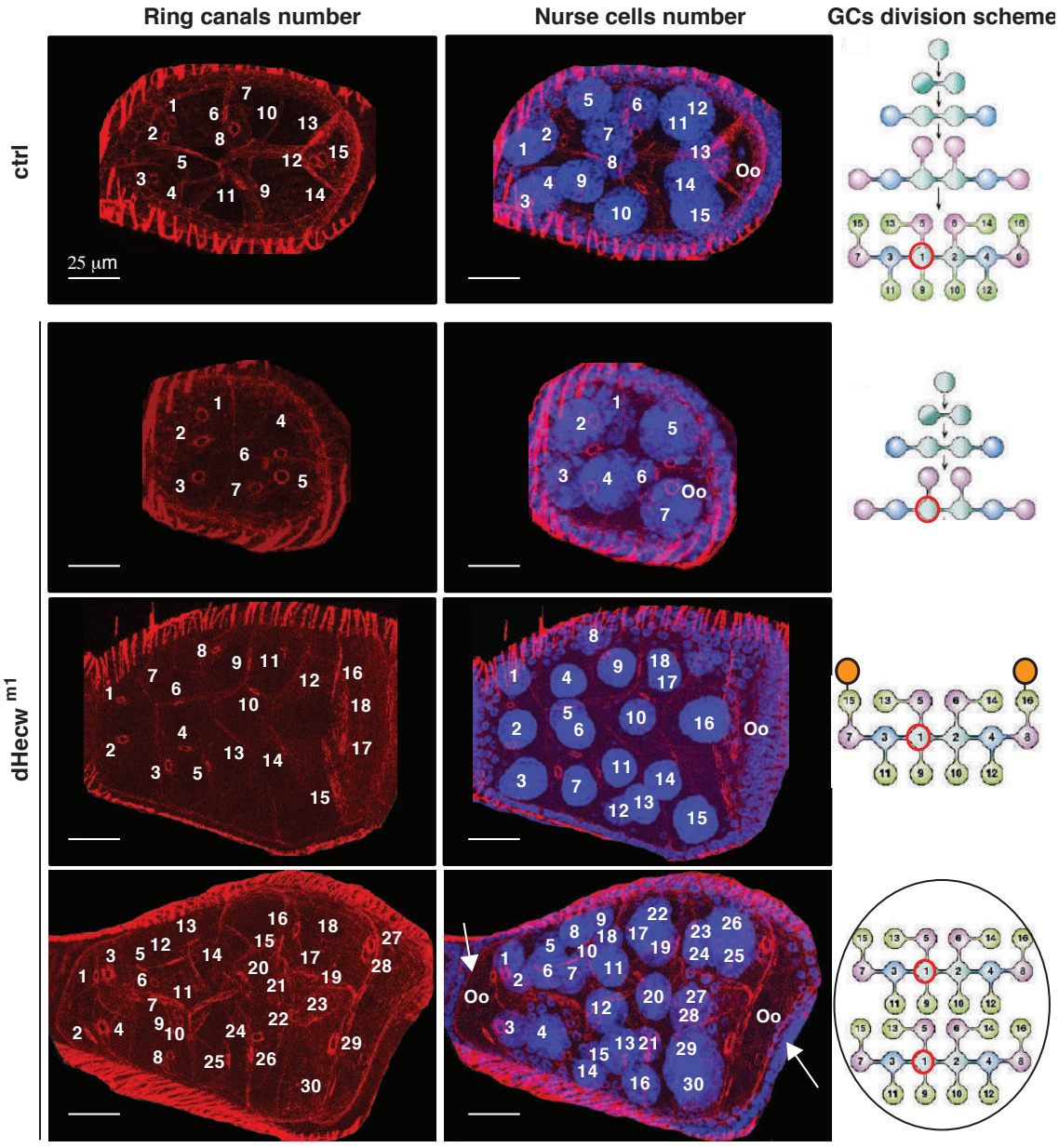

Figure 22. dHecw mutants display an aberrant oogenesis.

IF analysis of wild type (upper panels) and dHecw mutant (m1) fly egg chambers (lower panels). Phallodin in red, DAPI in blue. Observed defects include a reduced number of nurse cells (second line), an increased number of nurse cells (third line), and compound egg chambers (fourth line,

white arrows indicate the two oocytes). Right panel: schematic representation of germ cell (GCs) division of the corresponding egg chamber. The oocyte is highlighted in red, extra-numerary nurse cells in orange, black line encloses fused egg chambers. Scale bar: 25 µm.

As observed in the neurodegeneration phenotype, also oogenesis defects increase with age: the amount of aberrant egg chambers is 21% in young flies, almost doubles to 39% in 30 days old flies. Classification and quantification of the defects are summarized in **Table 1.**

Genotype	Flies age	NC, RC, Oo	Defects	Defective egg ch.(%)		
yw	3-day old	15,15,1	/	0/310 (0%)		
dHecw ^{m1}	3-day old	7,7,1	mitosis	19/338 (6%)	14%	dHecw^{m1} 3-day old tot: 21%
		7<NC, RC<15, 1	mitosis, synchronization	28/338 (8%)		
		15<NC, RC, 1	mitosis	6/338 (2%)	7%	
		30, 30, 2	encapsulation	16/338 (5%)		
yw	30-day old	15,15,1	/	0/150 (0%)		
dHecw ^{m1}	30-day old	7,7,1	mitosis	3/160 (2%)	9%	dHecw^{m1} 30-day old tot: 39%
		7<NC, RC<15, 1	mitosis, synchronization	11/160 (7%)		
		15<NC, RC, 1	mitosis	10/160 (6%)	30%	
		30, 30, 2	encapsulation	38/160 (24%)		

Table 1. Classification of dHecw mutant's defects in oogenesis.
Complete classification of the defects observed in dHecw mutant ovaries at the indicated time points. Numbers of nurse cells (NC), ring canals (RC), oocytes (Oo) are specified in the third column.

To visualize oocyte specification, we stained fly ovaries to detect Orb, which becomes enriched in the oocyte. 33% of the aberrant egg chambers present additional Orb-positive cells, indicating that the oocyte is misspecified (**Fig. 23**). The supernumerary Orb-positive cells generally exhibit more condensed nuclei in comparison with the surrounding nurse cells, further suggesting improper oocyte commitment.

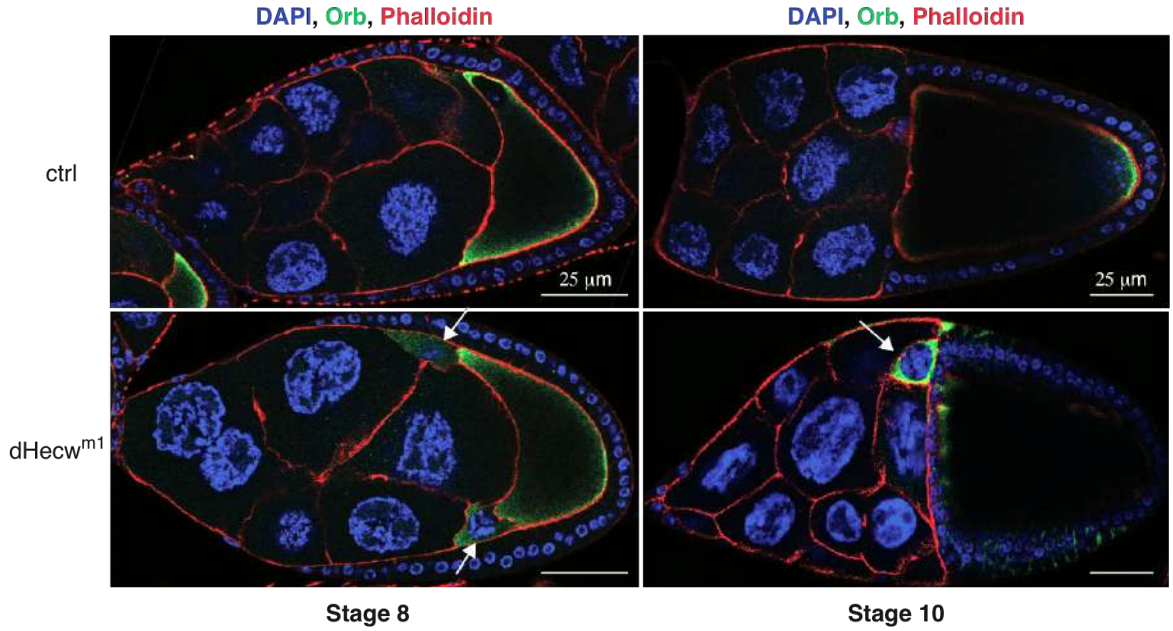

Figure 23. dHecw mutants present oocytes misspecification.

IF analysis of 3 days old wild type and dHecw mutant fly egg chambers with the indicated antibodies. Orb (green) marks the oocyte (wild type ctrl, upper panels). White arrows indicate additional Orb-positive cells present in the dHecw mutant fly eggs (lower panels). Scale bar: 25 µm.

2.3.1 The fusome is altered in dHecw mutant flies

The fusome is a vesicle-rich structure that arises from a spherical precursor (spectrosome) in GSC. The fusome has a key role in guiding the correct geometry of cyst division, synchrony and oocyte specification [188]. Therefore, we examined fusome morphology in dHecw mutant fly ovarioles by immunolabelling Hu-li tai shao (Hts), a specific fusome component. As shown in **Figure 24**, while in wild type controls the fusome possess a stereotypically branched shape, mutant cysts often contain fragmented or spherical fusomes. Spherical fusomes are frequently observed when cystoblasts fail to divide [257]. While in wild type samples, the fusome disassembles and is no longer visible by the middle of region 2a, the fusome persist as late as region 3 in a few dHecw mutant fly germaria [187]. The penetrance of these defects, consisting in about 25% of germaria of young mutant flies, which is similar to that observed in the aberrant fly egg chambers at later stages.

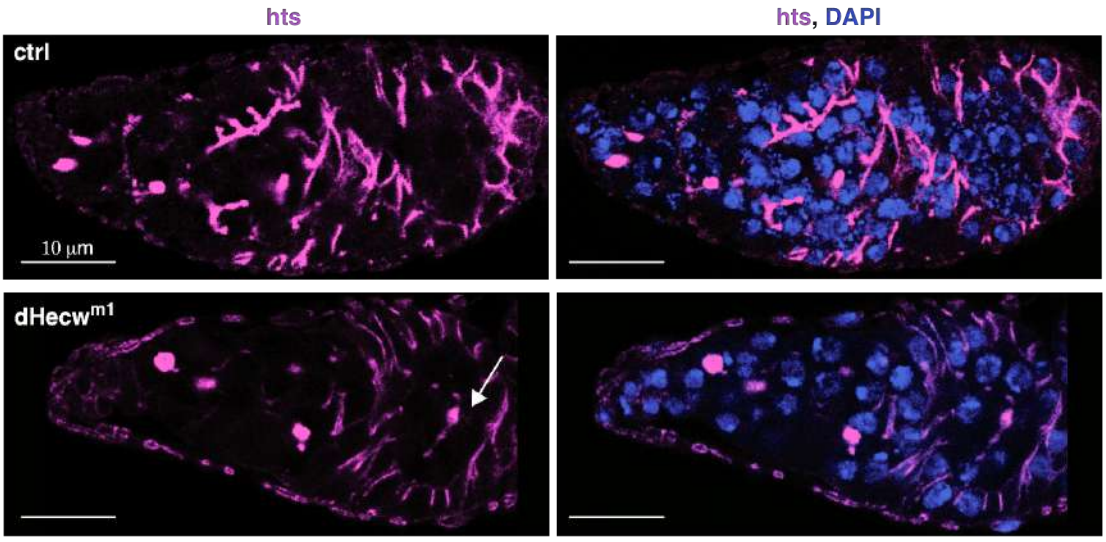

Figure 24. dHecw mutants present a fragmented fusome.

IF analysis of 3 days old wild type (upper panels) and dHecw mutant fly egg chambers (bottom panels) with the indicated antibodies. Hts (magenta) marks the fusome. White arrows indicate the retained fusome in region 3 of dHecw mutant germaria. Scale bar: 10 µm.

2.4 Generation and characterization of dHecw knock out flies

To assess whether the phenotypes observed in dHecw mutant flies represent a total loss of function or whether they are specific for the lack of catalytic activity, we generated knock out mutant flies by targeting CRISPR/Cas9 to generate an early premature stop codon and abrogate protein production. To this end, we designed the sgRNA guide to target the first exon and screened to isolate lines in which the expression of the protein is completely lost. Out of 50 lines, 35 lines presented mutations in the coding region around the target sequence, indicating that the mutagenesis was very efficient. Among the mutated lines, 23 led to the formation of premature stop codons at the level of 200 nucleotides. The remaining mutants led to formation of point mutations or smaller in-frame deletions. Surprisingly, by RT-PCR, we observed that the level of dHecw mRNA in the adult fly head is unchanged and decreases only mildly in the adult fly ovaries of putative knock out (KO) mutant lines (**Fig. 25**). Thus, we concluded that, in spite of the presence of premature stop codons at the 5' of *dHecw,* the corresponding transcripts are not subjected to NMD. Nonetheless, KO mutant lines with premature stop codons showed no sign of protein production, while a point mutation or small in frame

deletions recovered in the same round of mutagenesis (mA, B) displayed a detectable protein products (examples of IBs are reported in **Fig. 25B**). These data were also confirmed by immunoprecipitation (IP) of selected KO lysates (**Fig. 25C**).

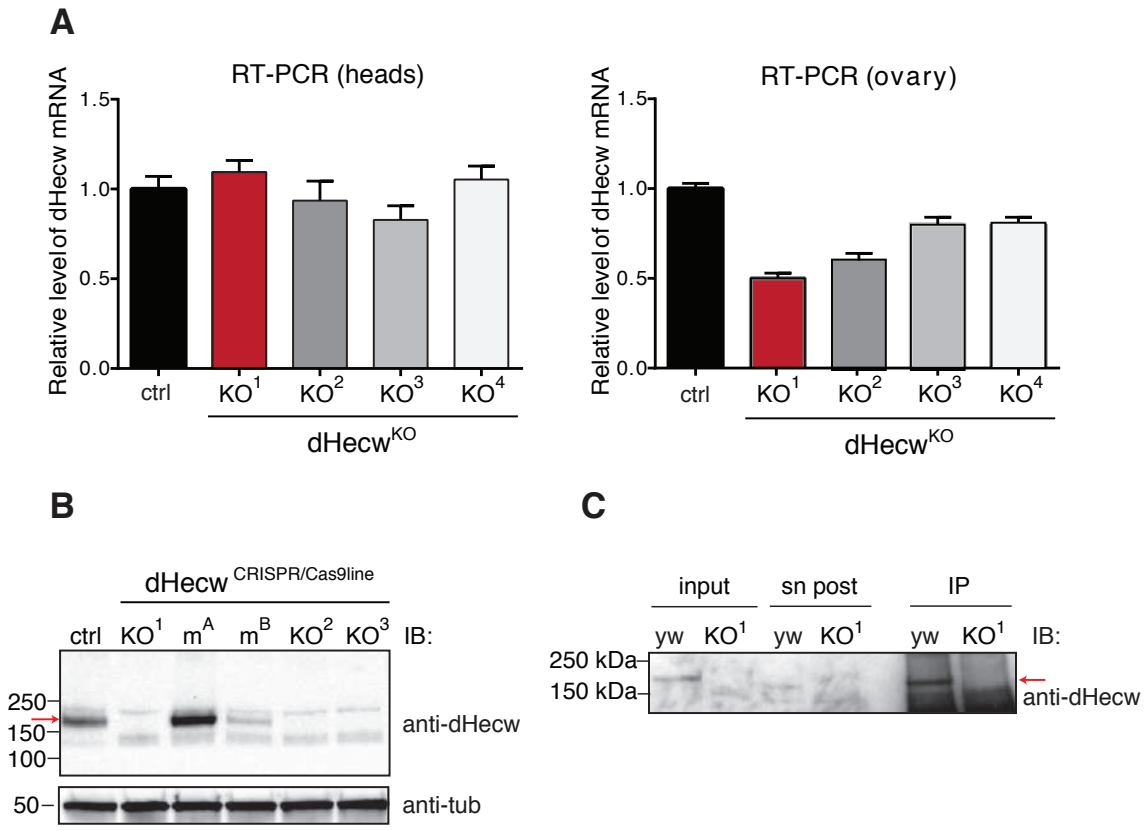

Figure 25. RT-PCR, WB and IP of dHecw KO flies.

*(**A**)The expression levels of mutated genes (four of the dHecwKO alleles with premature stop codon are shown as an example) were measured by RT-PCR in adult fly heads (right panel) and ovaries (right panel). The reported expression levels are relative to wild type (ctrl) and SD is calculated over three technical replicates. (**B**) Protein levels were measured by IB analysis with the indicated antibodies in adult fly ovaries. Mutant and KO fly strains were generated with CRISPR/Cas9 mutagenesis on the first exon. KO indicates the potential KO allele (premature stop codon), m^A indicates mutant alleles (point mutations), and m^B indicates small in frame deletion. dHecw (indicated by the red arrow) was not detected in KO alleles. (**C**) IP and IB analysis were performed with a dHecw antibody, using wild type (yw) and dHecw-KO1 (KO1) fly ovary lysates. Supernatant post IP; (sn post). The red arrow indicates immunoprecipitated dHecw.*

2.5 dHecw knock out flies recapitulate dHecw mutants phenotypes

Similar to m1, m2, m3 mutants, homozygous KO flies are viable and do not show macroscopic morphological defects. Wild type and dHecw mutant flies were tested for neurodegenerative defects, egg laying and presence of egg chamber alterations. Different KO lines tested exhibit the same defects, and one is shown in the following paragraph as example (KO1). All tests revealed similar results to those observed in dHecw m1, m2, m3 mutants: the lifespan of KO flies was decreased, with a median survival that was reduced by 24% (**Fig. 26A**). KO flies presented a significant premature decline in motor function, as assessed by negative geotaxis assay, comparable to that of dHecw mutants (**Fig. 26B**). Microscopy analysis of paraffin embedded frontal sections of KO adult fly brain highlighted an extended tissue vacuolization (**Fig. 26C**.).

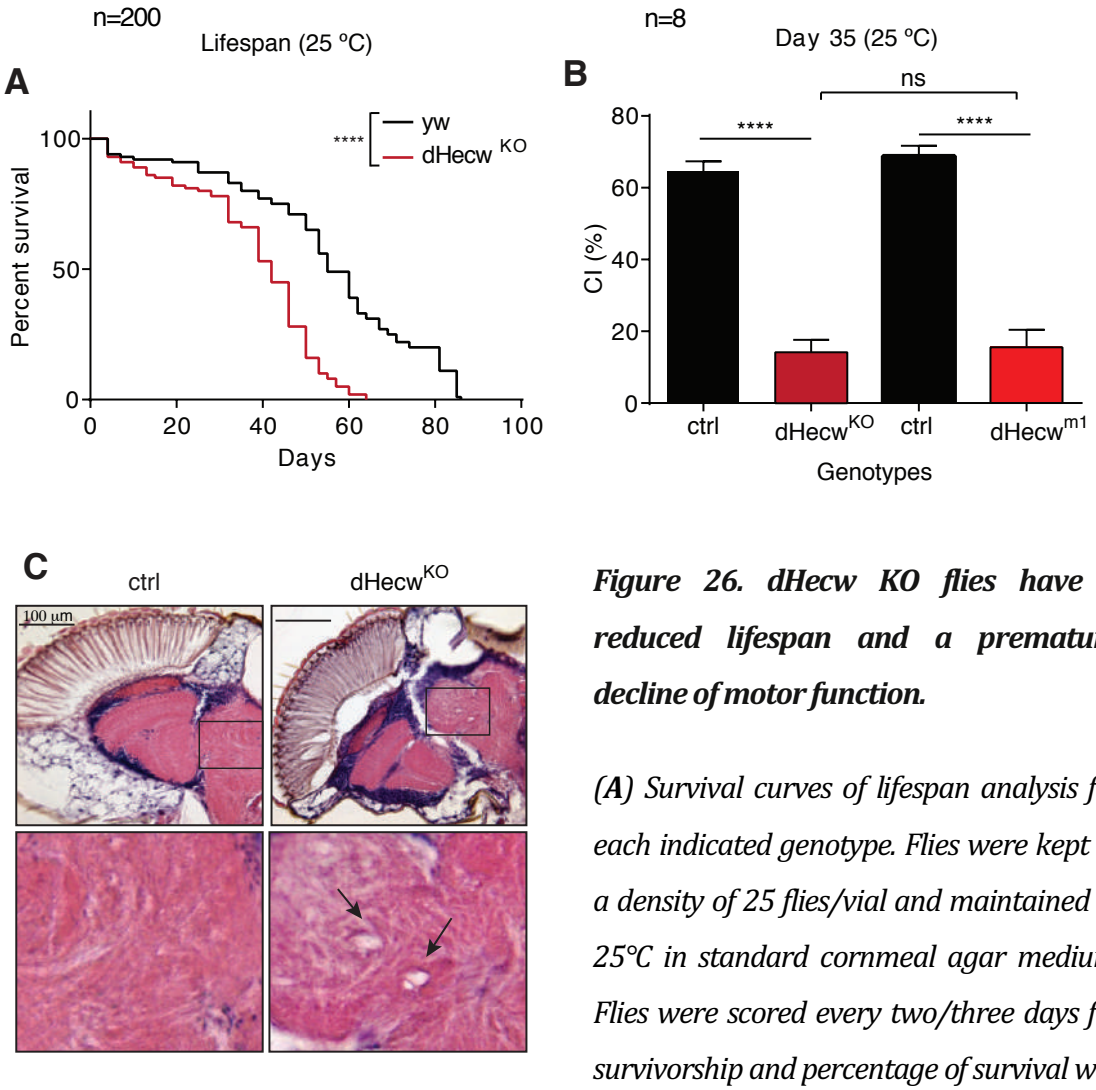

Figure 26. dHecw KO flies have a reduced lifespan and a premature decline of motor function.

*(**A**) Survival curves of lifespan analysis for each indicated genotype. Flies were kept at a density of 25 flies/vial and maintained at 25°C in standard cornmeal agar medium. Flies were scored every two/three days for survivorship and percentage of survival was*

*calculated over 100 animals per genotype. dHecw KO flies show a significant decrease in lifespan compared with the control line (log-rank test, p-value <0,001). (**B**) Motor function was measured during aging, using the negative geotaxis assay. Flies were gently tapped to the bottom of a plastic vial and flies that could climb over the threshold (7 cm) in 15seconds were scored. KO flies show a climbing deficit that is comparable with dHecw mutant flies. Results are presented as a mean of 8 repetitions ± SEM, and differences were measured with multiple comparison test (one-way ANOVA) and Mann Whitney test for single comparison. (**C**) Frontal sections of 35 days old flies were stained with H&E and examined by bright-field microscopy. Scale bar: 100 μm. Magnified views of central brain regions corresponding to the respective boxed areas.*

Finally, dHecw KO ovary and egg chamber morphology analysis revealed similar defects in oogenesis to those encountered in dHecw mutant flies (**Fig. 27**).

The total frequency of defects observed was very similar between the two genotypes, as indicated in **Table 2.** A difference was observed in young flies: while in m1 mutants the majority of the aberrant egg chambers (75%) showed a decreased number of nurse cells, the most prominent defect observed in KO fly ovaries was compound egg chambers. In older flies, in both genotypes, the majority of aberrant egg chambers had supernumerary GCs, and the more recurrent defect was compound egg chambers. Furthermore, as in dHecw mutants, also KO fly ovaries presented misspecification of additional oocytes.

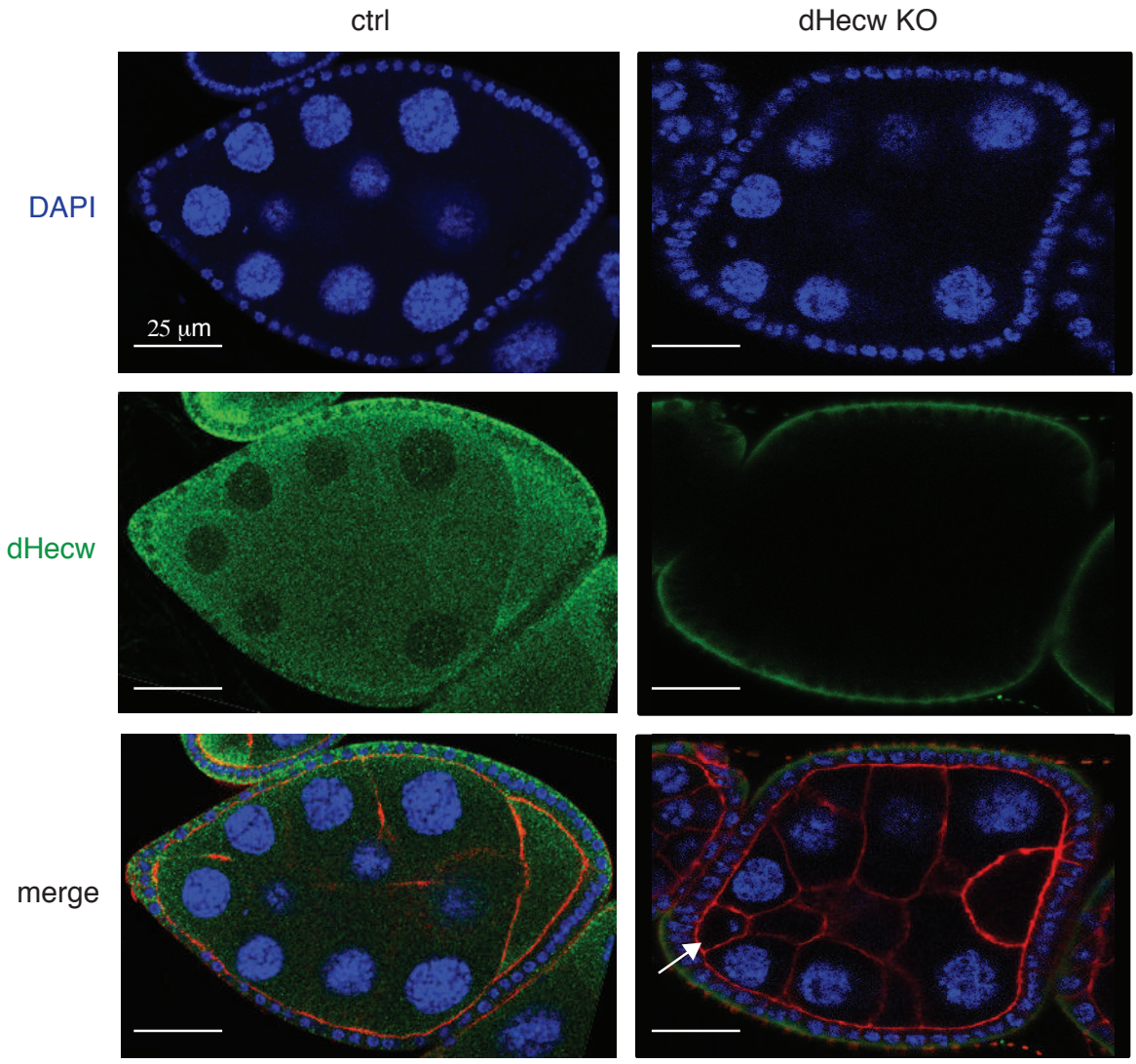

Figure 27. dHecw KO flies have an aberrant oogenesis.

IF analysis of wild type (left panels) and dHecw KO (right panels) fly ovaries were performed with the indicated antibodies. An example of aberrant egg chambers is present in dHecw KO ovaries. White arrows indicate the oocytes of the fused egg chamber at the anterior pole (dHecw KO). dHecw staining is absent in KO fly ovaries. Scale bar: 25 µm

Genotype	Flies age	NC, RC <15	NC, RC >15	Compound egg ch.	Total defective egg ch.
dHecw m1	3-day old	47/338 (**14%**)	6/338 (**2%**)	16/338 (**5%**)	69/338 **(21%)**
dHecw KO	3-day old	8/176 (**5%**)	4/176 (**2,2%**)	17/176 (**9,7%**)	29/176 **(17%)**
dHecw m1	30-day old	14/160 (**9%**)	10/160 (**6%**)	38/160 (**24%**)	62/160 **(39%)**
dHecw KO	30-day old	6/100 (**6%**)	7/100 (**7%**)	22/100 (**22%**)	35/100 **(35%)**

Table 2. Comparison of dHecw mutant and KO defects in oogenesis.

Classification of the defects observed in dHecw mutant and KO fly ovaries, at the indicated time points. Defective egg chambers include reduced/increased number of nurse cells (NC), ring canals (RC), and fused egg chambers (compound egg chambers).

2.6 dHecw activity during oogenesis is germline-specific

Drosophila egg chambers are formed by germline cells (GCs) surrounded by a monolayer of somatic cells constituting the follicular epithelium (FE) (**Fig. 7**). These two tissues are in tight communication in order to coordinate egg development [193]. Thus, the defects in fly egg chamber development could be caused by a requirement for dHecw in the GCs, in the FE, or in both. dHecw appears to be expressed both in the GCs and in the FE. To directly investigate if the defects observed in oogenesis are attributable to functional alterations specifically in one of these two tissues, we took advantage of the UAS-Gal4 system to perform tissue-specific knock down dHecw in FE using the traffic jam-Gal4 driver (tj-Gal4), or in GCs using the nanos-Gal4 driver. Only knock down of dHecw with the GCs-specific driver recapitulated mutant fly phenotypes (**Fig. 28** and data not shown), demonstrating that dHecw regulates oogenesis in a germline specific way.

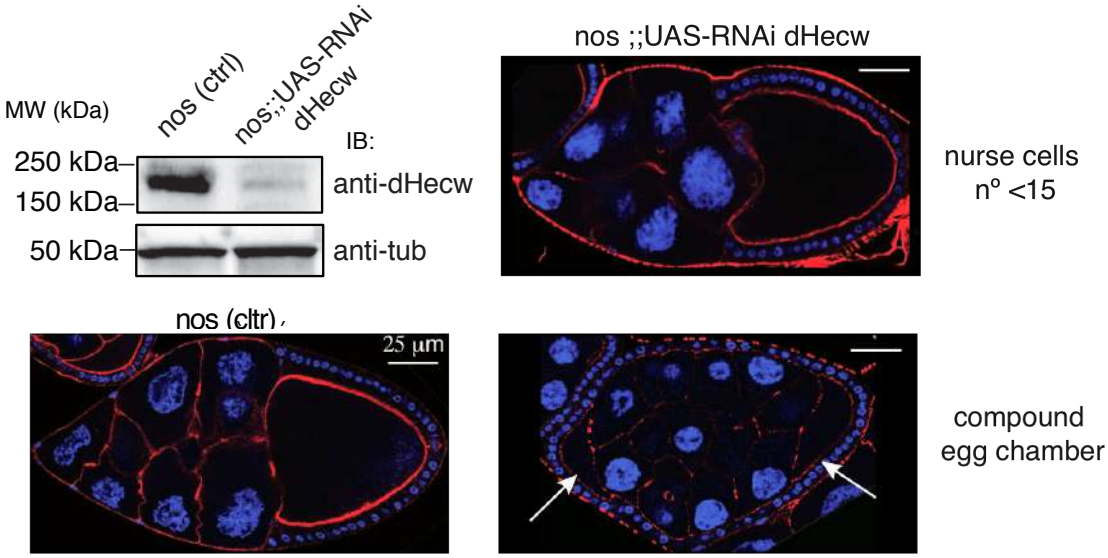

Figure 28. dHecw knock down in the germline recapitulates dHecw mutant and KO oogenesis defects.

Upper, left panel: protein levels in adult fly ovaries were measured by IB analysis with the indicated antibodies. The expression level of dHecw in the interfered fly ovaries (nos;;UAS-RNAi dHecw) is reduced in comparison with wild type control (driver nanos only).
IF analysis of 3 day old control (bottom, left panel) and dHecw KD fly egg chambers (right panels). Observed defects include aberrant number of nurse cells (an example is presented in the upper, right panel) and compound egg chambers (bottom, right panel). White arrows indicate two oocytes present in the fused egg chambers. DAPI, blue; phalloidin, red. Scale bar: 25 µm.

To further investigate the nature of dHecw function during oogenesis, we overexpressed the wild type protein in the germline, taking advantage of a UAS-RFP dHecw line that we generated. Despite the fact that UASt is not optimal for expression in the germline [258], we were able to overexpressed the tag-wild type protein, as shown by IB in **Figure 29**. Interestingly, overexpression of RFP-dHecw induced aberrant egg chamber formation, similar to that found in mutant flies or upon dHecw down modulation (**Fig. 29)**. These results strongly indicate that dHecw activity needs to be tightly regulated at the level of protein expression.

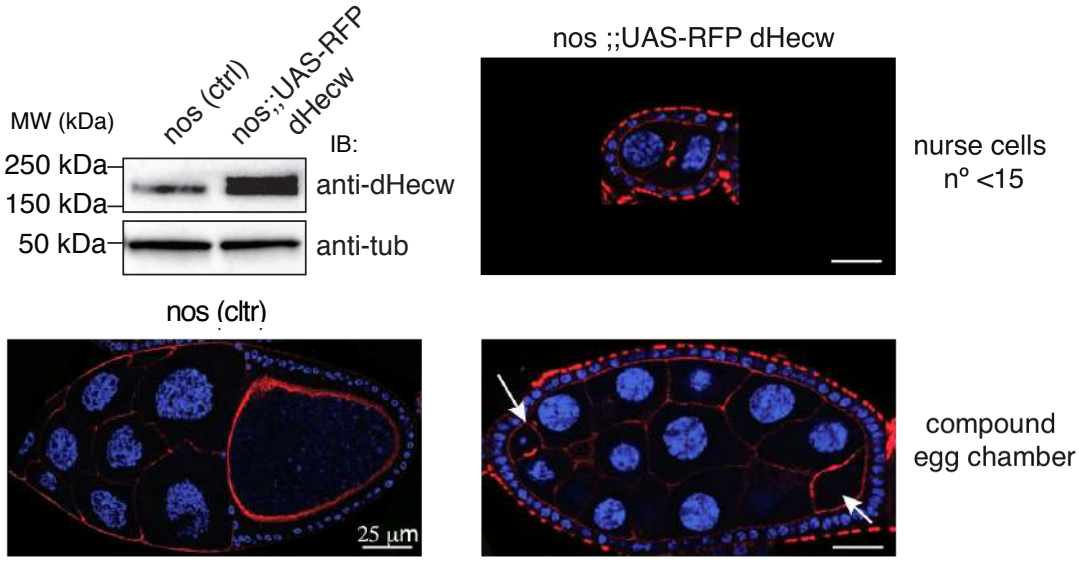

Figure 29. dHecw overexpression in the germline mimics dHecw mutant and KO oogenesis defects.

Upper, left panel: protein levels in adult fly ovaries were measured by IB analysis with the indicated antibodies. The expression level of RFP-tag dHecw in the overexpressed ovaries (nos;;UAS-RFP dHecw) is increased in comparison with wild type control (driver nanos only).
IF analysis of 3 days old control (bottom, left panel) and dHecw overexpression in fly egg chambers (right panels). Observed defects include aberrant number of nurse cells (example is presented in the upper, right panel) and compound egg chambers (bottom, right panel). White arrows indicate two oocytes present in the fused egg chambers. DAPI, blue; phalloidin; red. RFP tag of overexpressed dHecw in the germline is not detectable by IF. Scale bar: 25 µm.

2.7 Ectopic overexpression of dHecw induces the enlargement of endosomal compartment

While tissue-specific knock down in FE did not cause any evident phenotype, ectopic overexpression of RFP-dHecw, using tj-Gal4, led to the formation of large RFP-dHecw puncta. The RFP signal fully co-localized with the signal detected by the anti-Hecw antibody confirming the presence of the dHecw protein (**Fig. 30**).

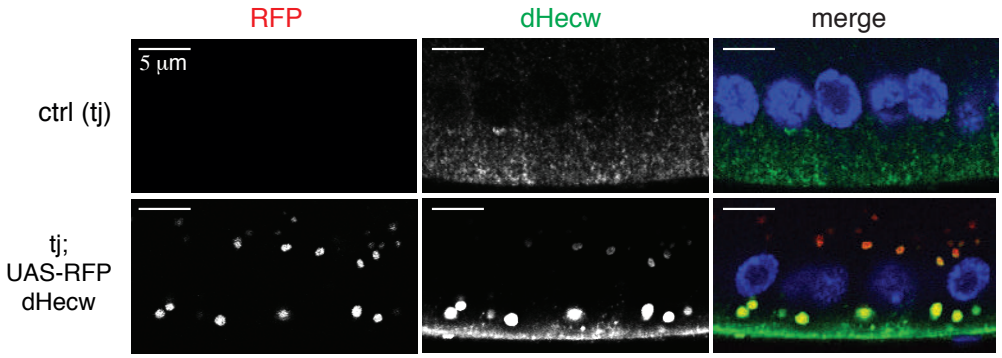

Figure 30. RFP-dHecw overexpression in fly follicle cells.

IF analysis of Drosophila follicle cells with the indicated antibodies/fluorescent tag. Lateral section: RFP-dHecw is overexpressed in follicle cells with the traffic jam-Gal4 driver (tj).
Upper panel: control (tj driver only) shows no RFP signal but a broad dHecw staining in the cytoplasm. Lower panel: overexpression of RFP-dHecw shows RFP puncta that co-localizes with dHecw antibody signal (green). Scale bar: 5 µm.

Because the Nedd4 family members often act during internalization of endocytic cargoes and to characterize the nature of the puncta, we performed a co-localization analysis with known markers of endocytic compartments. We found that dHecw puncta did not co-localize with the early endosome marker syntaxin 7/Avalanche, but partial co-localization was detected with Hrs, a component of the ESCRT0 complex involved in endosomal sorting, which often decorated a subdomain on the surface of some of the puncta (**Fig. 31A**). These data suggest that dHecw might associate with the sorting compartment of maturing endosomes. Indeed, staining with the multivescicular body marker Shrub, an ESCRT III component, revealed a complete co-localization with RFP-dHecw puncta (**Fig. 31A**). Shrub puncta were not present to such extent in non-overexpressing cells, indicating that the dHecw compartment is a neomorphic and possibly enlarged late endosomal organelle. In line with these results, the largest puncta in overexpressing cells accumulate on the basal membrane of the FE, where late endosomes and lysosomes localized, while puncta on the apical side are smaller (**Fig. 31B**).

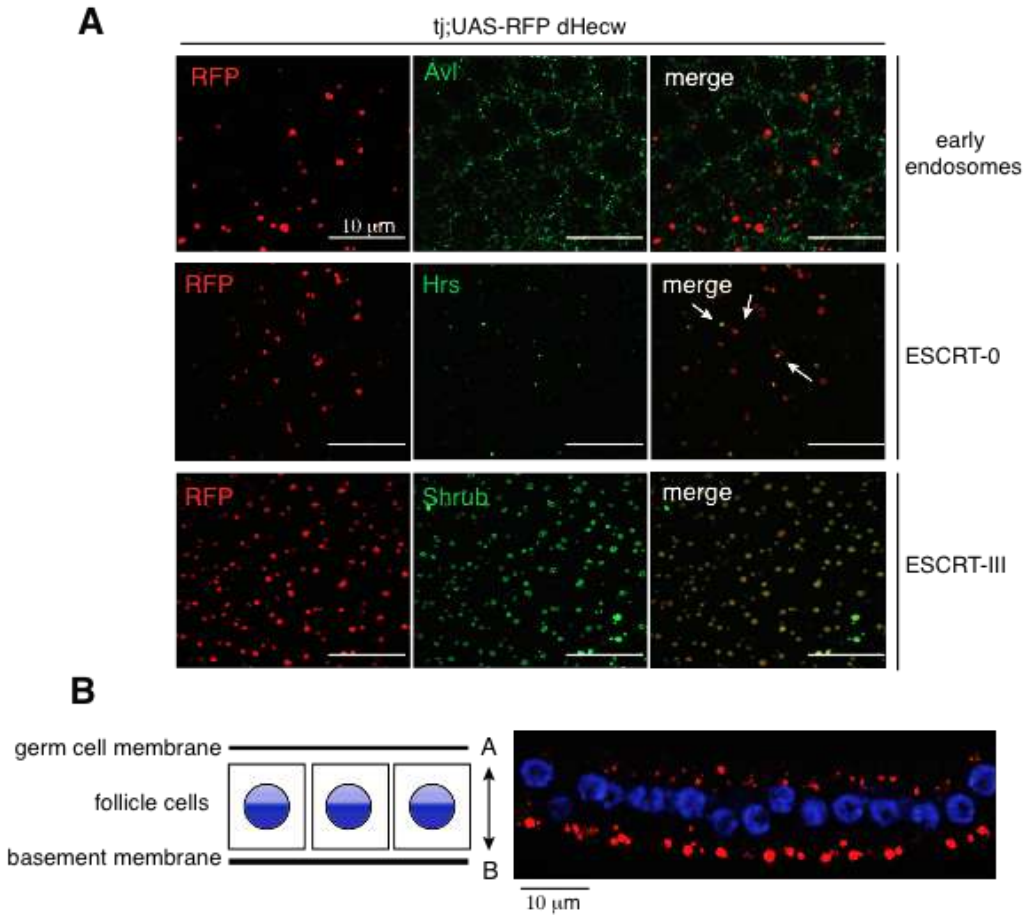

Figure 31. RFP-dHecw in fly follicle cells co-localizes with a MVB marker.

*IF analysis of Drosophila follicle cells with the indicated antibodies/fluorescent tag. RFP-dHecw is overexpressed in follicle cells with the traffic jam-Gal4 driver (tj). (**A**) Upon RFP-dHecw overexpression, RFP puncta do not co-localize with the early endosome marker Avalance (Avl), and partially co-localizes with the ESCRT-0 component Hrs (white arrow). High levels of co-localization are observed between RFP-dHecw and the ESCRTIII component (Shrub).*

*(**B**) Schematic representation of follicle cell epithelium; right, lateral section of follicle cell epithelium. Left: RFP-dHecw puncta are smaller under the apical FC surface and increase in size at the basal side. DAPI, blue; phalloidin; red. Scale bar: 10 µm.*

To gain more insights into the nature of the dHecw puncta, we took advantage of a fly line transgenic for the transmembrane portion of the glycoprotein CD8 fused with GFP (UAS-CD8 GFP) to label membranes, expressed in the larval wing disc pouch using the MS1096-Gal4 driver. Ectopic overexpression of RFP-dHecw in this line also led to the formation of dHecw puncta that co-localize with GFP-CD8, indicating that the dHecw ectopic puncta are likely organelles surrounded by membranes (**Fig. 32**).

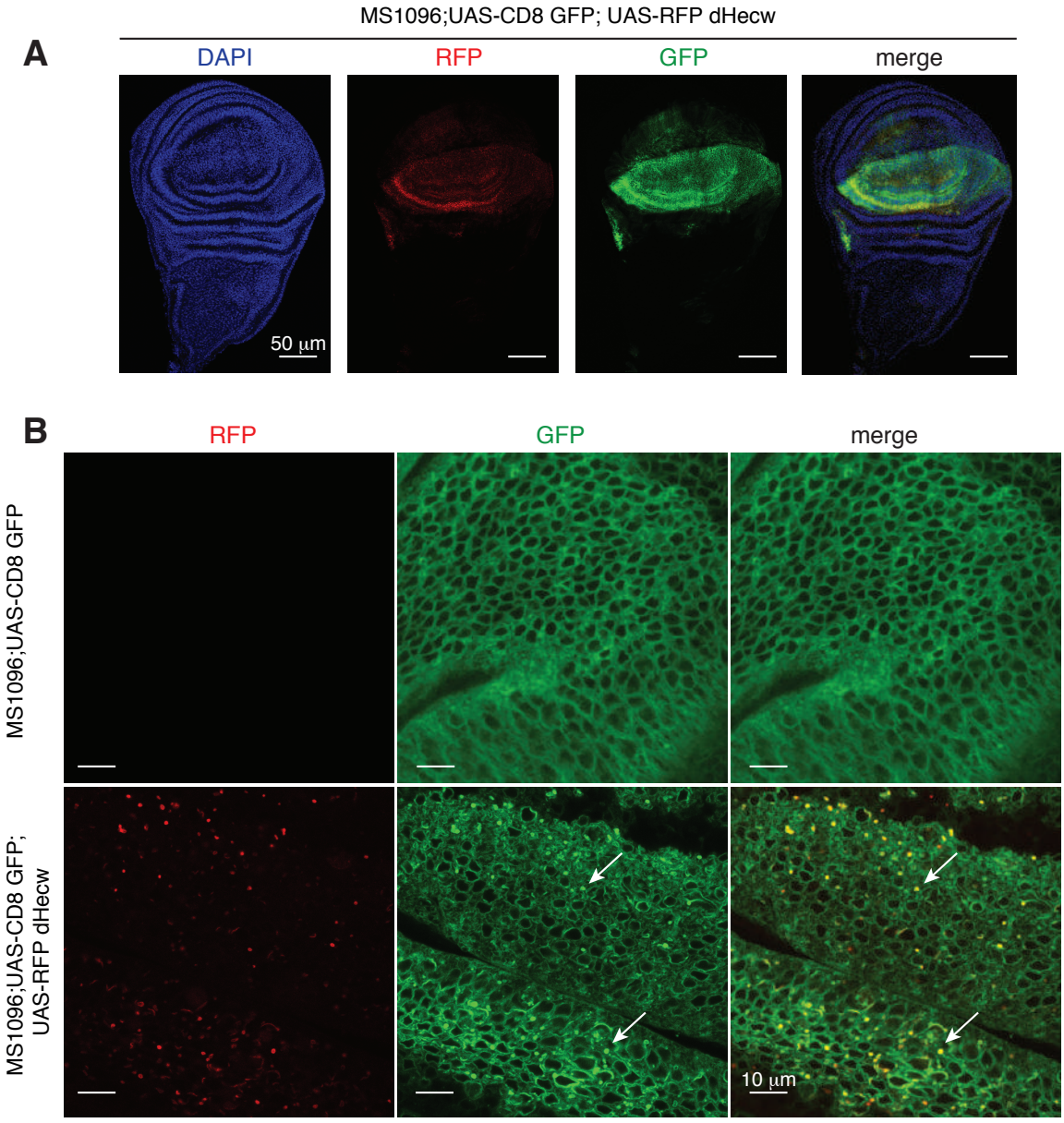

Figure 32. RFP-dHecw overexpression in the fly wing disc.

*IF analysis of Drosophila larval wing disc. (**A**) RFP-dHecw and CD8-GFP are overexpressed under the MS1096-Gal4 driver (dorsal wing disc pouch). Scale bar; 50 µm. (**B**) Upon RFP-dHecw overexpression, the membrane marker GFP-CD8 forms dots (white arrow, central bottom panel) that co-localize with RFP-positive puncta (white arrow, bottom left panel). Scale bar; 10 µm*

As shown in **Figure 33A**, dHecw puncta are positive for ubiquitin, which seems to massively re-localize from a diffuse cytoplasmic staining (visible in the control) to dHecw puncta. Staining with ubiquitin chain-specific antibody indicated the presence of K63-linked ubiquitin-modified substrates. This suggests that dHecw, as HECW1 and the other NEDD4

members [58],[259], is capable of generating K63-specific ubiquitin chains not only *in vitro* but also *in vivo*. K63-linked ubiquitin chains are known to be involved in endocytosis [17] and in autophagy as the autophagic receptor Ref(2)P - p62 in human - binds these specific chains with high affinity [260]. We, thus, stained dHecw overexpressing follicle cells with Ref(2)p and found co-localization with RFP-dHecw puncta (**Fig. 33B**). These data indicate that the late endocytic organelles induced by excess dHecw contain autophagy cargoes and, thus, could be tentatively classified as amphisomes, the organelles formed by the fusion of autophagosomes with multivescicular bodies [261].

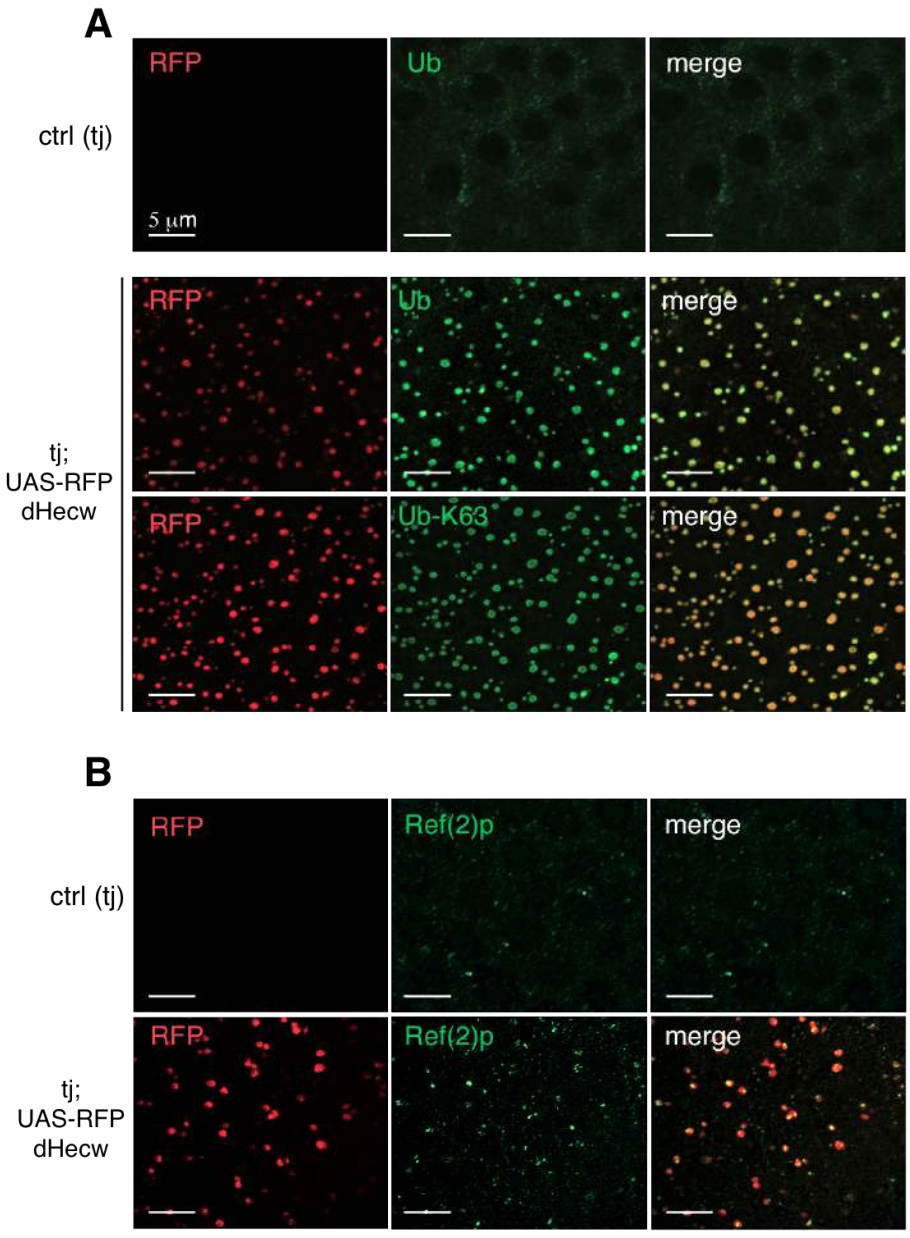

Figure 33. RFP-dHecw in follicle cells co-localizes with Ref(2)p, Ub and Ub-K63.

*IF analysis of Drosophila follicle cells with the indicated antibodies/fluorescent tag. RFP-dHecw is overexpressed in follicle cells with the traffic jam-Gal4 driver (tj). (**A**) RFP positive dHecw puncta (red) co-localizes with Ub and Ub-K63 chains (green). (**B**) RFP positive dHecw puncta co-localizes with the autophagic receptor Ref(2)p (green). Scale bar: 5 µm.*

2.8 dHecw is involved in autophagy Atg7

To test how dHecw might act on autophagy, we overexpressed tag-dHecw wild type in fly ovaries with traffic jam-Gal4 and in fly heads with elav-Gal4, and analyzed the levels of Ref(2)p in protein extracts. IB analysis showed a sharp decrease in Ref2P levels in dHecw overexpressed heads and ovaries compared with controls (**Fig. 34**).

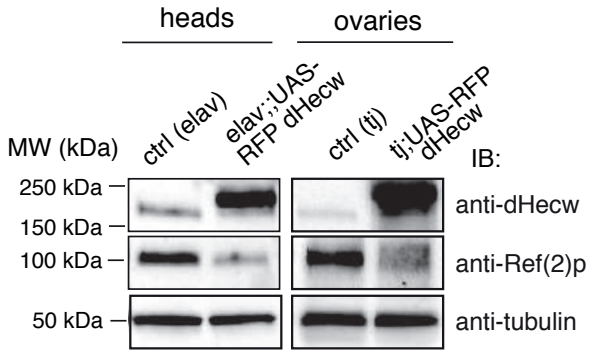

Figure 34. Immunoblot of dHecw overexpression in adult fly brain and ovaries.

IB analysis of proteins from RFP-dHecw overexpression in adult fly heads (elav-Gal4 driver) and ovarian follicle cells (tj, traffic jam-Gal4 driver). The level of Ref(2)p is decreased compared with the control line (drivers only).

Reduced Ref(2)p level is a feature often associated with an induction of the autophagic flux [262]. If dHecw would play a role in autophagy induction, its lack should lead to the accumulation of Ref(2)p, typical sign of autophagic flux impairment [262]. We, thus, assessed Ref(2)p levels in extracts of dHecw mutant fly heads and detected a major increase in the level of Ref(2)p (**Fig. 35**). Consistent with the possibility that dHecw might contribute to the induction of autophagy, the neurodegenerative phenotypes observed for dHecw mutant and KO flies closely resemble the ones caused by the lack of the positive autophagy regulator *Atg7*

[263]. Atg7 encodes for a non-essential evolutionarily conserved E1-activating enzyme that is strictly required to induce *de novo* formation of an autophagosome around Ref(2)P-positive cargoes to be degraded.

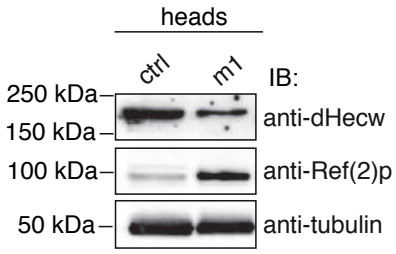

Figure 35. Immunoblot of dHecw mutant adult fly heads. *IB analysis of proteins of dHecw mutant adult fly brain lysates (3 day old flies). The level of Ref(2)p is increased in dHecw mutant (m1) compared with the control line (yw, ctrl).*

The comparison of brain tissue vacuolarization in Atg7 and dHecw mutants revealed similar amount of vacuoles in both mutant genotypes (**Fig. 36 A,B**).

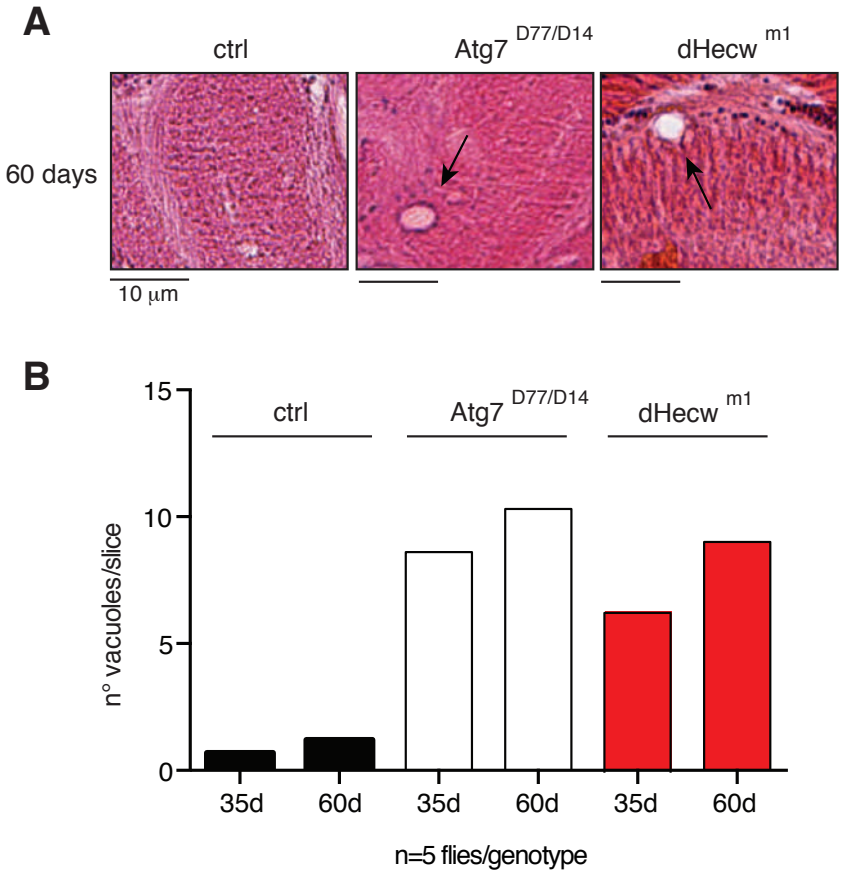

Figure 36. dHecw and Atg7 mutants present comparable fly brain vacuolarization.
Upper panel: a zoom of frontal sections of 60 days old fly brains were stained with H&E and examined by bright-field microscopy. Bottom panel: quantification of the vacuoles (>2 μm) in various brain slices of 5 flies/genotype. The results are presented as mean ± SEM (left panel). Wild type control (black), Atg7 mutant (white), dHecw mutant (red). Scale bar; 10 μm.

To understand how dHecw acts in autophagy, we compared the effect of lack of Atg7 or dHecw on the induction of autophagy by fly starvation on agar-molasses medium. The ovary is a nutrition-sensitive organ, and starvation is well known to inhibit ovary development with clear consequences in terms of egg production and ovary size [264]. The autophagic pathway has previously been shown to be activated under starvation conditions specifically in the germarium, during (stage7-8 previtellogenic) and late oogenesis (stage 12-13, nurse cells degeneration) [265]. In fed condition, few small Ref(2)P puncta are present in the germaria (**Fig. 37A**). Upon 48 hours starvation of wild-type females, autophagic induction results in the formation of Ref2P positive autophagosomes, which are ubiquitin positive (**Fig. 37B**). In sheer contrast, in $Atg7^{D77/D14}$ mutants, in which the autophagic flux is blocked, the large Ref(2)P- and ubiquitin-positive accumulation of cargoes are present also in fed conditions (**Fig. 37C**). Strikingly, in both the dHecw m1 mutant and the KO mutant, the Ref(2)P and ubiquitin puncta are not forming as it occurs in fed germaria (**Fig. 37 F,H**). These preliminary results indicate that dHecw might be required for the induction of the autophagy upstream of Atg7, possibly at the level of the autophagic cargoes organization.

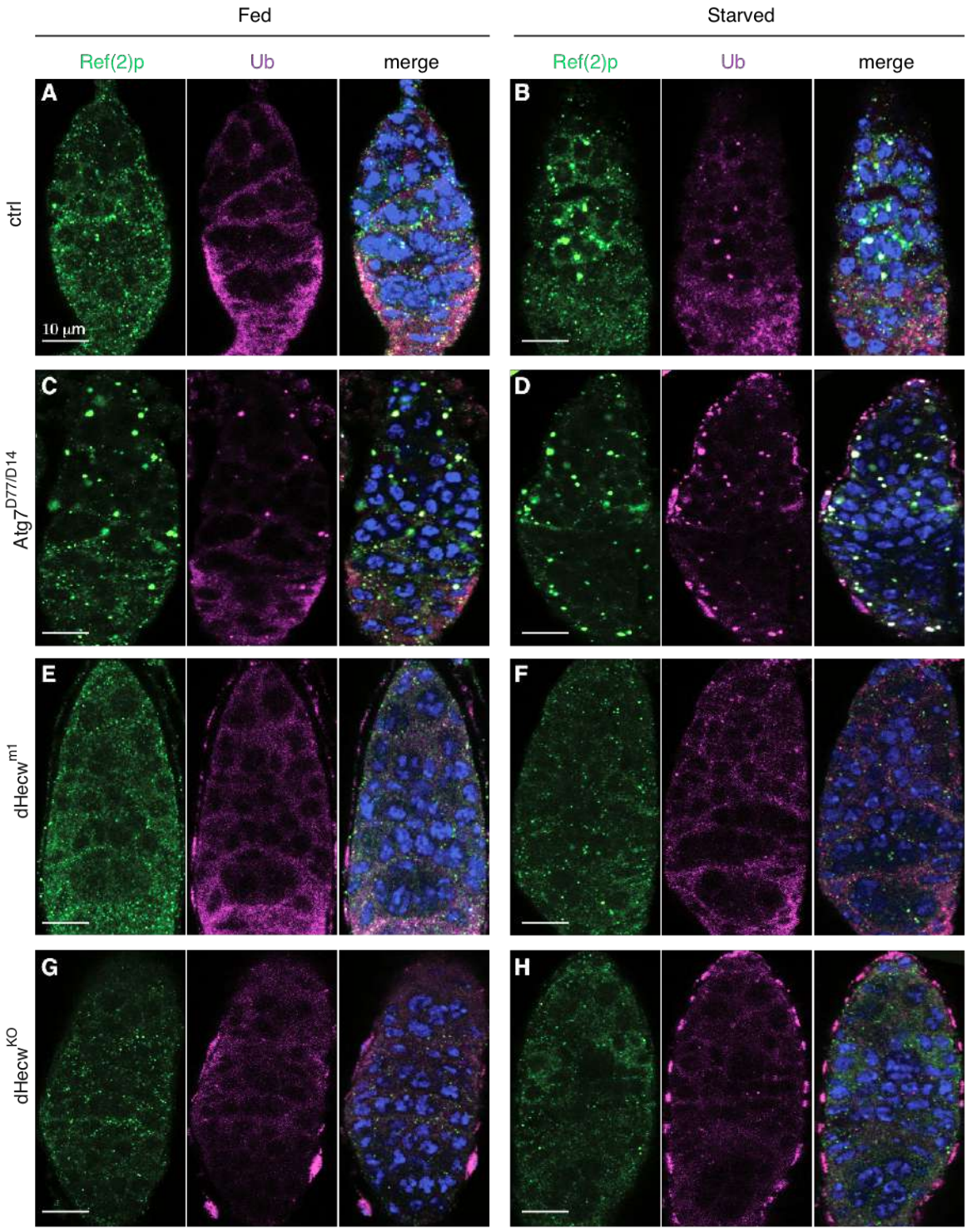

Figure 37. Starvation induces autophagy in fly ovaries.

*IF analysis of germaria of fed (**A, C, E, G**) and starved flies (**B, D, F, H**). Starvation was performed for 48 hours on agar-molasses medium. (**B**) Germaria from starved flies accumulate autophagy adaptor Ref2p in big puncta, in which the ubiquitin signal is re-localized. (**C**) Atg7$^{D77/D14}$ mutants present Ref2p-ubiquitin puncta also in fed condition. (**F, H**) On the contrary, dHecw^{m1} and dHecw^{KO} do not show any puncta in starved conditions. Scale bar; 10 µm.*

3. dHecw interacts with mRNA processing proteins

3.1 Identification of dHecw physical interactors with mass spectrometry

To gain insights into dHecw molecular function, we searched for its interactors and substrates, using two biochemical approaches. First, we took advantage of the antibody we generated to immunoprecipitate endogenous dHecw from *Drosophila* S2 cells that express good levels of the dHecw protein (**Fig. 38**).

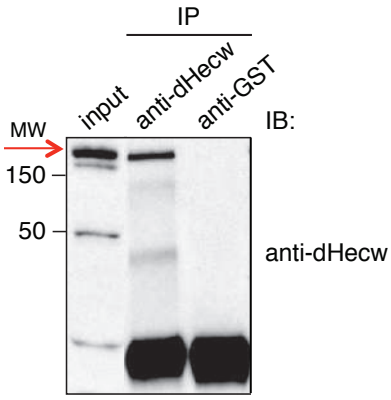

Figure 38. dHecw immunoprecipitation from S2 cells. *An example of IP and IB analysis of S2 cell lysate performed with dHecw antibody. Anti-GST antibody was used as control for the IP. The red arrow indicates dHecw.*

Second, we used a GST-tagged dHecw fragment that encodes the WW domains (aa 637-831) to pulldown interactors from S2 cellular lysate. The pulldown/immunoprecipitated proteins were visualized by gel electrophoresis and identified by mass spectrometry in collaboration with the IFOM proteomic facility. Candidate interactors are listed in **Table 3.** The interactome identified for dHecw with these approaches is relatively small, as pulling together the IP and two pulldown experiments resulted in 55 candidates. However, by GO, we observed an evident enrichment in specific protein categories, the most prominent being that of mRNA binding proteins implicated at various steps of mRNA processing. Among them there are some known mRNA translational repressors like Fmrp, Hrp48 and Glorund that have been implicated in the control of mRNA local translation in the *Drosophila* oocyte [206], [266]. We also identified several cytoskeleton and motor proteins, like kinesin, which are known to take part in the transport of ribonucleoparticles (RNPs). These are structures responsible for temporal and

spatial control of mRNA translation. Proteins involved in mRNA processing are the top hit category also in the human HECW1 interactome, characterized in a parallel study performed in the laboratory. Among the identified proteins, the Fragile X-mental retardation proteins (FMRPs), identified in both the human (data not shown) and the *Drosophila* datasets (**Table 3**), are of particular interest due to their disease implications and thus, we further examined the relationship between dHecw and dFmrp.

gene name	function	GST-pull down	IP	WW interaction motif
Hrb27C/Hrp48	Heterogeneous nuclear ribonucleoprotein at 27C	X		PY
Hrb98DE/Hrp38	Heterogeneous nuclear ribonucleoprotein at 98DE		X	PY(x2), PR
Fmr1 *	Fragile X mental retardation syndrome-related protein	X		PR
bel	ATP-de ndent RNA helicase bel	X		PR (x3)
larp	La-related protein 1, mRNA binding repressor	X		PR(x5), PY
Ef1alpha	Elongation factor 1-alpha	X	X	PY
EF2	Elongation factor 2	X		PR
eIF-4a	Eukaryotic initiation factor 4a		X	/
CG10077	ATP-dependent RNA helicase DEAD-box	X		PR (x2), PY
Rpll215	DNA-directed RNA polymerase II subunit RPB1	X		PR(x5), PY
nito	spenito,mRNA binding protein, splicing	X		PR(x5), PY (x4)
lig	linger, mRNA binding protein	X		PR, PY
glo	glorund, mRNA binding protein	X		PY(x2)
nonA	No-on-transient A, putative RNA binding protein	X		PR (x3), PY
abs	abstrakt,DEAD-box helicase		X	PY(x2), PR
Acn	Acinus, mRNA splicing, autophagy regulation		X	PR (x2)
CG7878	DEAD box RNA helicase	X		PR
unkempt	mRNA binding, ubiquitin			PPxY, PY(x2), PR(x3)
HBS1	GTPase. Pelo-Hbs1 mRNA surveillance complex		X	PR (x2)
Hsc70-3	Heat shock 70-kDa protein cognate 3	X		PR (x2)
Hsp60	60 kDa heat shock protein, mitochondria	X		PY
Hsc70-4-RA	Heat shock protein cognate 4	X		/
CG7033	Heat Shock Protein 60 chaperonins	X		PR
betetub56D	Tubulin beta-1 chain	X		PR(x4), PY
betetub60D	Tubulin beta-3 chain	X		PR (x3), PY
Act5C	Actin 5C	X		PR (x2)
zip	myo II	X		PR, PY
Eb1	Eb1, myosin and microtubule binding	X		PR
CG5787	microtubule associated complex	X		PR (x2), PY (x2)
tsr	Cofilin/actin-depolymerizing factor homolog		X	/
Chc	Clathrin heavy chain		X	PY(x2), PR
Khc	Kinesin heavy chain OS		X	PR (x2), PY
ck	Myosin VII		X	PR (x2), PY
RhoGAP15B	RhoGAP15B, isoform B	X		PR(x4), PY, PPXY (x2)
14-3-3zeta	E3 adaptor, signaling	X		/
Ack	Activated Cdc42 kinase	X		PR, PY
Rack1	Receptor of activated protein kinase C 1	X		/
His1	Histone1	X	X	/
mod(mdg4)	Modifier of mdg4		X	PR, PY
mod	DNA-binding protein modulo		X	PR (x3)
stnw	Stonewall, transcriptional factor		X	PR(x7)
jub	Ajuba LIM protein	X		PR (x2), PY
l(1)G0193	Lethal (1) G0193	X		PR (x2)
CG3800	zinc ion binding; nucleic acid binding	X		/
Vhc55	Vacuolar H[+]-ATPase 55kD B subunit, isoform C	X		PR (x3)
Aldh	Aldehyde dehydrogenase	X		PY
blw	ATP synthase subunit alpha, mitochondrial OS	X		PY
ATPsyn-beta	ATP synthase subunit beta	X		PY
Ns1	Guanine nucleotide-binding protein-like 3		X	PR (x2)
pxn	Peroxidasin		X	PR(x4)
CG1516	pyruvate carboxilase		X	PR(x5), PY(x2)
Phb2	Prohibitin, Lethal (2) 03709, isoform E		X	PR, PY
Cyp4d20	Probable cytochrome P450 4d20		X	PR, PY
CG7028	protein serine/threonine kinase activity		X	PR (x3), PY (x2)
RpS3	40S ribosomal protein S3	X	X	/
sta	40S ribosomal protein SA	X	X	PR

Table 3. dHecw interactome.

Complete list of dHecw candidate interactors identified by mass spectrometry analysis and not present in GST control. Red, proteins involved in mRNA binding and processing, grey, cytoskeleton and motor proteins.

3.2 dHecw and dFmrp interact genetically

The defects in oogenesis of dHecw mutant flies strongly resemble the ones described for *dfmr1* loss of function flies [206]: indeed, both mutants present an altered number of nurse cells, compound egg chambers and oocyte misspecification with similar penetrance, suggesting that these two proteins might act in the same pathway (**Fig. 39**).

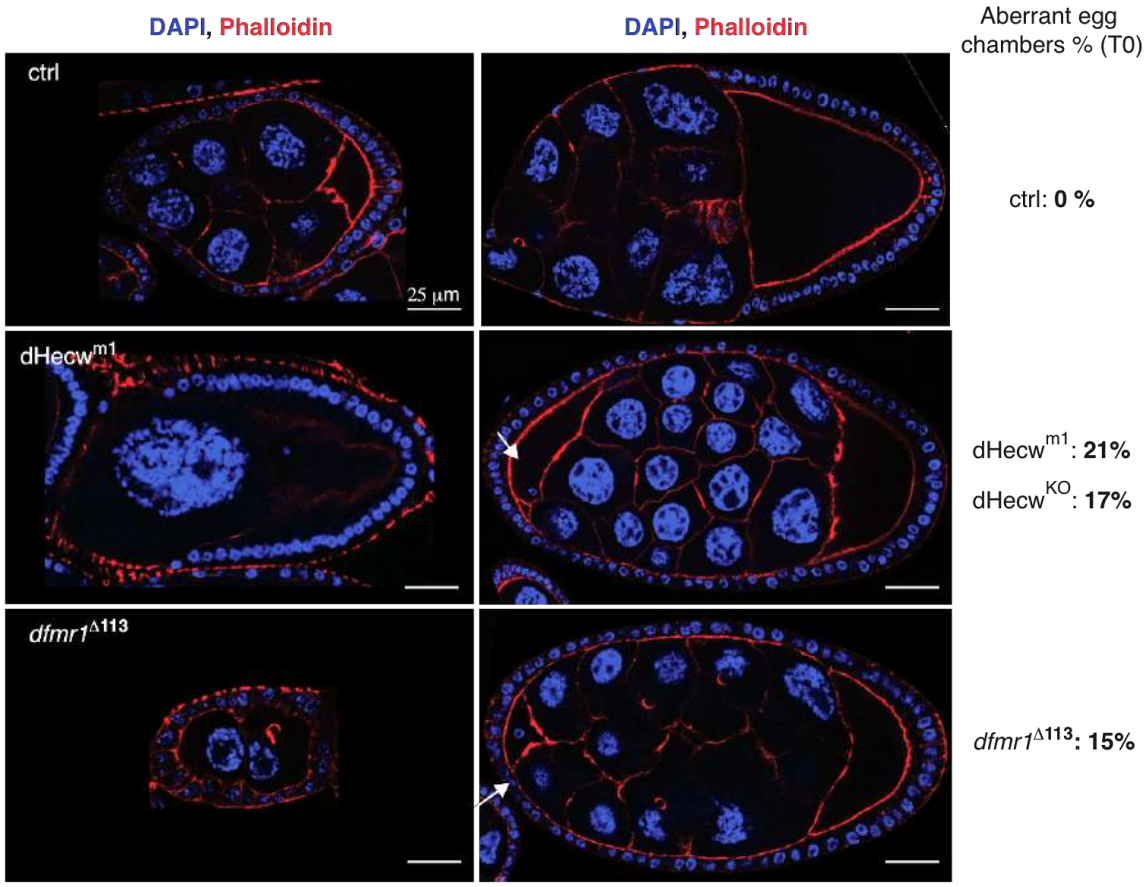

Figure 39. Aberrant egg chambers in dHecw mutant/KO and dFmr1 mutant flies.
IF analysis of 3 days old (T0) wild type, dHecw (dHecw^{m1}) and dFmr1 mutant (dfmr1$^{\Delta 113}$) fly egg chambers. An example of aberrant egg chambers is present in both dFmr1 and dHecw mutant flies: egg chambers with less than 15 nurse cells (left panels) and compound egg chambers (right panels). The white arrows indicate the oocytes of the fused egg chamber at the anterior pole. Percentages of the defects are indicated on the right. Scale bar; 25 µm.

To test whether *dHecw* and *dFmr1* interact genetically, we crossed our dHecw lines with Fmrp loss of function mutants *dfmr* $^{\Delta 113}$ [267]. Since this allele is not viable in homozygosis, we analyzed the effect of *dfmr* $^{\Delta 113}$ heterozygosity in the context of homozygous dHecw mutants. In

this genetic background, the percentage of egg chambers with altered number of nurse cells or fused egg chambers was not altered. However, we observed that 94% of egg chambers presented nurse cells with nuclei of different size, suggesting a massive loss of nurse endocycle synchronization (**Fig. 40A**). We observed this phenotype in single dHecw mutant with low frequency. A second defect that increased was oocyte misspecification: while in dHecw^{m1} 7% of total egg chambers presented this aberration, in dHecw$^{m1/m1}$- *dfmr* $^{\Delta 113/+}$ almost 70% of egg chambers had this defect (**Fig. 40B**). In dHecw$^{m1/m1}$-*dfmr*$^{\Delta 113/+}$ ovaries we also noticed the presence of several apoptotic egg chambers (33.2%). dHecw^{m1} flies presented about 4% apoptotic egg chambers in fed condition, while this number was close to 0 % in wild type fed flies (n=150). Overall, these data support our hypothesis that dHecw and dFmrp could work on the same axis, and be responsible for a subset of the functions of dHecw.

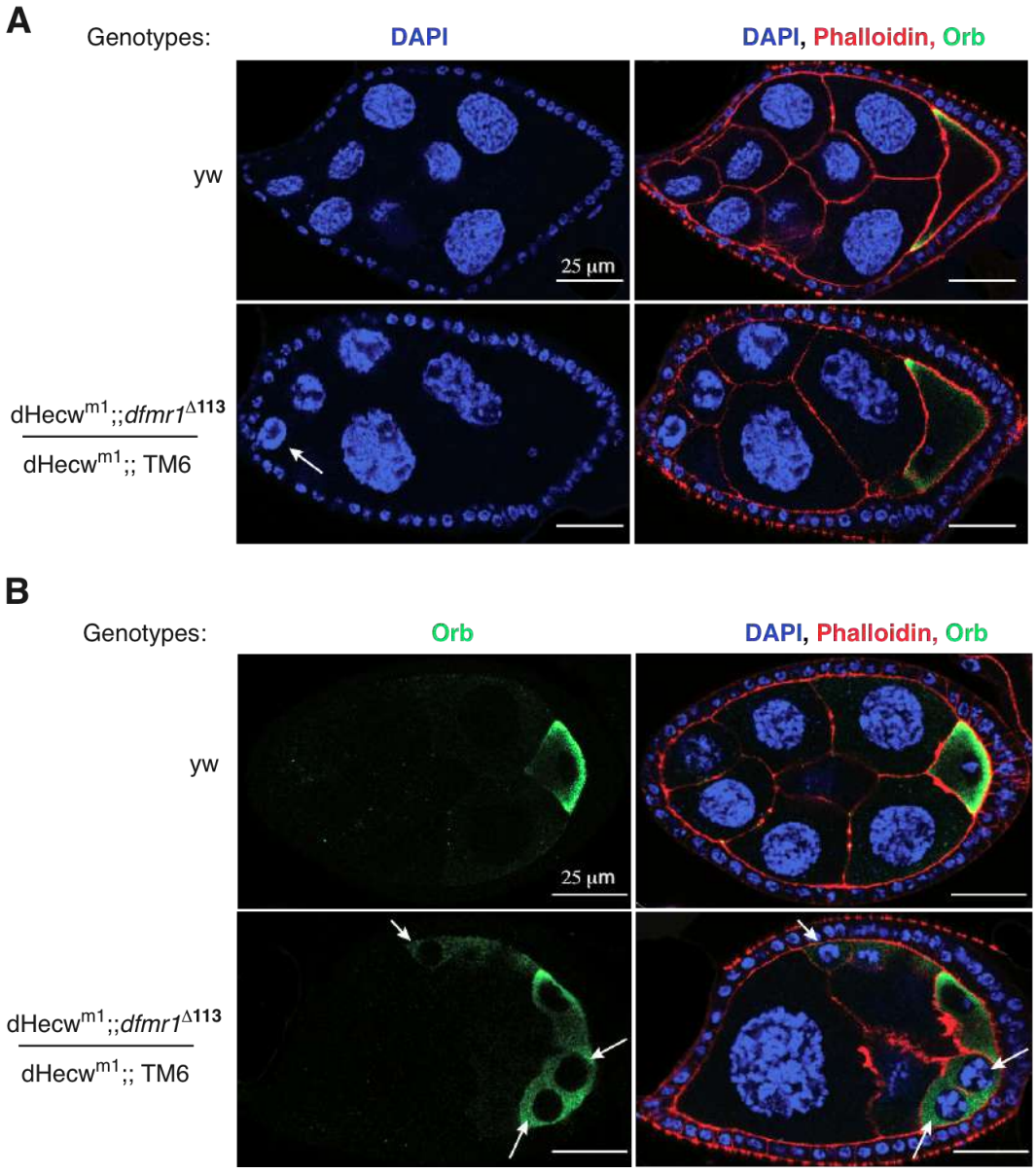

Figure 40. dHecw- dFmr1 genetic interaction.

*IF analysis of 3 days old wild type (yw) and dHecw-dFmr1 mutants (dHecw^{m1}-dfmr1$^{\Delta 113}$) fly egg chambers. The dHecw mutation is in homozygosis while the dFmr1 null allele is balanced over a 3rd chromosome balancer (TM6). (**A**) In many double mutant egg chambers, nurse cells have condensed nuclei of different sizes (white arrow). (**B**) dHecw^{m1}-dfmr1 $^{\Delta 113}$ mutant flie present extensive oocyte misspecification, indicated by extra-Orb positive germ cells (white arrows). Scale bar; 25 µm.*

3.3 dFmrp is a potential substrate of dHecw

FMRPs are nucleo-cytoplasmic shuttling proteins that are integral parts of RNP complexes and that control mRNA stability, localization and translational repression [268]. While in humans three genes belong to this family, *Drosophila* possesses a single ortholog, called *dFmr1*, whose structural domain composition is reported in **Fig. 41A**. Of note, dFmr1 possesses two proline-rich domains (PRs) at its C-terminal, which could be recognized by WW domains.

To test whether dFmr1 is a substrate of dHecw, we took advantage of our *in vitro* ubiquitination assay. *dFmr1* gene was cloned by PCR into a pET43, using as a template the cDNA obtained from wild type fly ovaries, where the gene is highly expressed. The His-MBP-tagged dFmr1 was produced in bacteria, purified and used as a substrate for GST-dHecw. As negative control for the reaction, we performed the same assay without the E2 or without the E3, and with the previously characterized dHecw catalytically inactive mutant (C1394W). Strikingly, we found that dFmrp is ubiquitinated *in vitro* by dHecw, as indicated by the ubiquitin signal starting from the molecular weight of the His-MBP-dFmrp (120kDa), but not by catalytically inactive dHecw (**Fig. 41B**).

To further investigate a possible functional relationship between dHecw and dFmrp, we examined their physiological subcellular localization in ovaries of wild type flies (**Fig. 42**). Published data show that dFmrp has a broad pattern of expression in the egg chamber, localizing both in follicle cells and in the germline, and that, during previtellogenesis (stages 1–7 of oogenesis), dFmrp concentrates at the posterior end of the oocyte [206]Despite some penetration problems with the antibodies, this expression pattern closely resembled the one we observed for dHecw, and co-localization by IF confirmed this data (**Fig. 42**).

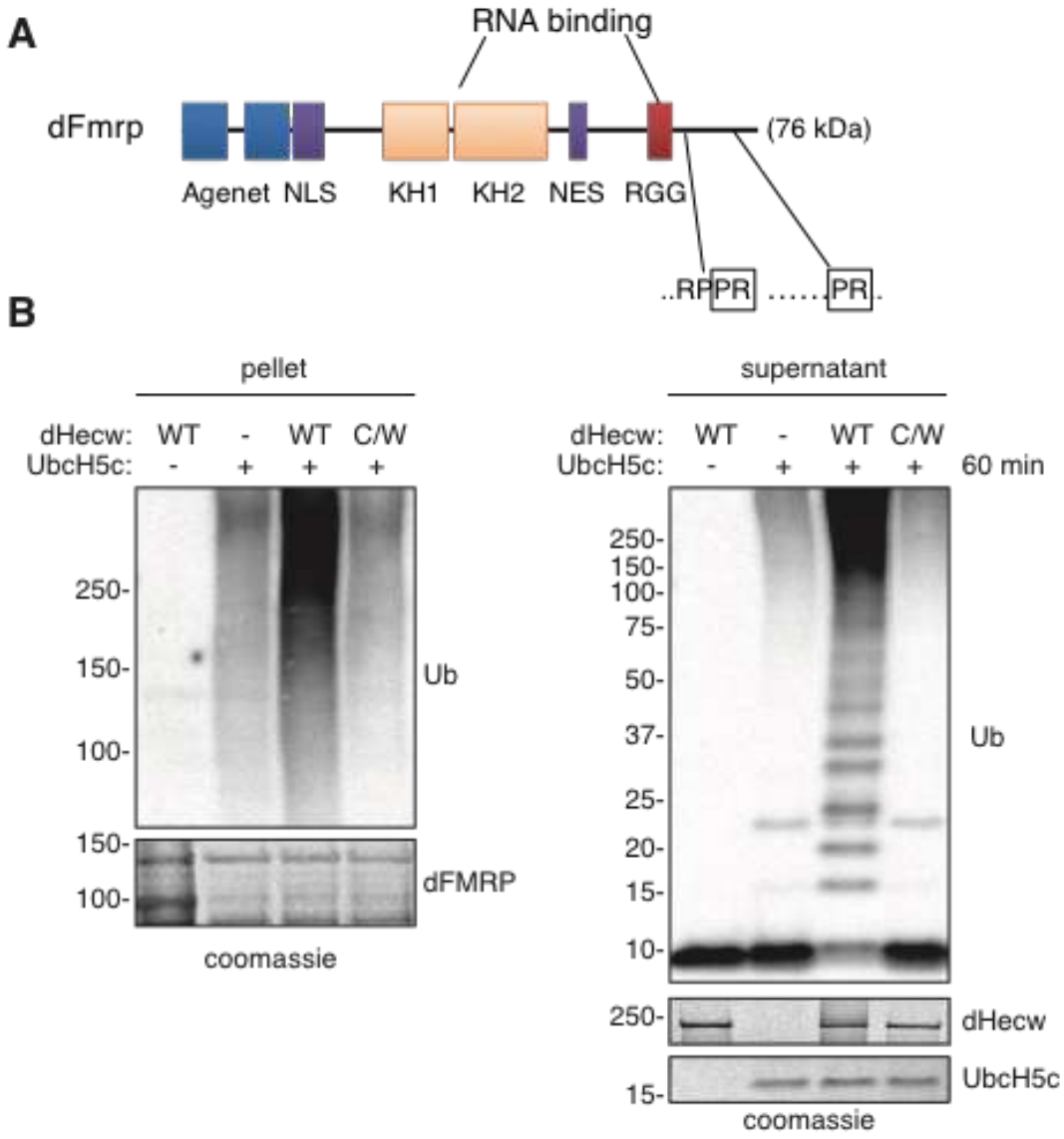

Figure 41. dFmrp is ubiquitinated by dHecw in vitro

*(**A**) Schematic representation of Drosophila Fmrp protein. From the N-terminus, domain architecture is composed of two Agenet domains (blue), a Nuclear Localization Sequence (NLS, violet), two KH1 domains (pink), one Nuclear Export Sequence (violet), and a RGG box (red). RNA binding domains are highlighted. Two proline-rich regions are present in the C-terminus part of the protein. (**B**) In vitro ubiquitination assay of dFmrp with the indicated recombinant E2 and E3 enzymes, analyzed by IB anti-ubiquitin (upper panels). Left panels: IB of proteins present in the reaction pellet (substrate). Right panels: IB of proteins present in the reaction supernatant (enzymes). The coomassie staining shows comparable levels of loaded protein (lower panels).*

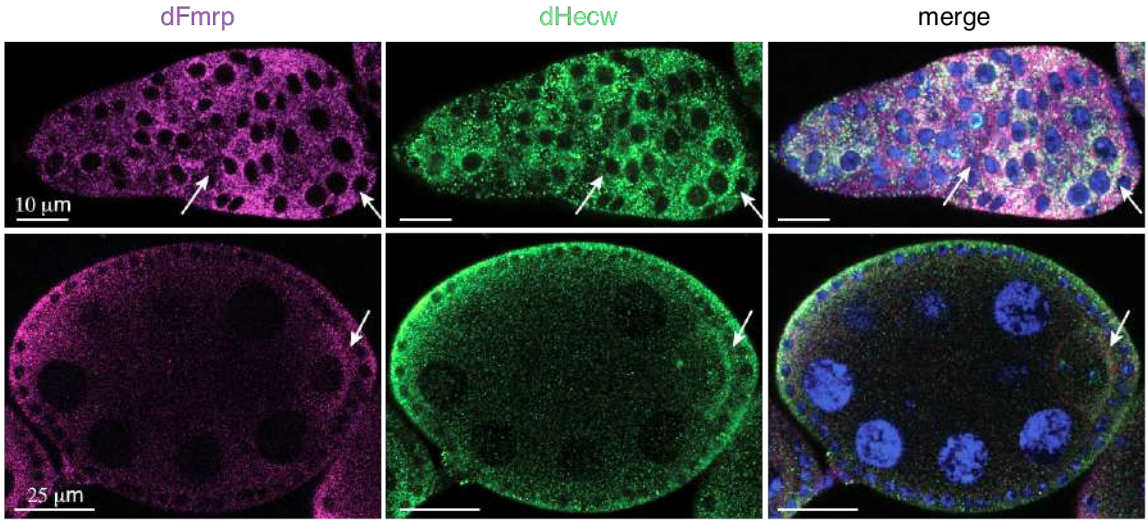

Figure 42. dHecw and dFmrp localization in fly ovarioles.

IF analysis of Drosophila ovarioles with the indicated antibodies. Upper panels: in the germarium, dFmrp and dHecw have a broad expression pattern with some preferential accumulation in the presumptive cyst (white arrow). Scale bar; 10 µm. At later stages (bottom panels), dFmrp and dHecw accumulate in the oocyte at the posterior pole (white arrow). Scale bar; 25 µm.

In addition, virtual *in situ* hybridization analysis of dHecw and dFmr mRNA expression in the *Drosophila* embryo at stage 6 using the online DVEX tool [252] predicted that they are co-expressed in cells of the dorsal/anterior and dorsal/posterior pole of the developing embryo, where the axis of the future animal and the primordial germ cells (pole cells) are forming (**Fig. 43**). These data indicate that dHecw might act on dFmrp to regulate egg and embryo formation.

3.4 dHecw and dFmrp interact functionally

To evaluate the impact of dHecw-dependent ubiquitination on dFmrp, we examined its protein levels in wild type, dHecw mutant and KO fly ovaries. IB analysis of young flies did not show an alteration in dFmrp levels in comparison with wild type control flies (**Fig. 44A**), suggesting that the absence of dHecw function does not alter dFmrp stability.

To investigate other ways in which dHecw could influence dFmrp, we examined known dFmrp interactors. Interestingly, one of the main targets of dFmrp repression in the oocyte

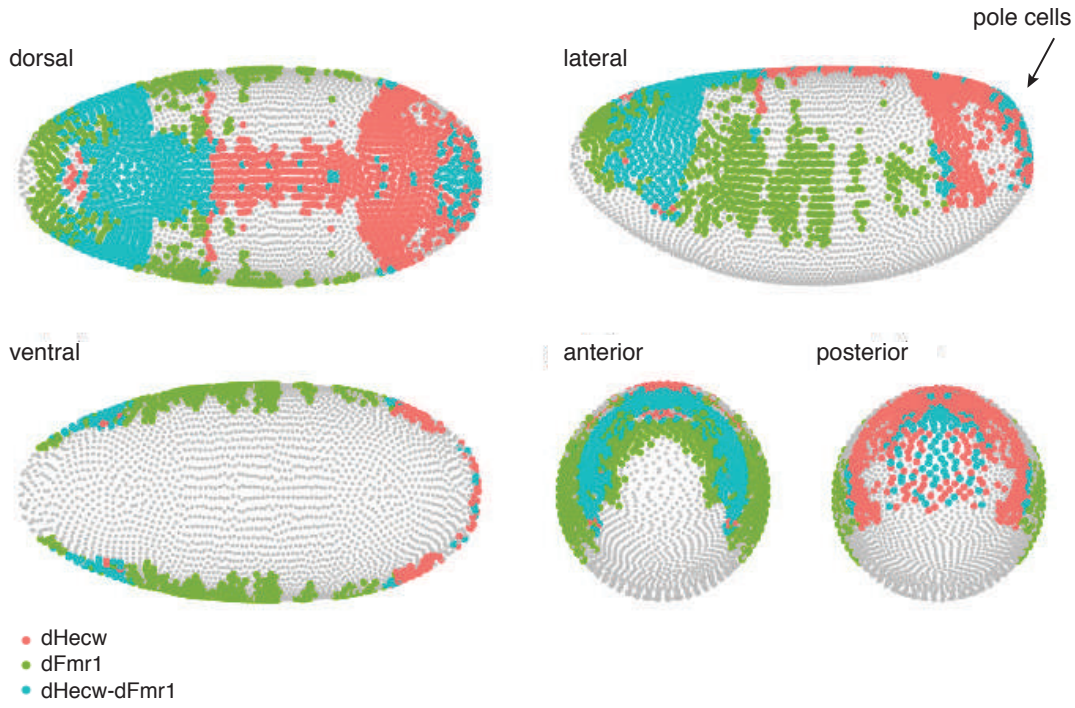

Figure 43. dHecw and dFmr1 virtual expression in fly embryos.

Prediction of spatial expression patterns of dHecw and dFmr1 genes with the virtual in situ hybridization tool DVEX in stage 6 embryos. Five different embryo orientations are shown. dHecw-expressing cells are shown in pink, dFmr1 in green and co-expressing cells in blue. Pole cells are indicated by a black arrow.

---

is the CPEB protein Orb [206]. Thus, we first evaluated Orb expression levels in dHecw mutant flies and found that Orb expression is higher in dHecw mutant and KO fly ovaries, relative to wild type control (**Fig. 44A**). A similar situation has been reported in a *dfmr1* loss of function mutant [206]. On the contrary, upon dHecw overexpression in germline tissue using the nos-Gal4 driver, Orb is strongly down-modulated (**Fig. 44B**). Collectively our results indicate that dHecw acts in the dFmrp-Orb axis and is likely a positive regulator of dFmrp repressive activity.

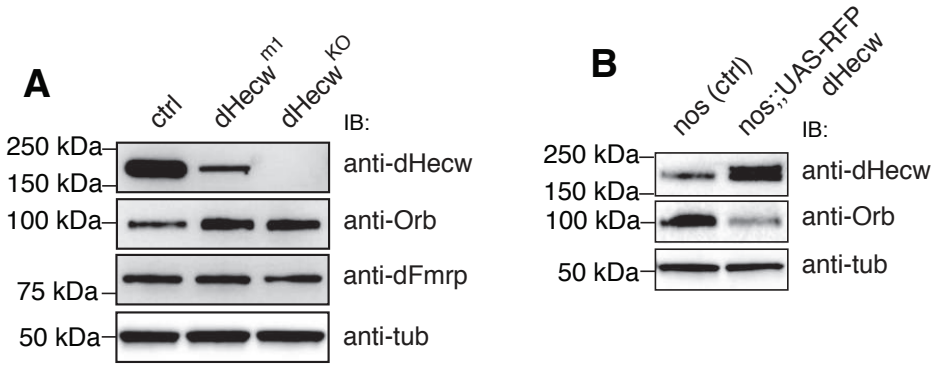

Figure 44. Orb protein levels in dHecw mutant and KO flies.

*(**A**) IB analysis of proteins from wild type (ctrl), dHecw mutant (dHecw^{m1}) and KO (dHecw ^{KO}) fly ovaries with the indicated antibodies. The levels of the Orb protein is increased in dHecw mutant and KO flies compared with the control line (yw, ctrl). dFmrp levels are similar between the analyzed samples. (**B**) IB analysis of proteins from wild type and RFP-dHecw fly ovaries in the germline (nos-Gal4). Upon dHecw overexpression in the germline, Orb levels are decreased in comparison with the control line (driver only).*

3.5 dHecw is required for Gurken and Oskar localization in the germline

It is well established that Orb is responsible for localized cytoplasmic polyadenylation of the *gurken* mRNA during mid to late oogenesis, thereby determining Gurken (Grk) protein accumulation in the dorsal/anterior corner of the oocyte [269]. This is a key step for formation of the dorso-ventral axis, and flies carrying mutations in the gene encoding Orb lay ventralized eggs. Thus, to determine how dHecw might act on RNP-containing dFmrp and Orb, we examined the proteins regulated by them at the mRNA level. Notably, by immunolocalizing Grk in mid oogenesis egg chamber of dHecw mutant flies, we found that a good proportion of egg chambers displayed ectopic Grk localization in the follicle cells at the ventral side of the oocyte (**Fig. 45**).

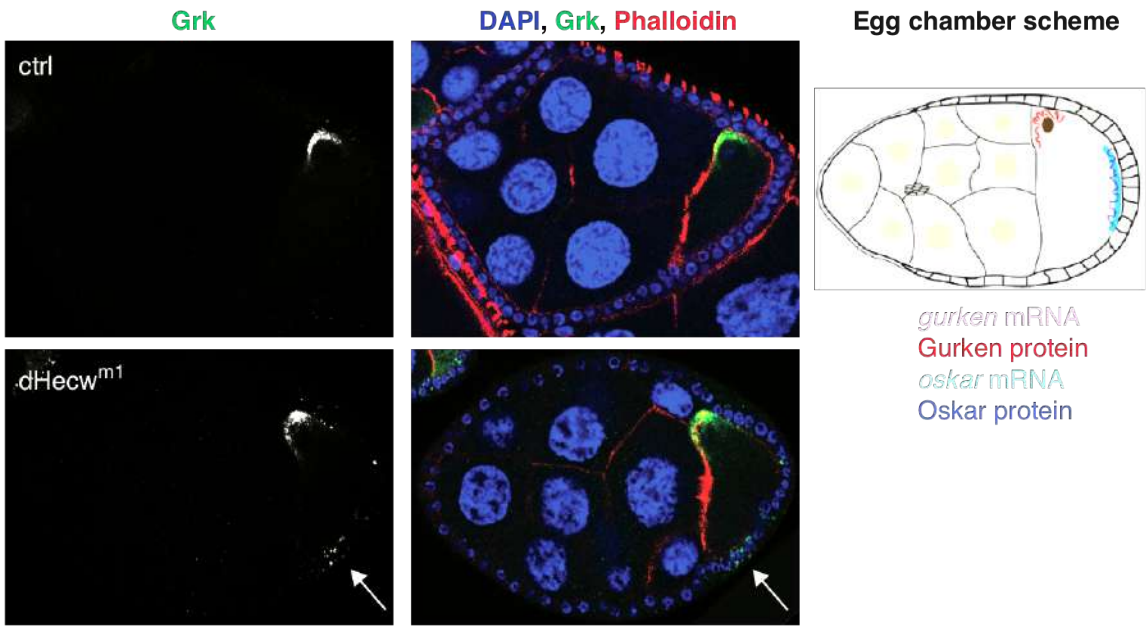

Figure 45. Gurken mislocalization in dHecw mutant flies.

IF analysis of 3 days old wild type and dHecw mutant (dHecw m1) fly egg chambers with the indicated antibodies. Gurken (Grk, green) is localized at the dorso-ventral corner of the oocyte in wild type control (upper panels). White arrows indicate mislocalized Grk at the ventral side of the oocyte in dHecw mutant fly egg chambers (lower panels). mRNA and protein localization is schematized on the right [adapted from McDermott, et al. Biology Open, 2012].

A second target of Orb is *oskar* mRNA, whose protein product its crucial for the localization of posterior determinants and the formation of pole plasm, where the pole cell of the embryo will organize the future germline [192]. Interestingly, by immunolocalization of the Oskar (Osk) protein in dHecw mutant fly ovaries, we observed occasional Osk mislocalization away from the posterior of the oocyte (**Fig. 46**).

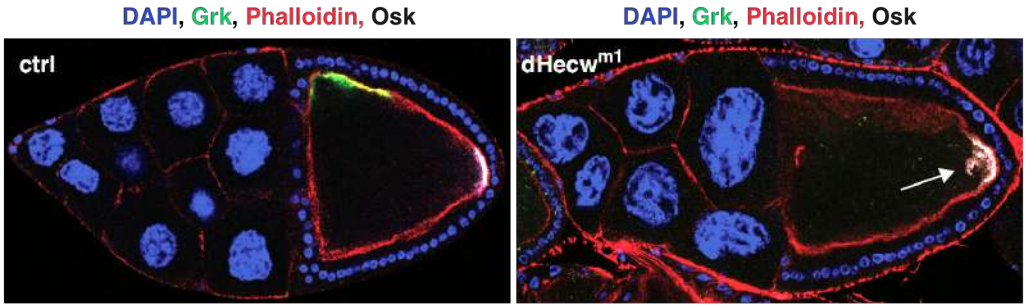

Figure 46. Oskar mis-localization in dHecw mutants.

IF analysis of 3 days old wild type and dHecw mutant (dHecwm1) fly egg chambers with the indicated antibodies. Oskar (Osk, white) is localized at the posterior margin of the oocyte, in wild type control (left panel). White arrows indicate mis-localized Osk in the dHecw mutant flies (right panel).

Taken together, these data suggest that dHecw acts with dFmrp and Orb in localization and/or translational silencing of RNPs involved in oocyte determination.

DISCUSSION

In this thesis, we present the characterization of a novel dNedd4 E3 ligase, dHecw, the unique *Drosophila* ortholog of the two poorly investigated human HECW1 and HECW2. We aimed at unravelling the biological function of this E3 HECT ligase in the context of a model organism by taking advantage of the single uncharacterized *Drosophila* ortholog. Our results have uncovered that dHecw is mainly expressed in fly ovaries and central nervous system, and dHecw mutation or depletion leads to pathological implications in both compartments. We identified dFmrp as a substrate of dHecw ubiquitination and provided evidences that dHecw might contribute to controlling the homeostasis of ribonucleoproteins (RNPs). The implications of our findings are detailed here below.

1. dHecw is a new member of the dNedd4 family

The *Drosophila* Nedd4 family includes three characterized members: dNedd4, the single ortholog of NEDD4 and NEDD4L, dSmurf, the ortholog of SMURF1 and SMURF2, and Su(dx), which is clustered with WWP2, WWP1 and AIP4/ITCH, as in the phylogenetic tree in **Figure 3.** By searching the *Drosophila* database Flybase, using a BLAST algorithm, we identified a single ortholog of *HECW1* and *HECW2* genes: CG42797, which we named dHecw. The protein behaves as an active ubiquitin E3 ligase and shares high sequence identity with its human orthologs within the catalytic HECT domain and the two substrate-binding WW domains, while it differs in the N-terminal region.

The N-terminal region is a distinct feature of HECW1 and HECW2 among NEDD4 members as it is extended before the C2 domain and includes a low complexity region between the C2 domain and the first WW domain. Notably, a recent NMR structure of the extended HECW2 N-terminal region (residues 42-162, PDB 2LFE) generated by Northeast structural genomics consortium (NESG) revealed the presence of an

uncharacterized structural domain. We modeled this region together with the C2 with Phyre2 and we identified a novel hypothetical domain, which bears striking similarity with the SKICH domain present in the autophagy-associated protein Nuclear dot protein 52 (NDP52).

dHecw does not have an N-terminal C2 domain, nor a possible SKICH domain. Secondary structure prediction shows a highly unstructured N-terminus, with possibly 8 alpha helixes and two short beta-strands, but without signs of a tertiary structure, according to Phyre2. This characteristic makes dHecw quite unique among Nedd4 members also in terms of regulation. Indeed, it was previously shown that the N-terminal C2 domain is critical in maintaining the protein in a closed, inactive conformation, in the absence of *bona fide* substrates [66], [47]. Overexpression of RFP-tagged full-length dHecw, which naturally lacks the C2 domain, leads to the formation of big puncta in the cytoplasm to which ubiquitin re-localizes. Strikingly, overexpression of human GFP tagged HECW1ΔC2 generates similar ubiquitin-positive aggregates (data not shown). These data suggest that dHecw is a constitutively active HECT, although a different type of regulation cannot be excluded. Indeed, another autoinhibitory mechanism has recently been described for WWP1/2 and ITCH [270], [70], [47], where a short helical linker located between the first and the second WW domains is capable of interacting with the HECT, thus, locking it in an inactive state. According to PSIPRED secondary structure prediction, an 11-residues alpha helix in the region between the two WW domains of dHecw may work in an analogous way. Whether dHecw, HECW1 and HECW2 are capable of assuming a closed, inactive conformation similarly to the other human NEDD4 proteins remains to be established.

2. dHecw is a potential modulator of neuronal homeostasis

It was previously shown that HECW1 and HECW2 are highly expressed in the central nervous system [105], [111]. Not surprisingly, HECW1 has been linked to neurodegenerative diseases, ALS in particular [105], while HECW2 has been shown to be involved in enteric neuronal development [113]. Interestingly, while HECW2 KO mice die within two weeks after birth for intestinal aganglionosis and kidney failure, HECW1-deficient mice are viable and fertile [114]. Moreover, transgenic mice that ubiquitously overexpressed human HECW show loss of neurons in the spinal cord, muscular atrophy and microglia activation, which are common features of ALS [106].

As for human HECW1 and HECW2, the characterization of the *Drosophila* ortholog revealed its preferential expression in the central nervous system, both at mRNA and protein level. Strikingly, our dHecw catalytically inactive mutants, presented many neurodegenerative phenotypes, including reduced lifespan, prematurely impaired climbing ability, and brain vacuolization. However, due to residual expression of the mutant proteins, it is difficult to exclude that dHecw performs additional functions and generated, thus, full dHecw-knock out (KO) flies to investigate this possibility. We did not observe any change in neurodegenerative defectors, nor additional phenotypes, thus, we concluded that the premature neurodegeneration observed in dHecw mutant flies is mainly caused by the lack of the catalytic activity of dHecw. We now intend to investigate in detail the status of the motoneurons (MNs), which are the specific neurons mainly implicated in ALS and similar diseases. In addition, it would be interesting to see if the overexpression of wild type dHecw in MN could clear the aggregates and rescue the phenotypes associated with neurodegenerative diseases, as was demonstrated for dNedd4 [271]. Interestingly, in a model of Parkinson disease, the overexpression of dNedd4 with a pan neuronal driver (elav-gal4) prevents alpha-synuclein-induced locomotive defects [271].

Although, dHecw, similarly to HECW1ΔC2, shows a natural tendency to form aggregates upon overexpression. This aggregation-prone behavior might be caused by the N-terminal low complexity region of the protein and appears to be potentially deleterious for flies' homeostasis. Indeed, in a preliminary experiment, we observed that pan-neuronal overexpression of wild type dHecw causes a decrease in the lifespan of the flies (not shown). Therefore, to rescue the KO phenotypes, it would be fundamental to tightly modulate the expression of this protein. To this end, we will take advantage of the temperature sensitivity of the Gal4-UAS system (see methods), and perform targeted overexpression at low temperature (18ºC), where Gal4 is less efficient [250]. Another possible option for the rescue is to take advantage of a transgenic fly line carrying the clone of the P[acman] BAC library [272] that contains a duplication of *dHecw* locus in a different chromosome, allowing physiological expression levels of the gene.

3. dHecw in autophagy

We observed that the expression of wild type dHecw is down modulated during aging, a pattern characteristic of proteins responsible for protein homeostasis and quality control [273]. Thus, this E3 might be important to maintain the fitness of the organism, working at the level of the ubiquitin proteasome system (UPS) and/or the autophagy pathway. The activity of these pathways is reduced with increasing age and this explains the late clinical onset of neurodegenerative diseases. Like other members of the family [259], dHecw is able to generate K63-linked ubiquitin chains, a signal that is not involved in proteasomal degradation, but appears to modulate selective autophagy [260].

Autophagy is considered to be the first response that is activated by virtually any kind of intracellular and extracellular stress and is the principal mechanism for turning over cellular organelles and protein aggregates that are too large to be

degraded by the proteasome [213]. The autophagy process is crucial for postmitotic neurons in which aggregated proteins and dysfunctional organelles are not diluted by means of cell division [213, 274]. Besides neuronal homeostasis, autophagy is also used for the continuous remodeling of neuronal terminals, which is required to support neuronal plasticity [275], [276]. Thus, it is not surprising that alterations in the autophagy system are intimately linked to several neurodegenerative diseases, such as Alzheimer's disease, Parkinson's disease, Huntington's disease, and Amyotrophic Lateral Sclerosis [277], [213], [278].

Intriguingly, fly mutants of the E1 enzyme Atg7, specific for autophagy [263], manifest neurodegenerative-like phenotypes comparable to that of dHecw mutants in flies. In addition, we identified the autophagy receptor SQSTM1/p62 as a potential interactor/substrate for HECW1 (data not shown), and found that the fly ortholog Ref(2)p is capable of re-localizing in cytoplasmic puncta after dHecw overexpression. Preliminary experiments of starvation-induced autophagy in the ovaries of dHecw mutant and KO flies suggest a possible autophagic impairment in the absence of this E3 ligase. All these evidences suggest a potential role of dHecw in the autophagy pathway and needs to be further investigated. It is worth mentioning that recent exciting studies have linked a few members of Nedd4 family to autophagy: SMURF1 has been shown to be required for viral autophagy and mitophagy [224], knockdown of NEDD4L in cultured cells suppressed both basal autophagy and ER stress-induced autophagy [144], and NEDD4 has been shown to bind and to mediate K11- and K63-linked ubiquitylation of Beclin1 [63].

Future dedicated experiments will be instrumental to examine the impact of dHecw in selective autophagy.

4. The dHecw interactome

To gain insights into the underlying molecular mechanisms of dHecw function, we searched for its interactors and substrates, using S2 cell lysates and IP/pulldown coupled with mass spectrometry analysis, and identified 55 candidates. The small size of the interactome may reflect technical issues related to the cellular context; S2 cells are amenable for such biochemical experiments, but tissue specific interactors and developmental targets are certainly missing. *Orb* gene for example, is not expressed in S2 cells. Moreover, identification of substrates is always troublesome for ubiquitin ligases due to the transient nature of the E3-substrate interaction.

Performing pull down using only the substrate binding domains of the protein it is a strategy that can help coping with the transitory ligase-substrate binding: in absence of the catalytic activity the interacting protein remain in contact longer with the enzyme WW domains, thus working as a 'trap' for substrates. This could explain why the majority of candidate interactors were identified in the GST-pull down assay rather than the IP experiment.

Despite the small size of the candidate interactor list, we found a clear GO enrichment in mRNA binding proteins involved in several aspects of mRNA processing. Among these proteins, there are members of the hnRNP family (Hrp48, Hrb98D, Glorund); RNA helicases (Belle, Abstrakt); splicing factors (Spenito), translation initiator (eIF4A) and elongation factors (EF1alpha, EF2); and known mRNA translational repressors (dFmrp, Larp, Glorund). Interestingly, many of these candidates are part of RNP complexes, which have a role in temporal and spatial control of mRNA expression. Of note, controlled transcripts localization and translation is of fundamental importance for the establishment of cell polarity during oogenesis and neuronal development, and for synaptic plasticity in differentiated neurons. A second protein category that we found enriched in the dHecw interactome

is composed of cytoskeleton/motor proteins such as kinesin heavy chain and clathrin heavy chain, which are involved in mRNA transport in polarizing oocytes [175], [174]. This is particularly interesting since RNP transport occurs mainly via a kinesin-dynein motor on a microtubule 'highway' [145]. Notably, among 55 putative interactors identified, 47 (85%) possess proline-rich motifs such as PPXY, PY, and PR, typically recognized by WW domains [46], and are therefore potential substrates that we intend to validate taking advantage of our set *in vitro* ubiquitination assay, as described in the next paragraph. To improve the identification of functionally relevant dHecw interaction we will perform Co-Immunoprecipitation (CoIP) and IP coupled with MS directly from fly ovary, where the protein is highly expressed and we hypothesize having a relevant function. It would be interesting to investigate dHecw interactors specific for a certain contexts or pathways: as we hypothesize dHecw involvement in autophagy, we could study candidates in condition of induction (e.g. starvation) or inhibition of the autophagy pathway in fly ovaries. It would be also highly informative to perform SILAC-proteomic analysis (stable isotope labeling with amino acids in cell culture) comparing wild type with dHecw mutant/KO fly ovary.

5. dFmrp is the first identified dHecw substrate

The proteomic data that we obtained from *Drosophila* analysis are further supported by the human HECW1 interactome that we generated in parallel (data not shown). dFmrp, the single fly ortholog of human FMRP genes is found among the common interactors. Two proteins of the human family (FMR1 and FXR1) were identified in the human HECW1 interactome, suggesting that this interaction and its functional meaning are possibly conserved throughout evolution.

In humans, loss of FMRP is associated with Fragile X-associated disorders, which cover a range of inherited mental, motor and reproductive disabilities including

Fragile X–associated tremor/ataxia syndrome (FXTAS) and Fragile X-related primary ovarian insufficiency (FXPOI) [279]. *Drosophila* has already been a useful tool to model this disease and has revealed new insights into the pathological mechanisms underlying the Fragile X syndrome [249].

Interestingly, dHecw and dFmrp present a highly similar pattern of expression in fly ovaries: they are expressed both in somatic follicular cells and in germline cells, with a preferential enrichment in the oocyte. Another striking feature that suggests a functional connection between the two proteins is that *dfmr1* loss of function flies [206] present the same oogenesis defects that we observed in dHecw mutant and KO flies, including aberrant number of nurse cells, compound egg chambers, and misspecification of an additional oocyte. To investigate the dHecw-dFmr1 relationship from the genetic point of view, we crossed our dHecw mutant flies with heterozygous *dfmr1* loss of function flies (*dfmr* $^{\Delta 1}$*^{13}*, [267]). As in single mutant flies, in dHecw^{m1}- *dfmr* $^{\Delta 113}$ ovaries we observed egg chambers with aberrant numbers of germ cells. This defect showed a similar frequency in both the single mutant flies and the dHecw^{m1}- *dfmr* $^{\Delta 113}$ flies. Interestingly, the two mutations seem to have a synergic effect on the oocyte mislocalization, as this defect was observed in 70% of the total egg chambers, ten times more than in the single mutants. Additionally, we observed an uncommon high number of apoptotic egg chambers, which is probably a sign of an even more compromised oogenesis. This data reinforces the functional relationship between dHecw and dFmr1.

Being an E3 ligase, we asked whether dFmrp could be a direct target of the enzymatic activity of dHecw. To this end, we performed an *in vitro* ubiquitination assay with purified proteins and our results clearly show that dFmrp is ubiquitinated by dHecw. Looking at possible recognition sites for dHecw WW domains, we found in dFmrp C-terminus two proline-rich domains (PR) that we are currently investigating

by a classical structure-function approach. To test dHecw-dependent dFmrp ubiquitination in a functionally relevant context *in vivo*, we will perform Co-IP analysis directly from wild type and mutant/KO ovaries and verify dFmrp ubiquitination state in both conditions.

6. dHecw-dFmrp functional relationship

The next step that we intend to pursue is the identification of the functional outcome of dHecw-dependent ubiquitination of dFmrp. The easiest hypothesis is dFmrp degradation upon ubiquitination. Notably, dFmrp stability is modulated by ubiquitination in rat hippocampal neurons [210]. Upon metabotropic glutamate receptor (mGluR) stimulation, a rapid dephosphorylation of FMRP by protein phosphatase 2a (PP2A) is induced [183], causing its ubiquitination and ubiquitin/proteasome-mediated degradation [210] by the anaphase promoting complex (APC)-Cdh1 [211]. To verify this hypothesis, we assessed dFmrp expression in the ovary of dHecw mutant and KO flies but found no alteration at the protein level in comparison with the wild type control. Furthermore, the level of dFmrp remains stable upon dHecw overexpression, suggesting that dHecw-mediated ubiquitination does not cause dFmrp degradation. Although local effect of dHecw on Fmrp in the germline could be masked in the whole ovary lysate, these results corroborate the idea that dHecw, as the other NEDD4 family members, is a K63-specific enzyme not involved in proteasomal degradation [58].

The covalent attachment of ubiquitin to proteins is not simply a sign of destruction but it can be a regulatory signal that alters localization, activity, and ultimate fate of the target proteins. dHecw down-modulation (mutation or KO) did not alter dFmrp localization in the ovaries. Therefore, we focused our attention on the dFmrp protein network that might well be modulated by K63 ubiquitination. One known dFmrp interactor in the ovaries is the cytoplasmic polyA binding element

(CPEB) Orb [206], an mRNA binding protein that acts mainly as a translational activator in the oocyte [184]. dFmrp is a negative regulator of Orb, possibly interfering with Orb positive autoregulatory loop [206], [205]. Immunoblot analysis of dHecw mutant and KO ovaries revealed an increased level of Orb protein, as in *dfmr* loss of function mutants [206]. Strikingly, upon dHecw overexpression in the germline (nos-Gal4 driver), Orb protein levels are decreased, demonstrating that dHecw levels impact functionally on the Orb-dFmrp interaction.

To monitor the consequences of the alteration of the potential dHecw-dFmrp-Orb axis in fly ovaries, we investigated two downstream targets of Orb, *gurken (grk)* and *oskar (osk)* mRNAs, which are responsible for the formation of the dorso/ventral axis and of the posterior axis of the embryo, respectively [269], [192]. In mid-oogenesis *grk* is localized and transcribed specifically at the dorso/anterior (D/A) corner of the oocyte where its EGF-like protein product signals to the follicle cells (FC) to dorsalize [195]. Together with local mRNA transport, it was suggested that the Grk D/A localization is also maintained through a rapid internalization of the Grk protein that diffuses laterally. Lateral and ventral FC quickly internalize the Grk-Torpedo (EGFR fly homolog) complex, directing it do lysosomal degradation [280]. Thus, in normal physiological conditions, the Grk protein is detectable only alt the D/A corner of the oocyte. Strickingly, in dHecw mutant flies, the Grk protein is visible not only in the D/A corner but also in the FC at the ventral side of the oocyte. This ventral localization of Grk could be due to either an aberrant mRNA transport to the ventral side, or to excessive *grk* translation. In the latter case, an excess of free Grk that diffuses to the ventral side could not be fully internalized and degraded by FCs, resulting in a visible signal at the ventral side of the follicular epithelium. Considering that in dHecw mutants Orb is upregulated, and that Orb is a translational activator of *grk* [269], Grk mislocalization is better explained by the latter hypothesis.

In some dHecw mutant stage 10-egg chambers, we observed Osk localization away from the posterior pole where it normally resides. Although this phenotype was not frequent, it might suggest an impairment also in the restriction of *osk* local translation at the posterior pole. Since Osk defect was observed only in late egg chambers, where the cytoskeleton is remodeled and cytoplasmic streaming starts, the phenotype observed might also indicate a problem in *osk* mRNA anchoring [197]. Interestingly, Osk mislocalization was observed in mutants of the RNP protein Hrp48, which represses Osk translation [281] and is found among dHecw immunoprecipitants in S2 cells. In *hrp48* mutants, the oocyte microtubule cytoskeleton is altered, thus, it will be important to determine if also dHecw is required for correct microtubule polarity, a prerequisite for RNP transport and translational activation. In addition, to better unravel the molecular details of dHecw-related phenotypes, it would be interesting to also perform fluorescence in situ hybridization (FISH) and analyze the mRNA pattern in the ovaries of dHecw mutants.

7. dHecw is a potential RNP regulator

The results that we obtained suggest that dHecw ubiquitination of dFmrp potentially have an impact on its translational repressor function. However, dFmrp is not the only RNP component identified in our interactome: notably, few potential interactors were mRNA binding proteins previously identified as part of the same RNP complex. In particular, Hrp48 and Glorund are two translational repressors involved in the regulation of *grk* and *osk* local translation [282]; thus, the mislocalization of Grk and Osk that we observed in dHecw mutant could also be due to an impairment in Hrp48 and Glorund regulation. Similarly, the candidate interactor Lingerer was found in an RNase-resistant RNP complex associated with Orb and dFmrp [206]. This protein possesses a ubiquitin-associated domain (UBA) with unknown function [283], further

suggesting that RNP components like dFrmp might be subjected to ubiquitination. An intriguing idea is that this post-translational modification (PTM) may regulate RNP assembly and transport.

Studies in yeast suggest that HECT E3 ligases might play a role in the regulation of mRNA local translation. Rsp5 and Tom1 were found to be required for mRNA nuclear export and processing in *Saccharomyces cerevisiae* [208], and, by targeting NANOS2 for degradation, NEDD4 participates in RNP regulation in testis germ cells in a mouse model [212]. Since dHecw is highly expressed in male gonads and dFmrp acts as a translational regulator also in testis [267], it would be interesting to verify if there are any defects in spermatogenesis in dHecw mutants and KO.

Moreover, mRNA local translation is a strictly regulated process also in the neuronal compartment, which is necessary both during development for axonal growth and in mature neurons for synaptic plasticity. Therefore, it would be fascinating to further investigate a potential role for dHecw in neurons, also considering the neurodegenerative defects observe in our mutant and KO flies. A growing body of evidences is now suggesting that neurodegenerative diseases are not only 'proteinopathies', but also 'ribonucleopathies' [284]. ALS, frontotemporal lobar degeneration (FTLD), fragile X syndrome, spinocerebellar ataxia-2 were indeed related to RNP defects [231]. The causes and dynamics of the pathologies are still not clear. RNA granules might work as a nucleation center for aggregation, either sequestering mRNAs and mRNA binding proteins from their normal function and/or generating toxic aggregates in neurons [285].

Despite the significant progresses in identifying components of RNP complexes, the precise regulation of RNP dynamic assembly, disassembly and transport needs further elucidation both in physiological and in pathological contexts. A growing body of evidence indicates that PTMs might have a crucial role in this

process; being largely reversible, PTMs represent a dynamic and fast way of regulation, without increasing genome size [286]. The networking capability of ubiquitin has been firmly established in the endocytic pathway in which it acts as an internalization signal at the plasma membrane [17], [287] and as a sorting signal at the level of the endosomes [288]. In this scenario, ubiquitin could modulate the organization of the RNP complex components, by influencing the interaction between them. It could also impact on the regulation of the adaptor proteins that act as a bridge between the RNPs and the motor protein, critical for their transport in the cell. Interestingly, this ubiquitin ligase is a member of the NEDD4 family, which has always been associated with the regulation of trafficking and endocytosis of transmembrane receptors. Collectively, our data suggest a potential novel and fundamental function of this type of E3 ligase in RNPs regulation.

ACKNOWLEDGEMENT

I would like to express my sincere gratitude to my supervisor Simona Polo, for the trust and support during my Ph.D study. I would like to thank Thomas Vaccari, who gave constant and precious contribution for the *Drosophila* part of the project.

I acknowledge my fellow lab-mates, present and past, in for the inspiring discussions and for the mutual moral support during this four years: I was very lucky to find such a stimulating and friendly environment to work in. Also, I have to thank all the members of the 'fly-group': it was a real pleasure to spend hours in the flyroom with you.

A very special thank goes out to my lab-coach Elena Maspero, for her precious teaching, practical and theoretical help, from the beginning to the end of my PhD and beyond!
I am also grateful to my other PhD colleagues and friends: the path is easier if you have someone to share it with. A special thank goes to Corey and his optimism, a fundamental ingredient for life and research.

I am grateful to my family, that provided me a 'scientific environment 'also at home, and for their moral and emotional encouragement.

This project was funded by PRIN 2015 grant 'Ubiquitin E3 ligases as critical sensors in physiological and pathological conditions' to Simona Polo and by TRIDEO-2014 grant 'HECTylomes in cancer' to Elena Maspero.

BIBLIOGRAPHY

1. Dye, B. T. & Schulman, B. A. (2007) Structural mechanisms underlying posttranslational modification by ubiquitin-like proteins, *Annu Rev Biophys Biomol Struct.* **36**, 131-50.
2. Pickart, C. M. (2001) Mechanisms underlying ubiquitination, *Annu Rev Biochem.* **70**, 503-33.
3. Vijay-Kumar, S., Bugg, C. E. & Cook, W. J. (1987) Structure of ubiquitin refined at 1.8 A resolution, *J Mol Biol.* **194**, 531-44.
4. Belgareh-Touze, N., Leon, S., Erpapazoglou, Z., Stawiecka-Mirota, M., Urban-Grimal, D. & Haguenauer-Tsapis, R. (2008) Versatile role of the yeast ubiquitin ligase Rsp5p in intracellular trafficking, *Biochem Soc Trans.* **36**, 791-6.
5. Schnell, J. D. & Hicke, L. (2003) Non-traditional functions of ubiquitin and ubiquitin-binding proteins, *J Biol Chem.* **278**, 35857-60.
6. Yau, R. & Rape, M. (2016) The increasing complexity of the ubiquitin code, *Nat Cell Biol.* **18**, 579-86.
7. Wertz, I. E. & Dixit, V. M. (2008) Ubiquitin-mediated regulation of TNFR1 signaling, *Cytokine Growth Factor Rev.* **19**, 313-24.
8. Branzei, D. & Foiani, M. (2008) Regulation of DNA repair throughout the cell cycle, *Nat Rev Mol Cell Biol.* **9**, 297-308.
9. Sumara, I., Maerki, S. & Peter, M. (2008) E3 ubiquitin ligases and mitosis: embracing the complexity, *Trends Cell Biol.* **18**, 84-94.
10. Swatek, K. N. & Komander, D. (2016) Ubiquitin modifications, *Cell Res.* **26**, 399-422.
11. Kulathu, Y. & Komander, D. (2012) Atypical ubiquitylation - the unexplored world of polyubiquitin beyond Lys48 and Lys63 linkages, *Nat Rev Mol Cell Biol.* **13**, 508-23.
12. Hicke, L. (2001) Protein regulation by monoubiquitin, *Nat Rev Mol Cell Biol.* **2**, 195-201.
13. Haglund, K., Di Fiore, P. P. & Dikic, I. (2003) Distinct monoubiquitin signals in receptor endocytosis, *Trends Biochem Sci.* **28**, 598-603.
14. Xu, P., Duong, D. M., Seyfried, N. T., Cheng, D., Xie, Y., Robert, J., Rush, J., Hochstrasser, M., Finley, D. & Peng, J. (2009) Quantitative proteomics reveals the function of unconventional ubiquitin chains in proteasomal degradation, *Cell.* **137**, 133-45.
15. Hoege, C., Pfander, B., Moldovan, G. L., Pyrowolakis, G. & Jentsch, S. (2002) RAD6-dependent DNA repair is linked to modification of PCNA by ubiquitin and SUMO, *Nature.* **419**, 135-41.
16. Stewart, G. S., Panier, S., Townsend, K., Al-Hakim, A. K., Kolas, N. K., Miller, E. S., Nakada, S., Ylanko, J., Olivarius, S., Mendez, M., Oldreive, C., Wildenhain, J., Tagliaferro, A., Pelletier, L., Taubenheim, N., Durandy, A., Byrd, P. J., Stankovic, T., Taylor, A. M. & Durocher, D. (2009) The RIDDLE syndrome protein mediates a ubiquitin-dependent signaling cascade at sites of DNA damage, *Cell.* **136**, 420-34.
17. Acconcia, F., Sigismund, S. & Polo, S. (2009) Ubiquitin in trafficking: the network at work, *Exp Cell Res.* **315**, 1610-8.
18. Spence, J., Gali, R. R., Dittmar, G., Sherman, F., Karin, M. & Finley, D. (2000) Cell cycle-regulated modification of the ribosome by a variant multiubiquitin chain, *Cell.* **102**, 67-76.
19. Song, E. J., Werner, S. L., Neubauer, J., Stegmeier, F., Aspden, J., Rio, D., Harper, J. W., Elledge, S. J., Kirschner, M. W. & Rape, M. (2010) The Prp19 complex and the Usp4Sart3 deubiquitinating enzyme control reversible ubiquitination at the spliceosome, *Genes Dev.* **24**, 1434-47.
20. Akutsu, M., Dikic, I. & Bremm, A. (2016) Ubiquitin chain diversity at a glance, *J Cell Sci.* **129**, 875-80.
21. Meyer, H. J. & Rape, M. (2014) Enhanced protein degradation by branched ubiquitin chains, *Cell.* **157**, 910-21.

22. Gatti, M., Pinato, S., Maiolica, A., Rocchio, F., Prato, M. G., Aebersold, R. & Penengo, L. (2015) RNF168 promotes noncanonical K27 ubiquitination to signal DNA damage, *Cell Rep.* **10**, 226-38.
23. Yuan, W. C., Lee, Y. R., Lin, S. Y., Chang, L. Y., Tan, Y. P., Hung, C. C., Kuo, J. C., Liu, C. H., Lin, M. Y., Xu, M., Chen, Z. J. & Chen, R. H. (2014) K33-Linked Polyubiquitination of Coronin 7 by Cul3-KLHL20 Ubiquitin E3 Ligase Regulates Protein Trafficking, *Mol Cell.* **54**, 586-600.
24. Iwai, K., Fujita, H. & Sasaki, Y. (2014) Linear ubiquitin chains: NF-kappaB signalling, cell death and beyond, *Nat Rev Mol Cell Biol.* **15**, 503-8.
25. Clague, M. J. & Urbe, S. (2010) Ubiquitin: same molecule, different degradation pathways, *Cell.* **143**, 682-5.
26. Herhaus, L. & Dikic, I. (2015) Expanding the ubiquitin code through post-translational modification, *EMBO Rep.* **16**, 1071-83.
27. Berndsen, C. E. & Wolberger, C. (2014) New insights into ubiquitin E3 ligase mechanism, *Nat Struct Mol Biol.* **21**, 301-7.
28. Buetow, L. & Huang, D. T. (2016) Structural insights into the catalysis and regulation of E3 ubiquitin ligases, *Nat Rev Mol Cell Biol.* **17**, 626-42.
29. Deshaies, R. J. & Joazeiro, C. A. (2009) RING domain E3 ubiquitin ligases, *Annu Rev Biochem.* **78**, 399-434.
30. Petroski, M. D. & Deshaies, R. J. (2005) Mechanism of lysine 48-linked ubiquitin-chain synthesis by the cullin-RING ubiquitin-ligase complex SCF-Cdc34, *Cell.* **123**, 1107-20.
31. Dou, H., Buetow, L., Hock, A., Sibbet, G. J., Vousden, K. H. & Huang, D. T. (2012) Structural basis for autoinhibition and phosphorylation-dependent activation of c-Cbl, *Nat Struct Mol Biol.* **19**, 184-92.
32. Plechanovova, A., Jaffray, E. G., Tatham, M. H., Naismith, J. H. & Hay, R. T. (2012) Structure of a RING E3 ligase and ubiquitin-loaded E2 primed for catalysis, *Nature.* **489**, 115-20.
33. Zheng, N., Wang, P., Jeffrey, P. D. & Pavletich, N. P. (2000) Structure of a c-Cbl-UbcH7 complex: RING domain function in ubiquitin-protein ligases, *Cell.* **102**, 533-9.
34. Mohapatra, B., Ahmad, G., Nadeau, S., Zutshi, N., An, W., Scheffe, S., Dong, L., Feng, D., Goetz, B., Arya, P., Bailey, T. A., Palermo, N., Borgstahl, G. E., Natarajan, A., Raja, S. M., Naramura, M., Band, V. & Band, H. (2013) Protein tyrosine kinase regulation by ubiquitination: critical roles of Cbl-family ubiquitin ligases, *Biochim Biophys Acta.* **1833**, 122-39.
35. Nakada, S. (2016) Opposing roles of RNF8/RNF168 and deubiquitinating enzymes in ubiquitination-dependent DNA double-strand break response signaling and DNA-repair pathway choice, *J Radiat Res.* **57 Suppl 1**, i33-i40.
36. Linke, K., Mace, P. D., Smith, C. A., Vaux, D. L., Silke, J. & Day, C. L. (2008) Structure of the MDM2/MDMX RING domain heterodimer reveals dimerization is required for their ubiquitylation in trans, *Cell Death Differ.* **15**, 841-8.
37. Vodermaier, H. C. (2004) APC/C and SCF: controlling each other and the cell cycle, *Curr Biol.* **14**, R787-96.
38. Rotin, D. & Kumar, S. (2009) Physiological functions of the HECT family of ubiquitin ligases, *Nat Rev Mol Cell Biol.* **10**, 398-409.
39. Huibregtse JM1, S. M., Beaudenon S, Howley PM. (1995) A family of proteins structurally and functionally related to the E6-AP ubiquitin-protein ligase., *PNAS.* **92**, 2563-25-67.
40. Kee, Y. & Huibregtse, J. M. (2007) Regulation of catalytic activities of HECT ubiquitin ligases, *Biochem Biophys Res Commun.* **354**, 329-33.
41. Scheffner, M. & Kumar, S. (2014) Mammalian HECT ubiquitin-protein ligases: biological and pathophysiological aspects, *Biochim Biophys Acta.* **1843**, 61-74.
42. Wenzel, D. M. & Klevit, R. E. (2012) Following Ariadne's thread: a new perspective on RBR ubiquitin ligases, *BMC Biol.* **10**, 24.
43. Metzger, M. B., Hristova, V. A. & Weissman, A. M. (2012) HECT and RING finger families of E3 ubiquitin ligases at a glance, *J Cell Sci.* **125**, 531-7.

44. Eisenhaber, B., Chumak, N., Eisenhaber, F. & Hauser, M. T. (2007) The ring between ring fingers (RBR) protein family, *Genome Biol.* **8**, 209.
45. Shimura, H., Mizuno, Y. & Hattori, N. (2012) Parkin and Parkinson disease, *Clin Chem.* **58**, 1260-1.
46. Ingham, R. J., Gish, G. & Pawson, T. (2004) The Nedd4 family of E3 ubiquitin ligases: functional diversity within a common modular architecture, *Oncogene.* **23**, 1972-84.
47. Fajner, V., Maspero, E. & Polo, S. (2017) Targeting HECT-type E3 ligases - insights from catalysis, regulation and inhibitors, *FEBS Lett.* **591**, 2636-2647.
48. Coussens, L., Parker, P. J., Rhee, L., Yang-Feng, T. L., Chen, E., Waterfield, M. D., Francke, U. & Ullrich, A. (1986) Multiple, distinct forms of bovine and human protein kinase C suggest diversity in cellular signaling pathways, *Science.* **233**, 859-66.
49. Corbalan-Garcia, S. & Gomez-Fernandez, J. C. (2014) Signaling through C2 domains: more than one lipid target, *Biochim Biophys Acta.* **1838**, 1536-47.
50. Verdecia, M. A., Bowman, M. E., Lu, K. P., Hunter, T. & Noel, J. P. (2000) Structural basis for phosphoserine-proline recognition by group IV WW domains, *Nat Struct Biol.* **7**, 639-43.
51. Sudol, M. & Hunter, T. (2000) NeW wrinkles for an old domain, *Cell.* **103**, 1001-4.
52. Ingham, R. J., Colwill, K., Howard, C., Dettwiler, S., Lim, C. S., Yu, J., Hersi, K., Raaijmakers, J., Gish, G., Mbamalu, G., Taylor, L., Yeung, B., Vassilovski, G., Amin, M., Chen, F., Matskova, L., Winberg, G., Ernberg, I., Linding, R., O'Donnell, P., Starostine, A., Keller, W., Metalnikov, P., Stark, C. & Pawson, T. (2005) WW domains provide a platform for the assembly of multiprotein networks, *Mol Cell Biol.* **25**, 7092-106.
53. Persaud, A., Alberts, P., Amsen, E. M., Xiong, X., Wasmuth, J., Saadon, Z., Fladd, C., Parkinson, J. & Rotin, D. (2009) Comparison of substrate specificity of the ubiquitin ligases Nedd4 and Nedd4-2 using proteome arrays, *Mol Syst Biol.* **5**, 333.
54. Huang L, K. E., Wang G, Beaudenon S, Howley PM, Huibregtse JM, Pavletich NP. (1999) Structure of an E6AP-UbcH7 complex: insights into ubiquitination by the E2-E3 enzyme cascade., *Science.* **12**, 1321-1326.
55. Verdecia MA, J. C., Wells NJ, Ferrer JL, Bowman ME, Hunter T, Noel JP. (2003) Conformational flexibility underlies ubiquitin ligation mediated by the WWP1 HECT domain E3 ligase., *Mol Cell.* **11**, 249-259.
56. Kamadurai, H. B., Souphron, J., Scott, D. C., Duda, D. M., Miller, D. J., Stringer, D., Piper, R. C. & Schulman, B. A. (2009) Insights into ubiquitin transfer cascades from a structure of a UbcH5B approximately ubiquitin-HECT(NEDD4L) complex, *Mol Cell.* **36**, 1095-102.
57. Kamadurai, H. B., Qiu, Y., Deng, A., Harrison, J. S., Macdonald, C., Actis, M., Rodrigues, P., Miller, D. J., Souphron, J., Lewis, S. M., Kurinov, I., Fujii, N., Hammel, M., Piper, R., Kuhlman, B. & Schulman, B. A. (2013) Mechanism of ubiquitin ligation and lysine prioritization by a HECT E3, *Elife.* **2**, e00828.
58. Maspero, E., Valentini, E., Mari, S., Cecatiello, V., Soffientini, P., Pasqualato, S. & Polo, S. (2013) Structure of a ubiquitin-loaded HECT ligase reveals the molecular basis for catalytic priming, *Nat Struct Mol Biol.* **20**, 696-701.
59. Sheng, Y., Hong, J. H., Doherty, R., Srikumar, T., Shloush, J., Avvakumov, G. V., Walker, J. R., Xue, S., Neculai, D., Wan, J. W., Kim, S. K., Arrowsmith, C. H., Raught, B. & Dhe-Paganon, S. (2012) A human ubiquitin conjugating enzyme (E2)-HECT E3 ligase structure-function screen, *Mol Cell Proteomics.* **11**, 329-41.
60. Kim, H. C. & Huibregtse, J. M. (2009) Polyubiquitination by HECT E3s and the determinants of chain type specificity, *Mol Cell Biol.* **29**, 3307-18.
61. Fang, N. N., Chan, G. T., Zhu, M., Comyn, S. A., Persaud, A., Deshaies, R. J., Rotin, D., Gsponer, J. & Mayor, T. (2014) Rsp5/Nedd4 is the main ubiquitin ligase that targets cytosolic misfolded proteins following heat stress, *Nat Cell Biol.* **16**, 1227-37.
62. French, M. E., Klosowiak, J. L., Aslanian, A., Reed, S. I., Yates, J. R., 3rd & Hunter, T. (2017) Mechanism of ubiquitin chain synthesis employed by a HECT domain ubiquitin ligase, *J Biol Chem.* **292**, 10398-10413.

63. Platta, H. W., Abrahamsen, H., Thoresen, S. B. & Stenmark, H. (2012) Nedd4-dependent lysine-11-linked polyubiquitination of the tumour suppressor Beclin 1, *Biochem J.* **441**, 399-406.
64. Shearwin-Whyatt, L., Dalton, H. E., Foot, N. & Kumar, S. (2006) Regulation of functional diversity within the Nedd4 family by accessory and adaptor proteins, *Bioessays.* **28**, 617-28.
65. Wiesner, S., Ogunjimi, A. A., Wang, H. R., Rotin, D., Sicheri, F., Wrana, J. L. & Forman-Kay, J. D. (2007) Autoinhibition of the HECT-type ubiquitin ligase Smurf2 through its C2 domain, *Cell.* **130**, 651-62.
66. Mari, S., Ruetalo, N., Maspero, E., Stoffregen, M. C., Pasqualato, S., Polo, S. & Wiesner, S. (2014) Structural and functional framework for the autoinhibition of Nedd4-family ubiquitin ligases, *Structure.* **22**, 1639-49.
67. Gallagher, E., Gao, M., Liu, Y. C. & Karin, M. (2006) Activation of the E3 ubiquitin ligase Itch through a phosphorylation-induced conformational change, *Proc Natl Acad Sci U S A.* **103**, 1717-22.
68. Bruce, M. C., Kanelis, V., Fouladkou, F., Debonneville, A., Staub, O. & Rotin, D. (2008) Regulation of Nedd4-2 self-ubiquitination and stability by a PY motif located within its HECT-domain, *Biochem J.* **415**, 155-63.
69. Riling, C., Kamadurai, H., Kumar, S., O'Leary, C. E., Wu, K. P., Manion, E. E., Ying, M., Schulman, B. A. & Oliver, P. M. (2015) Itch WW Domains Inhibit Its E3 Ubiquitin Ligase Activity by Blocking E2-E3 Ligase Trans-thiolation, *J Biol Chem.* **290**, 23875-87.
70. Chen, Z., Jiang, H., Xu, W., Li, X., Dempsey, D. R., Zhang, X., Devreotes, P., Wolberger, C., Amzel, L. M., Gabelli, S. B. & Cole, P. A. (2017) A Tunable Brake for HECT Ubiquitin Ligases, *Mol Cell.* **66**, 345-357 e6.
71. Polo, S. (2012) Signaling-mediated control of ubiquitin ligases in endocytosis, *BMC Biol.* **10**, 25.
72. Ogunjimi, A. A., Briant, D. J., Pece-Barbara, N., Le Roy, C., Di Guglielmo, G. M., Kavsak, P., Rasmussen, R. K., Seet, B. T., Sicheri, F. & Wrana, J. L. (2005) Regulation of Smurf2 ubiquitin ligase activity by anchoring the E2 to the HECT domain, *Mol Cell.* **19**, 297-308.
73. Wang, J., Peng, Q., Lin, Q., Childress, C., Carey, D. & Yang, W. (2010) Calcium activates Nedd4 E3 ubiquitin ligases by releasing the C2 domain-mediated auto-inhibition, *J Biol Chem.* **285**, 12279-88.
74. Escobedo, A., Gomes, T., Aragon, E., Martin-Malpartida, P., Ruiz, L. & Macias, M. J. (2014) Structural basis of the activation and degradation mechanisms of the E3 ubiquitin ligase Nedd4L, *Structure.* **22**, 1446-57.
75. Kamynina, E., Debonneville, C., Bens, M., Vandewalle, A. & Staub, O. (2001) A novel mouse Nedd4 protein suppresses the activity of the epithelial Na+ channel, *FASEB J.* **15**, 204-214.
76. Staub, O., Yeger, H., Plant, P. J., Kim, H., Ernst, S. A. & Rotin, D. (1997) Immunolocalization of the ubiquitin-protein ligase Nedd4 in tissues expressing the epithelial Na+ channel (ENaC), *Am J Physiol.* **272**, C1871-80.
77. Harvey, K. F. & Kumar, S. (1999) Nedd4-like proteins: an emerging family of ubiquitin-protein ligases implicated in diverse cellular functions, *Trends Cell Biol.* **9**, 166-9.
78. Rossier, B. C., Pradervand, S., Schild, L. & Hummler, E. (2002) Epithelial sodium channel and the control of sodium balance: interaction between genetic and environmental factors, *Annu Rev Physiol.* **64**, 877-97.
79. Harvey, K. F., Dinudom, A., Cook, D. I. & Kumar, S. (2001) The Nedd4-like protein KIAA0439 is a potential regulator of the epithelial sodium channel, *J Biol Chem.* **276**, 8597-601.
80. Snyder, P. M. (2005) Minireview: regulation of epithelial Na+ channel trafficking, *Endocrinology.* **146**, 5079-85.
81. Rotin, D., Kanelis, V. & Schild, L. (2001) Trafficking and cell surface stability of ENaC, *Am J Physiol Renal Physiol.* **281**, F391-9.

82. Abriel, H., Loffing, J., Rebhun, J. F., Pratt, J. H., Schild, L., Horisberger, J. D., Rotin, D. & Staub, O. (1999) Defective regulation of the epithelial Na+ channel by Nedd4 in Liddle's syndrome, *J Clin Invest.* **103**, 667-73.
83. Vina-Vilaseca, A., Bender-Sigel, J., Sorkina, T., Closs, E. I. & Sorkin, A. (2011) Protein kinase C-dependent ubiquitination and clathrin-mediated endocytosis of the cationic amino acid transporter CAT-1, *J Biol Chem.* **286**, 8697-706.
84. Katz, M., Shtiegman, K., Tal-Or, P., Yakir, L., Mosesson, Y., Harari, D., Machluf, Y., Asao, H., Jovin, T., Sugamura, K. & Yarden, Y. (2002) Ligand-independent degradation of epidermal growth factor receptor involves receptor ubiquitylation and Hgs, an adaptor whose ubiquitin-interacting motif targets ubiquitylation by Nedd4, *Traffic.* **3**, 740-51.
85. Cao, X. R., Lill, N. L., Boase, N., Shi, P. P., Croucher, D. R., Shan, H., Qu, J., Sweezer, E. M., Place, T., Kirby, P. A., Daly, R. J., Kumar, S. & Yang, B. (2008) Nedd4 controls animal growth by regulating IGF-1 signaling, *Sci Signal.* **1**, ra5.
86. Pham, N. & Rotin, D. (2001) Nedd4 regulates ubiquitination and stability of the guanine-nucleotide exchange factor CNrasGEF, *J Biol Chem.* **276**, 46995-7003.
87. Pak, Y., Glowacka, W. K., Bruce, M. C., Pham, N. & Rotin, D. (2006) Transport of LAPTM5 to lysosomes requires association with the ubiquitin ligase Nedd4, but not LAPTM5 ubiquitination, *J Cell Biol.* **175**, 631-45.
88. Shenoy, S. K., Xiao, K., Venkataramanan, V., Snyder, P. M., Freedman, N. J. & Weissman, A. M. (2008) Nedd4 mediates agonist-dependent ubiquitination, lysosomal targeting, and degradation of the beta2-adrenergic receptor, *J Biol Chem.* **283**, 22166-76.
89. Woelk, T., Oldrini, B., Maspero, E., Confalonieri, S., Cavallaro, E., Di Fiore, P. P. & Polo, S. (2006) Molecular mechanisms of coupled monoubiquitination, *Nat Cell Biol.* **8**, 1246-54.
90. Blot, V., Perugi, F., Gay, B., Prevost, M. C., Briant, L., Tangy, F., Abriel, H., Staub, O., Dokhelar, M. C. & Pique, C. (2004) Nedd4.1-mediated ubiquitination and subsequent recruitment of Tsg101 ensure HTLV-1 Gag trafficking towards the multivesicular body pathway prior to virus budding, *J Cell Sci.* **117**, 2357-67.
91. Ye, X., Wang, L., Shang, B., Wang, Z. & Wei, W. (2014) NEDD4: a promising target for cancer therapy, *Curr Cancer Drug Targets.* **14**, 549-56.
92. Wang, X., Trotman, L. C., Koppie, T., Alimonti, A., Chen, Z., Gao, Z., Wang, J., Erdjument-Bromage, H., Tempst, P., Cordon-Cardo, C., Pandolfi, P. P. & Jiang, X. (2007) NEDD4-1 is a proto-oncogenic ubiquitin ligase for PTEN, *Cell.* **128**, 129-39.
93. Fouladkou, F., Landry, T., Kawabe, H., Neeb, A., Lu, C., Brose, N., Stambolic, V. & Rotin, D. (2008) The ubiquitin ligase Nedd4-1 is dispensable for the regulation of PTEN stability and localization, *Proc Natl Acad Sci U S A.* **105**, 8585-90.
94. Chastagner, P., Israel, A. & Brou, C. (2008) AIP4/Itch regulates Notch receptor degradation in the absence of ligand, *PLoS One.* **3**, e2735.
95. Marchese, A., Raiborg, C., Santini, F., Keen, J. H., Stenmark, H. & Benovic, J. L. (2003) The E3 ubiquitin ligase AIP4 mediates ubiquitination and sorting of the G protein-coupled receptor CXCR4, *Dev Cell.* **5**, 709-22.
96. Liu, Y. C. (2007) The E3 ubiquitin ligase Itch in T cell activation, differentiation, and tolerance, *Semin Immunol.* **19**, 197-205.
97. Bernassola, F., Karin, M., Ciechanover, A. & Melino, G. (2008) The HECT family of E3 ubiquitin ligases: multiple players in cancer development, *Cancer Cell.* **14**, 10-21.
98. Chen, C., Sun, X., Guo, P., Dong, X. Y., Sethi, P., Zhou, W., Zhou, Z., Petros, J., Frierson, H. F., Jr., Vessella, R. L., Atfi, A. & Dong, J. T. (2007) Ubiquitin E3 ligase WWP1 as an oncogenic factor in human prostate cancer, *Oncogene.* **26**, 2386-94.
99. Laine, A. & Ronai, Z. (2007) Regulation of p53 localization and transcription by the HECT domain E3 ligase WWP1, *Oncogene.* **26**, 1477-83.
100. Chen, C., Sun, X., Guo, P., Dong, X. Y., Sethi, P., Cheng, X., Zhou, J., Ling, J., Simons, J. W., Lingrel, J. B. & Dong, J. T. (2005) Human Kruppel-like factor 5 is a target of the E3 ubiquitin ligase WWP1 for proteolysis in epithelial cells, *J Biol Chem.* **280**, 41553-61.

101. Komuro, A., Imamura, T., Saitoh, M., Yoshida, Y., Yamori, T., Miyazono, K. & Miyazawa, K. (2004) Negative regulation of transforming growth factor-beta (TGF-beta) signaling by WW domain-containing protein 1 (WWP1), *Oncogene.* **23**, 6914-23.
102. Zhang, Y., Chang, C., Gehling, D. J., Hemmati-Brivanlou, A. & Derynck, R. (2001) Regulation of Smad degradation and activity by Smurf2, an E3 ubiquitin ligase, *Proc Natl Acad Sci U S A.* **98**, 974-9.
103. Inoue, Y. & Imamura, T. (2008) Regulation of TGF-beta family signaling by E3 ubiquitin ligases, *Cancer Sci.* **99**, 2107-12.
104. Fukuchi, M., Fukai, Y., Masuda, N., Miyazaki, T., Nakajima, M., Sohda, M., Manda, R., Tsukada, K., Kato, H. & Kuwano, H. (2002) High-level expression of the Smad ubiquitin ligase Smurf2 correlates with poor prognosis in patients with esophageal squamous cell carcinoma, *Cancer Res.* **62**, 7162-5.
105. Miyazaki, K., Fujita, T., Ozaki, T., Kato, C., Kurose, Y., Sakamoto, M., Kato, S., Goto, T., Itoyama, Y., Aoki, M. & Nakagawara, A. (2004) NEDL1, a novel ubiquitin-protein isopeptide ligase for dishevelled-1, targets mutant superoxide dismutase-1, *J Biol Chem.* **279**, 11327-35.
106. Zhang, L., Haraguchi, S., Koda, T., Hashimoto, K. & Nakagawara, A. (2011) Muscle atrophy and motor neuron degeneration in human NEDL1 transgenic mice, *J Biomed Biotechnol.* **2011**, 831092.
107. Li, Y., Ozaki, T., Kikuchi, H., Yamamoto, H., Ohira, M. & Nakagawara, A. (2008) A novel HECT-type E3 ubiquitin protein ligase NEDL1 enhances the p53-mediated apoptotic cell death in its catalytic activity-independent manner, *Oncogene.* **27**, 3700-9.
108. Shinada, K., Tsukiyama, T., Sho, T., Okumura, F., Asaka, M. & Hatakeyama, S. (2011) RNF43 interacts with NEDL1 and regulates p53-mediated transcription, *Biochem Biophys Res Commun.* **404**, 143-7.
109. Li, Y., Zhou, Z., Alimandi, M. & Chen, C. (2009) WW domain containing E3 ubiquitin protein ligase 1 targets the full-length ErbB4 for ubiquitin-mediated degradation in breast cancer, *Oncogene.* **28**, 2948-58.
110. Mantripragada, K. K., Diaz de Stahl, T., Patridge, C., Menzel, U., Andersson, R., Chuzhanova, N., Kluwe, L., Guha, A., Mautner, V., Dumanski, J. P. & Upadhyaya, M. (2009) Genome-wide high-resolution analysis of DNA copy number alterations in NF1-associated malignant peripheral nerve sheath tumors using 32K BAC array, *Genes Chromosomes Cancer.* **48**, 897-907.
111. Miyazaki, K., Ozaki, T., Kato, C., Hanamoto, T., Fujita, T., Irino, S., Watanabe, K., Nakagawa, T. & Nakagawara, A. (2003) A novel HECT-type E3 ubiquitin ligase, NEDL2, stabilizes p73 and enhances its transcriptional activity, *Biochem Biophys Res Commun.* **308**, 106-13.
112. Lu, L., Hu, S., Wei, R., Qiu, X., Lu, K., Fu, Y., Li, H., Xing, G., Li, D., Peng, R., He, F. & Zhang, L. (2013) The HECT type ubiquitin ligase NEDL2 is degraded by anaphase-promoting complex/cyclosome (APC/C)-Cdh1, and its tight regulation maintains the metaphase to anaphase transition, *J Biol Chem.* **288**, 35637-50.
113. Wei, R., Qiu, X., Wang, S., Li, Y., Wang, Y., Lu, K., Fu, Y., Xing, G., He, F. & Zhang, L. (2015) NEDL2 is an essential regulator of enteric neural development and GDNF/Ret signaling, *Cell Signal.* **27**, 578-86.
114. Qiu, X., Wei, R., Li, Y., Zhu, Q., Xiong, C., Chen, Y., Zhang, Y., Lu, K., He, F. & Zhang, L. (2016) NEDL2 regulates enteric nervous system and kidney development in its Nedd8 ligase activity-dependent manner, *Oncotarget.* **7**, 31440-53.
115. O'Donnell, A. M., Coyle, D. & Puri, P. (2016) Decreased expression of NEDL2 in Hirschsprung's disease, *J Pediatr Surg.* **51**, 1839-1842.
116. Choi, K. S., Choi, H. J., Lee, J. K., Im, S., Zhang, H., Jeong, Y., Park, J. A., Lee, I. K., Kim, Y. M. & Kwon, Y. G. (2016) The endothelial E3 ligase HECW2 promotes endothelial cell junctions by increasing AMOTL1 protein stability via K63-linked ubiquitination, *Cell Signal.* **28**, 1642-51.
117. Jennings, B. H. (2011) Drosophila – a versatile model in biology & medicine, *Materials Today.* **14**, 190-195.

118. Pandey, U. B. & Nichols, C. D. (2011) Human disease models in Drosophila melanogaster and the role of the fly in therapeutic drug discovery, *Pharmacol Rev.* **63**, 411-36.
119. Adams, M. D.Celniker, S. E.Holt, R. A.Evans, C. A.Gocayne, J. D.Amanatides, P. G.Scherer, S. E.Li, P. W.Hoskins, R. A.Galle, R. F.George, R. A.Lewis, S. E.Richards, S.Ashburner, M.Henderson, S. N.Sutton, G. G.Wortman, J. R.Yandell, M. D.Zhang, Q.Chen, L. X.Brandon, R. C.Rogers, Y. H.Blazej, R. G.Champe, M.Pfeiffer, B. D.Wan, K. H.Doyle, C.Baxter, E. G.Helt, G.Nelson, C. R.Gabor, G. L.Abril, J. F.Agbayani, A.An, H. J.Andrews-Pfannkoch, C.Baldwin, D.Ballew, R. M.Basu, A.Baxendale, J.Bayraktaroglu, L.Beasley, E. M.Beeson, K. Y.Benos, P. V.Berman, B. P.Bhandari, D.Bolshakov, S.Borkova, D.Botchan, M. R.Bouck, J.Brokstein, P.Brottier, P.Burtis, K. C.Busam, D. A.Butler, H.Cadieu, E.Center, A.Chandra, I.Cherry, J. M.Cawley, S.Dahlke, C.Davenport, L. B.Davies, P.de Pablos, B.Delcher, A.Deng, Z.Mays, A. D.Dew, I.Dietz, S. M.Dodson, K.Doup, L. E.Downes, M.Dugan-Rocha, S.Dunkov, B. C.Dunn, P.Durbin, K. J.Evangelista, C. C.Ferraz, C.Ferriera, S.Fleischmann, W.Fosler, C.Gabrielian, A. E.Garg, N. S.Gelbart, W. M.Glasser, K.Glodek, A.Gong, F.Gorrell, J. H.Gu, Z.Guan, P.Harris, M.Harris, N. L.Harvey, D.Heiman, T. J.Hernandez, J. R.Houck, J.Hostin, D.Houston, K. A.Howland, T. J.Wei, M. H.Ibegwam, C., et al. (2000) The genome sequence of Drosophila melanogaster, *Science.* **287**, 2185-95.
120. Reiter, L. T., Potocki, L., Chien, S., Gribskov, M. & Bier, E. (2001) A systematic analysis of human disease-associated gene sequences in Drosophila melanogaster, *Genome Res.* **11**, 1114-25.
121. Lu, B. & Vogel, H. (2009) Drosophila models of neurodegenerative diseases, *Annu Rev Pathol.* **4**, 315-42.
122. Mandelkow, E. (1999) Alzheimer's disease. The tangled tale of tau, *Nature.* **402**, 588-9.
123. Feany, M. B. & Bender, W. W. (2000) A Drosophila model of Parkinson's disease, *Nature.* **404**, 394-8.
124. Warrick, J. M., Paulson, H. L., Gray-Board, G. L., Bui, Q. T., Fischbeck, K. H., Pittman, R. N. & Bonini, N. M. (1998) Expanded polyglutamine protein forms nuclear inclusions and causes neural degeneration in Drosophila, *Cell.* **93**, 939-49.
125. McBride, S. M., Choi, C. H., Wang, Y., Liebelt, D., Braunstein, E., Ferreiro, D., Sehgal, A., Siwicki, K. K., Dockendorff, T. C., Nguyen, H. T., McDonald, T. V. & Jongens, T. A. (2005) Pharmacological rescue of synaptic plasticity, courtship behavior, and mushroom body defects in a Drosophila model of fragile X syndrome, *Neuron.* **45**, 753-64.
126. Barry, W. E. & Thummel, C. S. (2016) The Drosophila HNF4 nuclear receptor promotes glucose-stimulated insulin secretion and mitochondrial function in adults, *Elife.* **5**.
127. Trinh, I. & Boulianne, G. L. (2013) Modeling obesity and its associated disorders in Drosophila, *Physiology (Bethesda).* **28**, 117-24.
128. Bogatan, S., Cevik, D., Demidov, V., Vanderploeg, J., Panchbhaya, A., Vitkin, A. & Jacobs, J. R. (2015) Talin Is Required Continuously for Cardiomyocyte Remodeling during Heart Growth in Drosophila, *PLoS One.* **10**, e0131238.
129. Hahn, N., Geurten, B., Gurvich, A., Piepenbrock, D., Kastner, A., Zanini, D., Xing, G., Xie, W., Gopfert, M. C., Ehrenreich, H. & Heinrich, R. (2013) Monogenic heritable autism gene neuroligin impacts Drosophila social behaviour, *Behav Brain Res.* **252**, 450-7.
130. Rudrapatna, V. A., Cagan, R. L. & Das, T. K. (2012) Drosophila cancer models, *Dev Dyn.* **241**, 107-18.
131. Mazaleyrat, S. L., Fostier, M., Wilkin, M. B., Aslam, H., Evans, D. A., Cornell, M. & Baron, M. (2003) Down-regulation of Notch target gene expression by Suppressor of deltex, *Dev Biol.* **255**, 363-72.
132. Wilkin, M. B., Carbery, A. M., Fostier, M., Aslam, H., Mazaleyrat, S. L., Higgs, J., Myat, A., Evans, D. A., Cornell, M. & Baron, M. (2004) Regulation of notch endosomal sorting and signaling by Drosophila Nedd4 family proteins, *Curr Biol.* **14**, 2237-44.
133. Shimizu, H., Woodcock, S. A., Wilkin, M. B., Trubenova, B., Monk, N. A. & Baron, M. (2014) Compensatory flux changes within an endocytic trafficking network maintain thermal robustness of Notch signaling, *Cell.* **157**, 1160-74.

134. Djiane, A., Shimizu, H., Wilkin, M., Mazleyrat, S., Jennings, M. D., Avis, J., Bray, S. & Baron, M. (2011) Su(dx) E3 ubiquitin ligase-dependent and -independent functions of polychaetoid, the Drosophila ZO-1 homologue, *J Cell Biol.* **192**, 189-200.
135. Sakata, T., Sakaguchi, H., Tsuda, L., Higashitani, A., Aigaki, T., Matsuno, K. & Hayashi, S. (2004) Drosophila Nedd4 regulates endocytosis of notch and suppresses its ligand-independent activation, *Curr Biol.* **14**, 2228-36.
136. Myat, A., Henry, P., McCabe, V., Flintoft, L., Rotin, D. & Tear, G. (2002) Drosophila Nedd4, a ubiquitin ligase, is recruited by Commissureless to control cell surface levels of the roundabout receptor, *Neuron.* **35**, 447-59.
137. Ing, B., Shteiman-Kotler, A., Castelli, M., Henry, P., Pak, Y., Stewart, B., Boulianne, G. L. & Rotin, D. (2007) Regulation of Commissureless by the ubiquitin ligase DNedd4 is required for neuromuscular synaptogenesis in Drosophila melanogaster, *Mol Cell Biol.* **27**, 481-96.
138. Zhong, Y., Shtineman-Kotler, A., Nguyen, L., Iliadi, K. G., Boulianne, G. L. & Rotin, D. (2011) A splice isoform of DNedd4, DNedd4-long, negatively regulates neuromuscular synaptogenesis and viability in Drosophila, *PLoS One.* **6**, e27007.
139. Podos, S. D., Hanson, K. K., Wang, Y. C. & Ferguson, E. L. (2001) The DSmurf ubiquitin-protein ligase restricts BMP signaling spatially and temporally during Drosophila embryogenesis, *Dev Cell.* **1**, 567-78.
140. Liang, Y. Y., Lin, X., Liang, M., Brunicardi, F. C., ten Dijke, P., Chen, Z., Choi, K. W. & Feng, X. H. (2003) dSmurf selectively degrades decapentaplegic-activated MAD, and its overexpression disrupts imaginal disc development, *J Biol Chem.* **278**, 26307-10.
141. Cao, L., Wang, P., Gao, Y., Lin, X., Wang, F. & Wu, S. (2014) Ubiquitin E3 ligase dSmurf is essential for Wts protein turnover and Hippo signaling, *Biochem Biophys Res Commun.* **454**, 167-71.
142. Besse, F. & Ephrussi, A. (2008) Translational control of localized mRNAs: restricting protein synthesis in space and time, *Nat Rev Mol Cell Biol.* **9**, 971-80.
143. Nevo-Dinur, K., Nussbaum-Shochat, A., Ben-Yehuda, S. & Amster-Choder, O. (2011) Translation-independent localization of mRNA in E. coli, *Science.* **331**, 1081-4.
144. Moffitt, J. R., Pandey, S., Boettiger, A. N., Wang, S. & Zhuang, X. (2016) Spatial organization shapes the turnover of a bacterial transcriptome, *Elife.* **5**.
145. Becalska, A. N. & Gavis, E. R. (2009) Lighting up mRNA localization in Drosophila oogenesis, *Development.* **136**, 2493-503.
146. Heasman, J., Quarmby, J. & Wylie, C. C. (1984) The mitochondrial cloud of Xenopus oocytes: the source of germinal granule material, *Dev Biol.* **105**, 458-69.
147. Lin, A. C. & Holt, C. E. (2007) Local translation and directional steering in axons, *EMBO J.* **26**, 3729-36.
148. Glock, C., Heumuller, M. & Schuman, E. M. (2017) mRNA transport & local translation in neurons, *Curr Opin Neurobiol.* **45**, 169-177.
149. Condeelis, J. & Singer, R. H. (2005) How and why does beta-actin mRNA target?, *Biol Cell.* **97**, 97-110.
150. Cody, N. A., Iampietro, C. & Lecuyer, E. (2013) The many functions of mRNA localization during normal development and disease: from pillar to post, *Wiley Interdiscip Rev Dev Biol.* **2**, 781-96.
151. Smith, R. (2004) Moving molecules: mRNA trafficking in Mammalian oligodendrocytes and neurons, *Neuroscientist.* **10**, 495-500.
152. Ainger, K., Avossa, D., Morgan, F., Hill, S. J., Barry, C., Barbarese, E. & Carson, J. H. (1993) Transport and localization of exogenous myelin basic protein mRNA microinjected into oligodendrocytes, *J Cell Biol.* **123**, 431-41.
153. Parker, R. & Sheth, U. (2007) P bodies and the control of mRNA translation and degradation, *Mol Cell.* **25**, 635-46.
154. Buchan, J. R. & Parker, R. (2009) Eukaryotic stress granules: the ins and outs of translation, *Mol Cell.* **36**, 932-41.

155. Anderson, P. & Kedersha, N. (2002) Stressful initiations, *J Cell Sci.* **115**, 3227-34.
156. Kedersha, N., Stoecklin, G., Ayodele, M., Yacono, P., Lykke-Andersen, J., Fritzler, M. J., Scheuner, D., Kaufman, R. J., Golan, D. E. & Anderson, P. (2005) Stress granules and processing bodies are dynamically linked sites of mRNP remodeling, *J Cell Biol.* **169**, 871-84.
157. Kiebler, M. A. & Bassell, G. J. (2006) Neuronal RNA granules: movers and makers, *Neuron.* **51**, 685-90.
158. Schisa, J. A. (2012) New insights into the regulation of RNP granule assembly in oocytes, *Int Rev Cell Mol Biol.* **295**, 233-89.
159. Bramham, C. R. & Wells, D. G. (2007) Dendritic mRNA: transport, translation and function, *Nat Rev Neurosci.* **8**, 776-89.
160. Anderson, P. & Kedersha, N. (2006) RNA granules, *J Cell Biol.* **172**, 803-8.
161. Kress, T. L., Yoon, Y. J. & Mowry, K. L. (2004) Nuclear RNP complex assembly initiates cytoplasmic RNA localization, *J Cell Biol.* **165**, 203-11.
162. Kuersten, S. & Goodwin, E. B. (2003) The power of the 3' UTR: translational control and development, *Nat Rev Genet.* **4**, 626-37.
163. Hachet, O. & Ephrussi, A. (2004) Splicing of oskar RNA in the nucleus is coupled to its cytoplasmic localization, *Nature.* **428**, 959-63.
164. Ghosh, S., Marchand, V., Gaspar, I. & Ephrussi, A. (2012) Control of RNP motility and localization by a splicing-dependent structure in oskar mRNA, *Nat Struct Mol Biol.* **19**, 441-9.
165. Schratt, G. M., Tuebing, F., Nigh, E. A., Kane, C. G., Sabatini, M. E., Kiebler, M. & Greenberg, M. E. (2006) A brain-specific microRNA regulates dendritic spine development, *Nature.* **439**, 283-9.
166. Napoli, I., Mercaldo, V., Boyl, P. P., Eleuteri, B., Zalfa, F., De Rubeis, S., Di Marino, D., Mohr, E., Massimi, M., Falconi, M., Witke, W., Costa-Mattioli, M., Sonenberg, N., Achsel, T. & Bagni, C. (2008) The fragile X syndrome protein represses activity-dependent translation through CYFIP1, a new 4E-BP, *Cell.* **134**, 1042-54.
167. Paquin, N., Menade, M., Poirier, G., Donato, D., Drouet, E. & Chartrand, P. (2007) Local activation of yeast ASH1 mRNA translation through phosphorylation of Khd1p by the casein kinase Yck1p, *Mol Cell.* **26**, 795-809.
168. Lin, D., Pestova, T. V., Hellen, C. U. & Tiedge, H. (2008) Translational control by a small RNA: dendritic BC1 RNA targets the eukaryotic initiation factor 4A helicase mechanism, *Mol Cell Biol.* **28**, 3008-19.
169. Huttelmaier, S., Zenklusen, D., Lederer, M., Dictenberg, J., Lorenz, M., Meng, X., Bassell, G. J., Condeelis, J. & Singer, R. H. (2005) Spatial regulation of beta-actin translation by Src-dependent phosphorylation of ZBP1, *Nature.* **438**, 512-5.
170. Zaessinger, S., Busseau, I. & Simonelig, M. (2006) Oskar allows nanos mRNA translation in Drosophila embryos by preventing its deadenylation by Smaug/CCR4, *Development.* **133**, 4573-83.
171. Chekulaeva, M., Hentze, M. W. & Ephrussi, A. (2006) Bruno acts as a dual repressor of oskar translation, promoting mRNA oligomerization and formation of silencing particles, *Cell.* **124**, 521-33.
172. Lipshitz, H. D. & Smibert, C. A. (2000) Mechanisms of RNA localization and translational regulation, *Curr Opin Genet Dev.* **10**, 476-88.
173. St Johnston, D. (2005) Moving messages: the intracellular localization of mRNAs, *Nat Rev Mol Cell Biol.* **6**, 363-75.
174. Vazquez-Pianzola, P., Adam, J., Haldemann, D., Hain, D., Urlaub, H. & Suter, B. (2014) Clathrin heavy chain plays multiple roles in polarizing the Drosophila oocyte downstream of Bic-D, *Development.* **141**, 1915-26.
175. Kanai, Y., Dohmae, N. & Hirokawa, N. (2004) Kinesin transports RNA: isolation and characterization of an RNA-transporting granule, *Neuron.* **43**, 513-25.

176. Bullock, S. L., Nicol, A., Gross, S. P. & Zicha, D. (2006) Guidance of bidirectional motor complexes by mRNA cargoes through control of dynein number and activity, *Curr Biol.* **16**, 1447-52.
177. Bullock, S. L. (2007) Translocation of mRNAs by molecular motors: think complex?, *Semin Cell Dev Biol.* **18**, 194-201.
178. Delanoue, R. & Davis, I. (2005) Dynein anchors its mRNA cargo after apical transport in the Drosophila blastoderm embryo, *Cell.* **122**, 97-106.
179. Mendez, R. & Richter, J. D. (2001) Translational control by CPEB: a means to the end, *Nat Rev Mol Cell Biol.* **2**, 521-9.
180. Huang, Y. S., Jung, M. Y., Sarkissian, M. & Richter, J. D. (2002) N-methyl-D-aspartate receptor signaling results in Aurora kinase-catalyzed CPEB phosphorylation and alpha CaMKII mRNA polyadenylation at synapses, *EMBO J.* **21**, 2139-48.
181. Andresson, T. & Ruderman, J. V. (1998) The kinase Eg2 is a component of the Xenopus oocyte progesterone-activated signaling pathway, *EMBO J.* **17**, 5627-37.
182. Ceman, S., O'Donnell, W. T., Reed, M., Patton, S., Pohl, J. & Warren, S. T. (2003) Phosphorylation influences the translation state of FMRP-associated polyribosomes, *Hum Mol Genet.* **12**, 3295-305.
183. Narayanan, U., Nalavadi, V., Nakamoto, M., Pallas, D. C., Ceman, S., Bassell, G. J. & Warren, S. T. (2007) FMRP phosphorylation reveals an immediate-early signaling pathway triggered by group I mGluR and mediated by PP2A, *J Neurosci.* **27**, 14349-57.
184. Weil, T. T. (2014) mRNA localization in the Drosophila germline, *RNA Biol.* **11**, 1010-8.
185. Spradling, A. C., de Cuevas, M., Drummond-Barbosa, D., Keyes, L., Lilly, M., Pepling, M. & Xie, T. (1997) The Drosophila germarium: stem cells, germ line cysts, and oocytes, *Cold Spring Harb Symp Quant Biol.* **62**, 25-34.
186. Ables, E. T. (2015) Drosophila oocytes as a model for understanding meiosis: an educational primer to accompany "corolla is a novel protein that contributes to the architecture of the synaptonemal complex of Drosophila", *Genetics.* **199**, 17-23.
187. Lin, H. & Spradling, A. C. (1995) Fusome asymmetry and oocyte determination in Drosophila, *Dev Genet.* **16**, 6-12.
188. de Cuevas, M. & Spradling, A. C. (1998) Morphogenesis of the Drosophila fusome and its implications for oocyte specification, *Development.* **125**, 2781-9.
189. Lilly, M. A., de Cuevas, M. & Spradling, A. C. (2000) Cyclin A associates with the fusome during germline cyst formation in the Drosophila ovary, *Dev Biol.* **218**, 53-63.
190. Parton, R. M., Hamilton, R. S., Ball, G., Yang, L., Cullen, C. F., Lu, W., Ohkura, H. & Davis, I. (2011) A PAR-1-dependent orientation gradient of dynamic microtubules directs posterior cargo transport in the Drosophila oocyte, *J Cell Biol.* **194**, 121-35.
191. Nilson, L. A. & Schupbach, T. (1999) EGF receptor signaling in Drosophila oogenesis, *Curr Top Dev Biol.* **44**, 203-43.
192. Ephrussi, A., Dickinson, L. K. & Lehmann, R. (1991) Oskar organizes the germ plasm and directs localization of the posterior determinant nanos, *Cell.* **66**, 37-50.
193. Gonzalez-Reyes, A., Elliott, H. & St Johnston, D. (1995) Polarization of both major body axes in Drosophila by gurken-torpedo signalling, *Nature.* **375**, 654-8.
194. Zhao, T., Graham, O. S., Raposo, A. & St Johnston, D. (2012) Growing microtubules push the oocyte nucleus to polarize the Drosophila dorsal-ventral axis, *Science.* **336**, 999-1003.
195. Roth, S., Neuman-Silberberg, F. S., Barcelo, G. & Schupbach, T. (1995) cornichon and the EGF receptor signaling process are necessary for both anterior-posterior and dorsal-ventral pattern formation in Drosophila, *Cell.* **81**, 967-78.
196. Zimyanin, V. L., Belaya, K., Pecreaux, J., Gilchrist, M. J., Clark, A., Davis, I. & St Johnston, D. (2008) In vivo imaging of oskar mRNA transport reveals the mechanism of posterior localization, *Cell.* **134**, 843-53.

197. Dahlgaard, K., Raposo, A. A., Niccoli, T. & St Johnston, D. (2007) Capu and Spire assemble a cytoplasmic actin mesh that maintains microtubule organization in the Drosophila oocyte, *Dev Cell.* **13**, 539-53.
198. Besse, F., Lopez de Quinto, S., Marchand, V., Trucco, A. & Ephrussi, A. (2009) Drosophila PTB promotes formation of high-order RNP particles and represses oskar translation, *Genes Dev.* **23**, 195-207.
199. Little, S. C., Sinsimer, K. S., Lee, J. J., Wieschaus, E. F. & Gavis, E. R. (2015) Independent and coordinate trafficking of single Drosophila germ plasm mRNAs, *Nat Cell Biol.* **17**, 558-68.
200. Lantz, V., Ambrosio, L. & Schedl, P. (1992) The Drosophila orb gene is predicted to encode sex-specific germline RNA-binding proteins and has localized transcripts in ovaries and early embryos, *Development.* **115**, 75-88.
201. Wong, L. C. & Schedl, P. (2011) Cup blocks the precocious activation of the orb autoregulatory loop, *PLoS One.* **6**, e28261.
202. Castagnetti, S. & Ephrussi, A. (2003) Orb and a long poly(A) tail are required for efficient oskar translation at the posterior pole of the Drosophila oocyte, *Development.* **130**, 835-43.
203. Davidson, A., Parton, Richard M., Rabouille, C., Weil, Timothy T. & Davis, I. (2016) Localized Translation of gurken/TGF-α mRNA during Axis Specification Is Controlled by Access to Orb/CPEB on Processing Bodies, *Cell Reports.* **14**, 2451-2462.
204. Weil, T. T., Parton, R. M., Herpers, B., Soetaert, J., Veenendaal, T., Xanthakis, D., Dobbie, I. M., Halstead, J. M., Hayashi, R., Rabouille, C. & Davis, I. (2012) Drosophila patterning is established by differential association of mRNAs with P bodies, *Nat Cell Biol.* **14**, 1305-13.
205. Tan, L., Chang, J. S., Costa, A. & Schedl, P. (2001) An autoregulatory feedback loop directs the localized expression of the Drosophila CPEB protein Orb in the developing oocyte, *Development.* **128**, 1159-69.
206. Costa, A., Wang, Y., Dockendorff, T. C., Erdjument-Bromage, H., Tempst, P., Schedl, P. & Jongens, T. A. (2005) The Drosophila fragile X protein functions as a negative regulator in the orb autoregulatory pathway, *Dev Cell.* **8**, 331-42.
207. Mansfield, J. H., Wilhelm, J. E. & Hazelrigg, T. (2002) Ypsilon Schachtel, a Drosophila Y-box protein, acts antagonistically to Orb in the oskar mRNA localization and translation pathway, *Development.* **129**, 197-209.
208. Iglesias, N., Tutucci, E., Gwizdek, C., Vinciguerra, P., Von Dach, E., Corbett, A. H., Dargemont, C. & Stutz, F. (2010) Ubiquitin-mediated mRNP dynamics and surveillance prior to budding yeast mRNA export, *Genes Dev.* **24**, 1927-38.
209. Hou, L., Antion, M. D., Hu, D., Spencer, C. M., Paylor, R. & Klann, E. (2006) Dynamic translational and proteasomal regulation of fragile X mental retardation protein controls mGluR-dependent long-term depression, *Neuron.* **51**, 441-54.
210. Nalavadi, V. C., Muddashetty, R. S., Gross, C. & Bassell, G. J. (2012) Dephosphorylation-induced ubiquitination and degradation of FMRP in dendrites: a role in immediate early mGluR-stimulated translation, *J Neurosci.* **32**, 2582-7.
211. Huang, J., Ikeuchi, Y., Malumbres, M. & Bonni, A. (2015) A Cdh1-APC/FMRP Ubiquitin Signaling Link Drives mGluR-Dependent Synaptic Plasticity in the Mammalian Brain, *Neuron.* **86**, 726-39.
212. Zhou, Z., Kawabe, H., Suzuki, A., Shinmyozu, K. & Saga, Y. (2017) NEDD4 controls spermatogonial stem cell homeostasis and stress response by regulating messenger ribonucleoprotein complexes, *Nat Commun.* **8**, 15662.
213. Wong, E. & Cuervo, A. M. (2010) Integration of clearance mechanisms: the proteasome and autophagy, *Cold Spring Harb Perspect Biol.* **2**, a006734.
214. Melendez, A. & Neufeld, T. P. (2008) The cell biology of autophagy in metazoans: a developing story, *Development.* **135**, 2347-60.
215. McPhee, C. K. & Baehrecke, E. H. (2009) Autophagy in Drosophila melanogaster, *Biochim Biophys Acta.* **1793**, 1452-60.

216. Glick, D., Barth, S. & Macleod, K. F. (2010) Autophagy: cellular and molecular mechanisms, *J Pathol.* **221**, 3-12.
217. Green, D. R. & Levine, B. (2014) To be or not to be? How selective autophagy and cell death govern cell fate, *Cell.* **157**, 65-75.
218. Yamano, K., Matsuda, N. & Tanaka, K. (2016) The ubiquitin signal and autophagy: an orchestrated dance leading to mitochondrial degradation, *EMBO Rep.* **17**, 300-16.
219. Khaminets, A., Behl, C. & Dikic, I. (2016) Ubiquitin-Dependent And Independent Signals In Selective Autophagy, *Trends Cell Biol.* **26**, 6-16.
220. Kuang, E., Qi, J. & Ronai, Z. (2013) Emerging roles of E3 ubiquitin ligases in autophagy, *Trends Biochem Sci.* **38**, 453-60.
221. McEwan, D. G. & Dikic, I. (2014) Cullins keep autophagy under control, *Dev Cell.* **31**, 675-6.
222. Li, Y., Zhang, L., Zhou, J., Luo, S., Huang, R., Zhao, C. & Diao, A. (2015) Nedd4 E3 ubiquitin ligase promotes cell proliferation and autophagy, *Cell Prolif.* **48**, 338-47.
223. Sun, A., Wei, J., Childress, C., Shaw, J. H. t., Peng, K., Shao, G., Yang, W. & Lin, Q. (2017) The E3 ubiquitin ligase NEDD4 is an LC3-interactive protein and regulates autophagy, *Autophagy.* **13**, 522-537.
224. Orvedahl, A., Sumpter, R., Jr., Xiao, G., Ng, A., Zou, Z., Tang, Y., Narimatsu, M., Gilpin, C., Sun, Q., Roth, M., Forst, C. V., Wrana, J. L., Zhang, Y. E., Luby-Phelps, K., Xavier, R. J., Xie, Y. & Levine, B. (2011) Image-based genome-wide siRNA screen identifies selective autophagy factors, *Nature.* **480**, 113-7.
225. Frankel, L. B., Lubas, M. & Lund, A. H. (2017) Emerging connections between RNA and autophagy, *Autophagy.* **13**, 3-23.
226. Sameshima, M., Liebhaber, S. A. & Schlessinger, D. (1981) Dual pathways for ribonucleic acid turnover in WI-38 but not in I-cell human diploid fibroblasts, *Mol Cell Biol.* **1**, 75-81.
227. Heydrick, S. J., Lardeux, B. R. & Mortimore, G. E. (1991) Uptake and degradation of cytoplasmic RNA by hepatic lysosomes. Quantitative relationship to RNA turnover, *J Biol Chem.* **266**, 8790-6.
228. Balavoine, S., Feldmann, G. & Lardeux, B. (1990) Rates of RNA degradation in isolated rat hepatocytes. Effects of amino acids and inhibitors of lysosomal function, *Eur J Biochem.* **189**, 617-23.
229. Guo, B., Huang, X., Zhang, P., Qi, L., Liang, Q., Zhang, X., Huang, J., Fang, B., Hou, W., Han, J. & Zhang, H. (2014) Genome-wide screen identifies signaling pathways that regulate autophagy during Caenorhabditis elegans development, *EMBO Rep.* **15**, 705-13.
230. Behrends, C., Sowa, M. E., Gygi, S. P. & Harper, J. W. (2010) Network organization of the human autophagy system, *Nature.* **466**, 68-76.
231. Buchan, J. R., Kolaitis, R. M., Taylor, J. P. & Parker, R. (2013) Eukaryotic stress granules are cleared by autophagy and Cdc48/VCP function, *Cell.* **153**, 1461-74.
232. Zhao, Y., Tian, E. & Zhang, H. (2009) Selective autophagic degradation of maternally-loaded germline P granule components in somatic cells during C. elegans embryogenesis, *Autophagy.* **5**, 717-9.
233. Sugimoto, A. (2009) Clearance of germ granules in the soma, *F1000 Biol Rep.* **1**, 49.
234. Mihailovic, M. K., Chen, A., Gonzalez-Rivera, J. C. & Contreras, L. M. (2017) Defective Ribonucleoproteins, Mistakes in RNA Processing, and Diseases, *Biochemistry.* **56**, 1367-1382.
235. Ito, D. & Suzuki, N. (2011) Conjoint pathologic cascades mediated by ALS/FTLD-U linked RNA-binding proteins TDP-43 and FUS, *Neurology.* **77**, 1636-43.
236. Didiot, M. C., Subramanian, M., Flatter, E., Mandel, J. L. & Moine, H. (2009) Cells lacking the fragile X mental retardation protein (FMRP) have normal RISC activity but exhibit altered stress granule assembly, *Mol Biol Cell.* **20**, 428-37.
237. Nonhoff, U., Ralser, M., Welzel, F., Piccini, I., Balzereit, D., Yaspo, M. L., Lehrach, H. & Krobitsch, S. (2007) Ataxin-2 interacts with the DEAD/H-box RNA helicase DDX6 and interferes with P-bodies and stress granules, *Mol Biol Cell.* **18**, 1385-96.

238. Dewey, C. M., Cenik, B., Sephton, C. F., Johnson, B. A., Herz, J. & Yu, G. (2012) TDP-43 aggregation in neurodegeneration: are stress granules the key?, *Brain Res.* **1462**, 16-25.
239. Kato, M., Han, T. W., Xie, S., Shi, K., Du, X., Wu, L. C., Mirzaei, H., Goldsmith, E. J., Longgood, J., Pei, J., Grishin, N. V., Frantz, D. E., Schneider, J. W., Chen, S., Li, L., Sawaya, M. R., Eisenberg, D., Tycko, R. & McKnight, S. L. (2012) Cell-free formation of RNA granules: low complexity sequence domains form dynamic fibers within hydrogels, *Cell.* **149**, 753-67.
240. Walsh, M. J., Cooper-Knock, J., Dodd, J. E., Stopford, M. J., Mihaylov, S. R., Kirby, J., Shaw, P. J. & Hautbergue, G. M. (2015) Invited review: decoding the pathophysiological mechanisms that underlie RNA dysregulation in neurodegenerative disorders: a review of the current state of the art, *Neuropathol Appl Neurobiol.* **41**, 109-34.
241. Aguzzi, A. & Rajendran, L. (2009) The transcellular spread of cytosolic amyloids, prions, and prionoids, *Neuron.* **64**, 783-90.
242. Arnold, E. S., Ling, S. C., Huelga, S. C., Lagier-Tourenne, C., Polymenidou, M., Ditsworth, D., Kordasiewicz, H. B., McAlonis-Downes, M., Platoshyn, O., Parone, P. A., Da Cruz, S., Clutario, K. M., Swing, D., Tessarollo, L., Marsala, M., Shaw, C. E., Yeo, G. W. & Cleveland, D. W. (2013) ALS-linked TDP-43 mutations produce aberrant RNA splicing and adult-onset motor neuron disease without aggregation or loss of nuclear TDP-43, *Proc Natl Acad Sci U S A.* **110**, E736-45.
243. Han, S. P., Tang, Y. H. & Smith, R. (2010) Functional diversity of the hnRNPs: past, present and perspectives, *Biochem J.* **430**, 379-92.
244. Udagawa, T., Fujioka, Y., Tanaka, M., Honda, D., Yokoi, S., Riku, Y., Ibi, D., Nagai, T., Yamada, K., Watanabe, H., Katsuno, M., Inada, T., Ohno, K., Sokabe, M., Okado, H., Ishigaki, S. & Sobue, G. (2015) FUS regulates AMPA receptor function and FTLD/ALS-associated behaviour via GluA1 mRNA stabilization, *Nat Commun.* **6**, 7098.
245. Fallini, C., Bassell, G. J. & Rossoll, W. (2012) Spinal muscular atrophy: the role of SMN in axonal mRNA regulation, *Brain Res.* **1462**, 81-92.
246. Ramaswami, M., Taylor, J. P. & Parker, R. (2013) Altered ribostasis: RNA-protein granules in degenerative disorders, *Cell.* **154**, 727-36.
247. Till, S. M. (2010) The developmental roles of FMRP, *Biochem Soc Trans.* **38**, 507-10.
248. Sherman, S. L., Curnow, E. C., Easley, C. A., Jin, P., Hukema, R. K., Tejada, M. I., Willemsen, R. & Usdin, K. (2014) Use of model systems to understand the etiology of fragile X-associated primary ovarian insufficiency (FXPOI), *J Neurodev Disord.* **6**, 26.
249. Bilen, J. & Bonini, N. M. (2005) Drosophila as a model for human neurodegenerative disease, *Annu Rev Genet.* **39**, 153-71.
250. Brand, A. H. & Perrimon, N. (1993) Targeted gene expression as a means of altering cell fates and generating dominant phenotypes, *Development.* **118**, 401-15.
251. Kondo, S. & Ueda, R. (2013) Highly improved gene targeting by germline-specific Cas9 expression in Drosophila, *Genetics.* **195**, 715-21.
252. Karaiskos, N., Wahle, P., Alles, J., Boltengagen, A., Ayoub, S., Kipar, C., Kocks, C., Rajewsky, N. & Zinzen, R. P. (2017) The Drosophila embryo at single-cell transcriptome resolution, *Science.* **358**, 194-199.
253. Chang, Y. F., Imam, J. S. & Wilkinson, M. F. (2007) The nonsense-mediated decay RNA surveillance pathway, *Annu Rev Biochem.* **76**, 51-74.
254. Tower, J. & Arbeitman, M. (2009) The genetics of gender and life span, *J Biol.* **8**, 38.
255. Piper, M. D., Skorupa, D. & Partridge, L. (2005) Diet, metabolism and lifespan in Drosophila, *Exp Gerontol.* **40**, 857-62.
256. Grotewiel, M. S., Martin, I., Bhandari, P. & Cook-Wiens, E. (2005) Functional senescence in Drosophila melanogaster, *Ageing Res Rev.* **4**, 372-97.
257. Mathe, E. (2003) Orbit/Mast, the CLASP orthologue of Drosophila, is required for asymmetric stem cell and cystocyte divisions and development of the polarised microtubule network that interconnects oocyte and nurse cells during oogenesis, *Development.* **130**, 901-915.
258. Rorth, P. (1998) Gal4 in the Drosophila female germline, *Mech Dev.* **78**, 113-8.

259. Tofaris, G. K., Kim, H. T., Hourez, R., Jung, J. W., Kim, K. P. & Goldberg, A. L. (2011) Ubiquitin ligase Nedd4 promotes alpha-synuclein degradation by the endosomal-lysosomal pathway, *Proc Natl Acad Sci U S A.* **108**, 17004-9.
260. Kirkin, V., McEwan, D. G., Novak, I. & Dikic, I. (2009) A role for ubiquitin in selective autophagy, *Mol Cell.* **34**, 259-69.
261. Sanchez-Wandelmer, J. & Reggiori, F. (2013) Amphisomes: out of the autophagosome shadow?, *EMBO J.* **32**, 3116-8.
262. Nagy, P., Varga, A., Kovacs, A. L., Takats, S. & Juhasz, G. (2015) How and why to study autophagy in Drosophila: it's more than just a garbage chute, *Methods.* **75**, 151-61.
263. Juhasz, G., Erdi, B., Sass, M. & Neufeld, T. P. (2007) Atg7-dependent autophagy promotes neuronal health, stress tolerance, and longevity but is dispensable for metamorphosis in Drosophila, *Genes Dev.* **21**, 3061-6.
264. Mendes, C. C. & Mirth, C. K. (2016) Stage-Specific Plasticity in Ovary Size Is Regulated by Insulin/Insulin-Like Growth Factor and Ecdysone Signaling in Drosophila, *Genetics.* **202**, 703-19.
265. Barth, J. M., Szabad, J., Hafen, E. & Kohler, K. (2011) Autophagy in Drosophila ovaries is induced by starvation and is required for oogenesis, *Cell Death Differ.* **18**, 915-24.
266. Richter, J. D. & Lasko, P. (2011) Translational control in oocyte development, *Cold Spring Harb Perspect Biol.* **3**, a002758.
267. Bozzetti, M. P., Specchia, V., Cattenoz, P. B., Laneve, P., Geusa, A., Sahin, H. B., Di Tommaso, S., Friscini, A., Massari, S., Diebold, C. & Giangrande, A. (2015) The Drosophila fragile X mental retardation protein participates in the piRNA pathway, *J Cell Sci.* **128**, 2070-84.
268. Lu, R., Wang, H., Liang, Z., Ku, L., O'Donnell W, T., Li, W., Warren, S. T. & Feng, Y. (2004) The fragile X protein controls microtubule-associated protein 1B translation and microtubule stability in brain neuron development, *Proc Natl Acad Sci U S A.* **101**, 15201-6.
269. Norvell, A., Wong, J., Randolph, K. & Thompson, L. (2015) Wispy and Orb cooperate in the cytoplasmic polyadenylation of localized gurken mRNA, *Dev Dyn.* **244**, 1276-85.
270. Zhu, K., Shan, Z., Chen, X., Cai, Y., Cui, L., Yao, W., Wang, Z., Shi, P., Tian, C., Lou, J., Xie, Y. & Wen, W. (2017) Allosteric auto-inhibition and activation of the Nedd4 family E3 ligase Itch, *EMBO Rep.* **18**, 1618-1630.
271. Davies, S. E., Hallett, P. J., Moens, T., Smith, G., Mangano, E., Kim, H. T., Goldberg, A. L., Liu, J. L., Isacson, O. & Tofaris, G. K. (2014) Enhanced ubiquitin-dependent degradation by Nedd4 protects against alpha-synuclein accumulation and toxicity in animal models of Parkinson's disease, *Neurobiol Dis.* **64**, 79-87.
272. Venken, K. J., Carlson, J. W., Schulze, K. L., Pan, H., He, Y., Spokony, R., Wan, K. H., Koriabine, M., de Jong, P. J., White, K. P., Bellen, H. J. & Hoskins, R. A. (2009) Versatile P[acman] BAC libraries for transgenesis studies in Drosophila melanogaster, *Nat Methods.* **6**, 431-4.
273. Vilchez, D., Saez, I. & Dillin, A. (2014) The role of protein clearance mechanisms in organismal ageing and age-related diseases, *Nat Commun.* **5**, 5659.
274. Nixon, R. A. (2013) The role of autophagy in neurodegenerative disease, *Nat Med.* **19**, 983-97.
275. Fimia, G. M., Stoykova, A., Romagnoli, A., Giunta, L., Di Bartolomeo, S., Nardacci, R., Corazzari, M., Fuoco, C., Ucar, A., Schwartz, P., Gruss, P., Piacentini, M., Chowdhury, K. & Cecconi, F. (2007) Ambra1 regulates autophagy and development of the nervous system, *Nature.* **447**, 1121-5.
276. Maday, S. & Holzbaur, E. L. (2016) Compartment-Specific Regulation of Autophagy in Primary Neurons, *J Neurosci.* **36**, 5933-45.
277. Nixon, R. A. (2006) Autophagy in neurodegenerative disease: friend, foe or turncoat?, *Trends Neurosci.* **29**, 528-35.
278. Nah, J., Yuan, J. & Jung, Y. K. (2015) Autophagy in neurodegenerative diseases: from mechanism to therapeutic approach, *Mol Cells.* **38**, 381-9.

279. Santoro, M. R., Bray, S. M. & Warren, S. T. (2012) Molecular mechanisms of fragile X syndrome: a twenty-year perspective, *Annu Rev Pathol.* **7**, 219-45.
280. Chang, W. L., Liou, W., Pen, H. C., Chou, H. Y., Chang, Y. W., Li, W. H., Chiang, W. & Pai, L. M. (2008) The gradient of Gurken, a long-range morphogen, is directly regulated by Cbl-mediated endocytosis, *Development.* **135**, 1923-33.
281. Yano, T., Lopez de Quinto, S., Matsui, Y., Shevchenko, A., Shevchenko, A. & Ephrussi, A. (2004) Hrp48, a Drosophila hnRNPA/B homolog, binds and regulates translation of oskar mRNA, *Dev Cell.* **6**, 637-48.
282. Kalifa, Y., Armenti, S. T. & Gavis, E. R. (2009) Glorund interactions in the regulation of gurken and oskar mRNAs, *Dev Biol.* **326**, 68-74.
283. Baumgartner, R., Stocker, H. & Hafen, E. (2013) The RNA-binding proteins FMR1, rasputin and caprin act together with the UBA protein lingerer to restrict tissue growth in Drosophila melanogaster, *PLoS Genet.* **9**, e1003598.
284. Robberecht, W. & Philips, T. (2013) The changing scene of amyotrophic lateral sclerosis, *Nat Rev Neurosci.* **14**, 248-64.
285. Li, Y. R., King, O. D., Shorter, J. & Gitler, A. D. (2013) Stress granules as crucibles of ALS pathogenesis, *J Cell Biol.* **201**, 361-72.
286. Tutucci, E. & Stutz, F. (2011) Keeping mRNPs in check during assembly and nuclear export, *Nat Rev Mol Cell Biol.* **12**, 377-84.
287. Sigismund, S., Polo, S. & Di Fiore, P. P. (2004) Signaling through monoubiquitination, *Curr Top Microbiol Immunol.* **286**, 149-85.
288. Piper, R. C., Dikic, I. & Lukacs, G. L. (2014) Ubiquitin-dependent sorting in endocytosis, *Cold Spring Harb Perspect Biol.* **6**.